Palladium(0) and Juglone: a New Alliance in the Fight Against Ovarian Cancer

Giovanni Tonon, Anna Rafaniello, Matteo Mauceri, Nicola Demitri, Thomas Scattolin*, Flavio Rizzolio*, Fabiano Visentin*

NMR SPECTRA

1D NMR and 2D NMR spectrum were recorded on Bruker 300 or 400 Advance spectrometers. Chemical shifts values (ppm) are given relative to TMS (^{1}H and ^{13}C), H_3PO_4 (^{31}P) and CCl_3F (^{19}F).

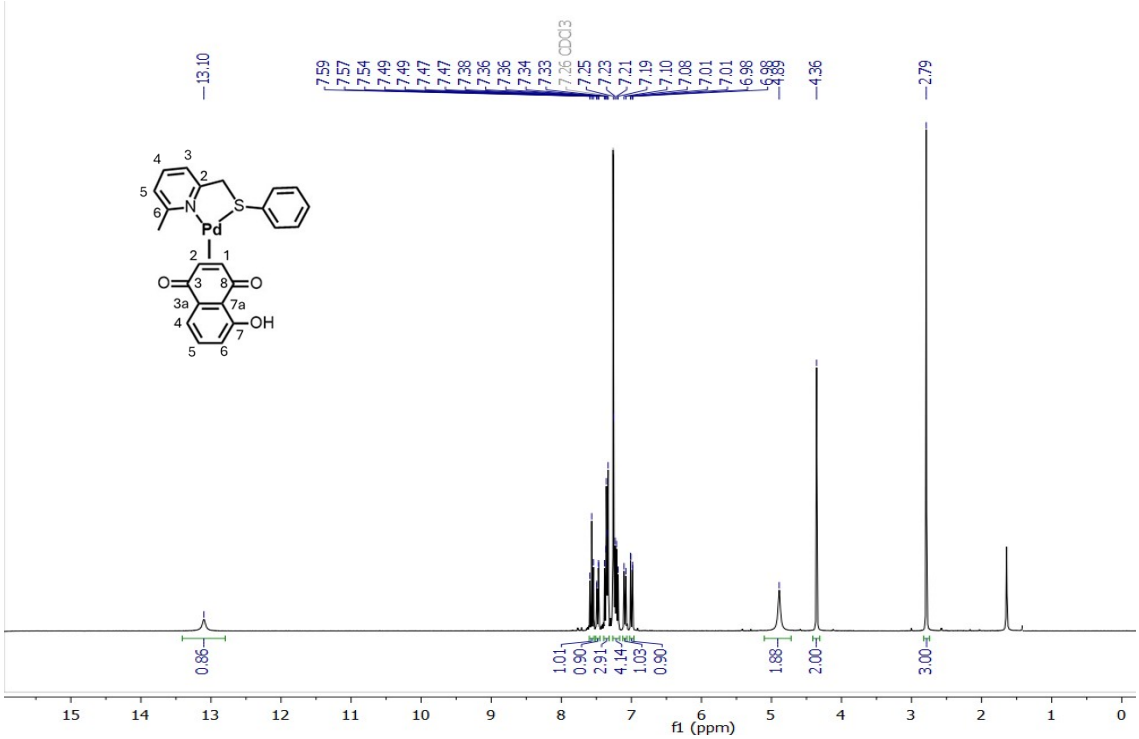

Figure **S1**. ^{1}H NMR spectrum of **A** in $CDCl_3$.

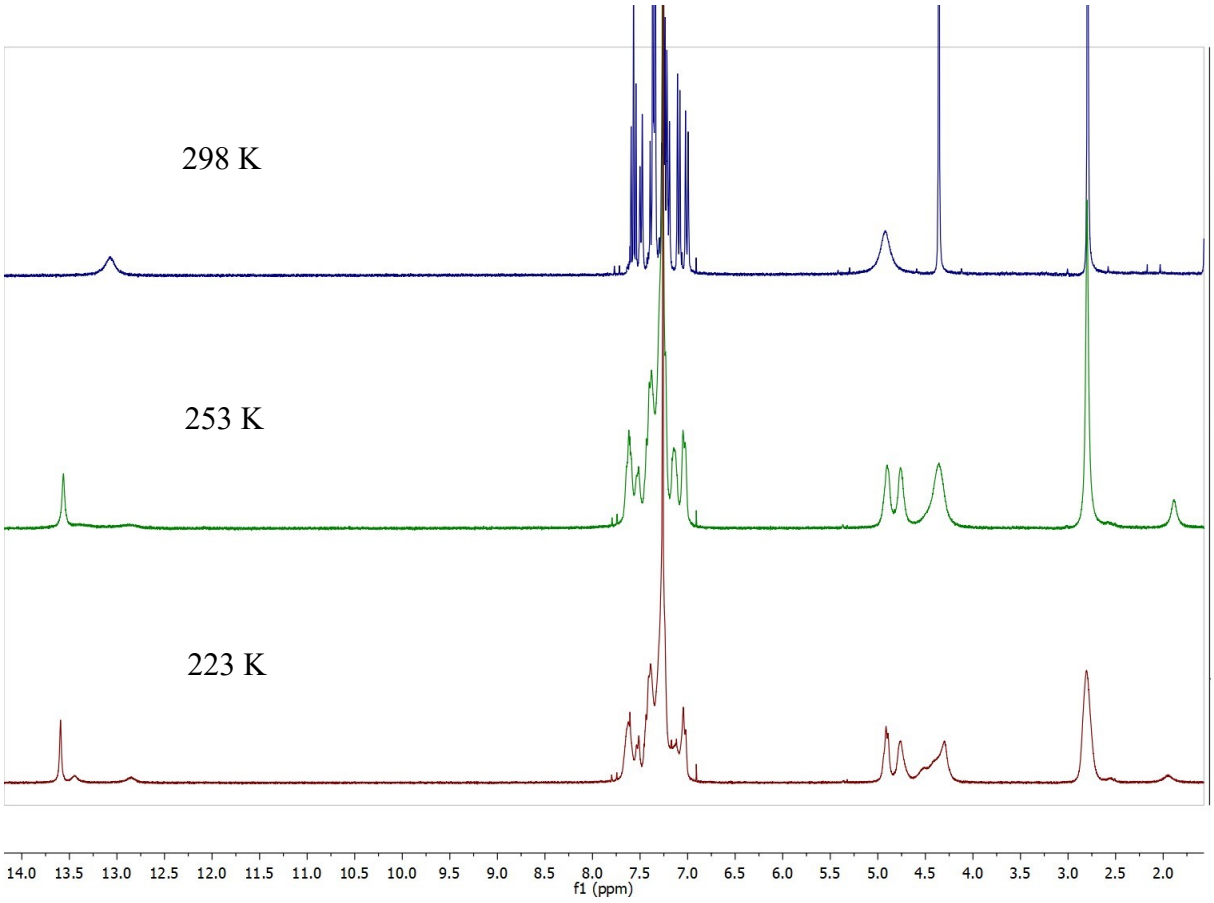

Figure **S2**. ^{1}H NMR spectrum of **A** in $CDCl_3$ at different temperatures.

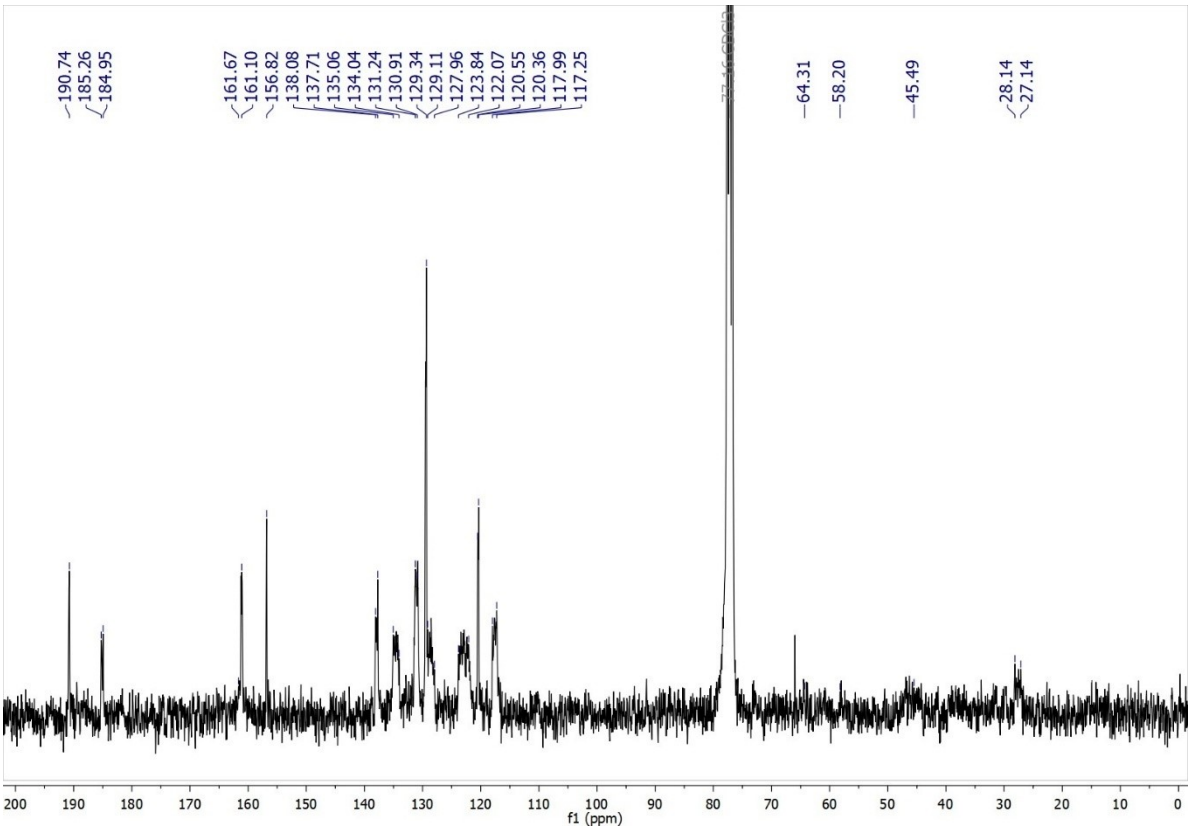

Figure **S3**. $^{13}C\{^{1}H\}$ NMR spectrum of **A** in $CDCl_3$ at 298K.

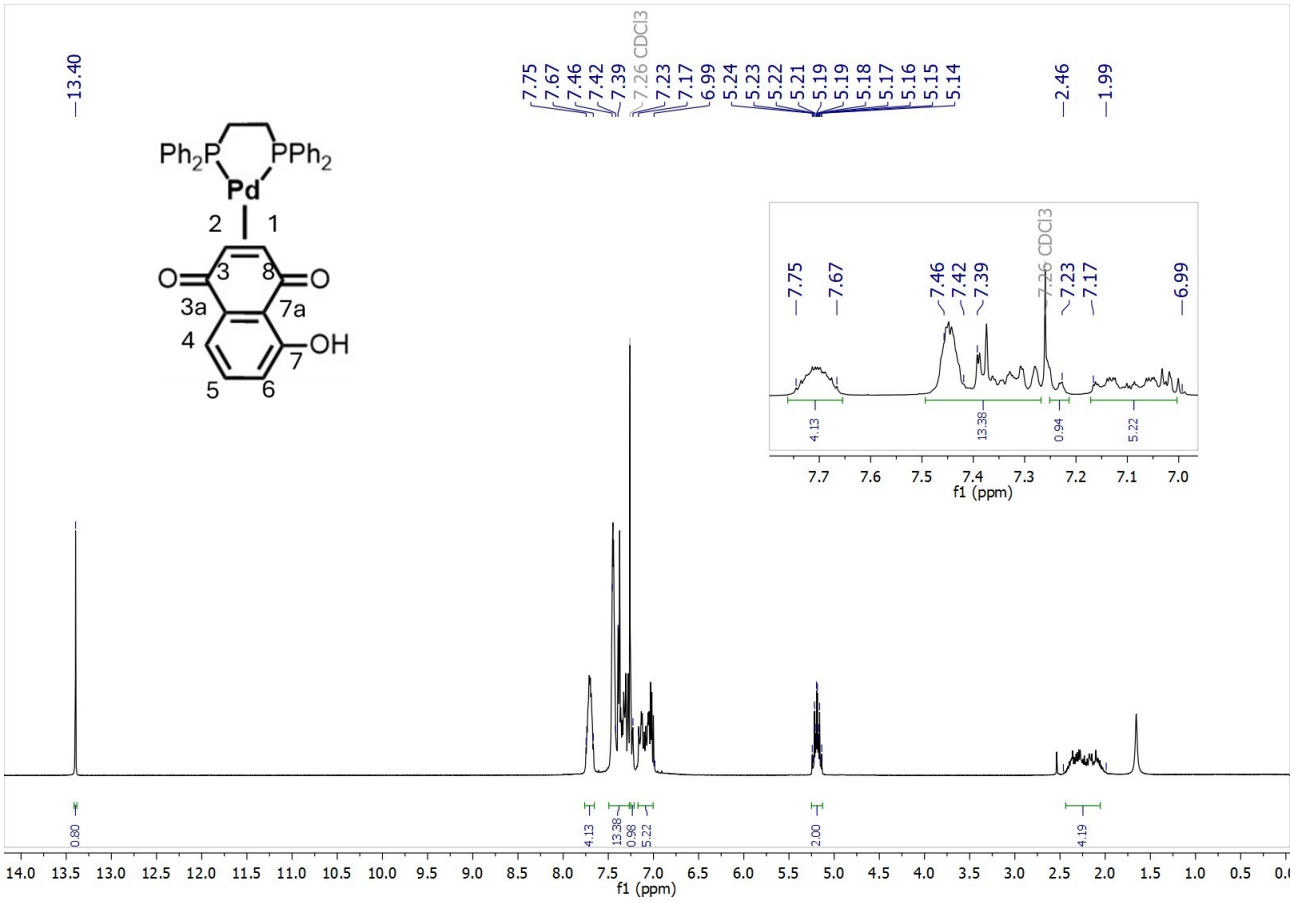

Figure **S4**. ^{1}H NMR spectrum of **1** in $CDCl_3$.

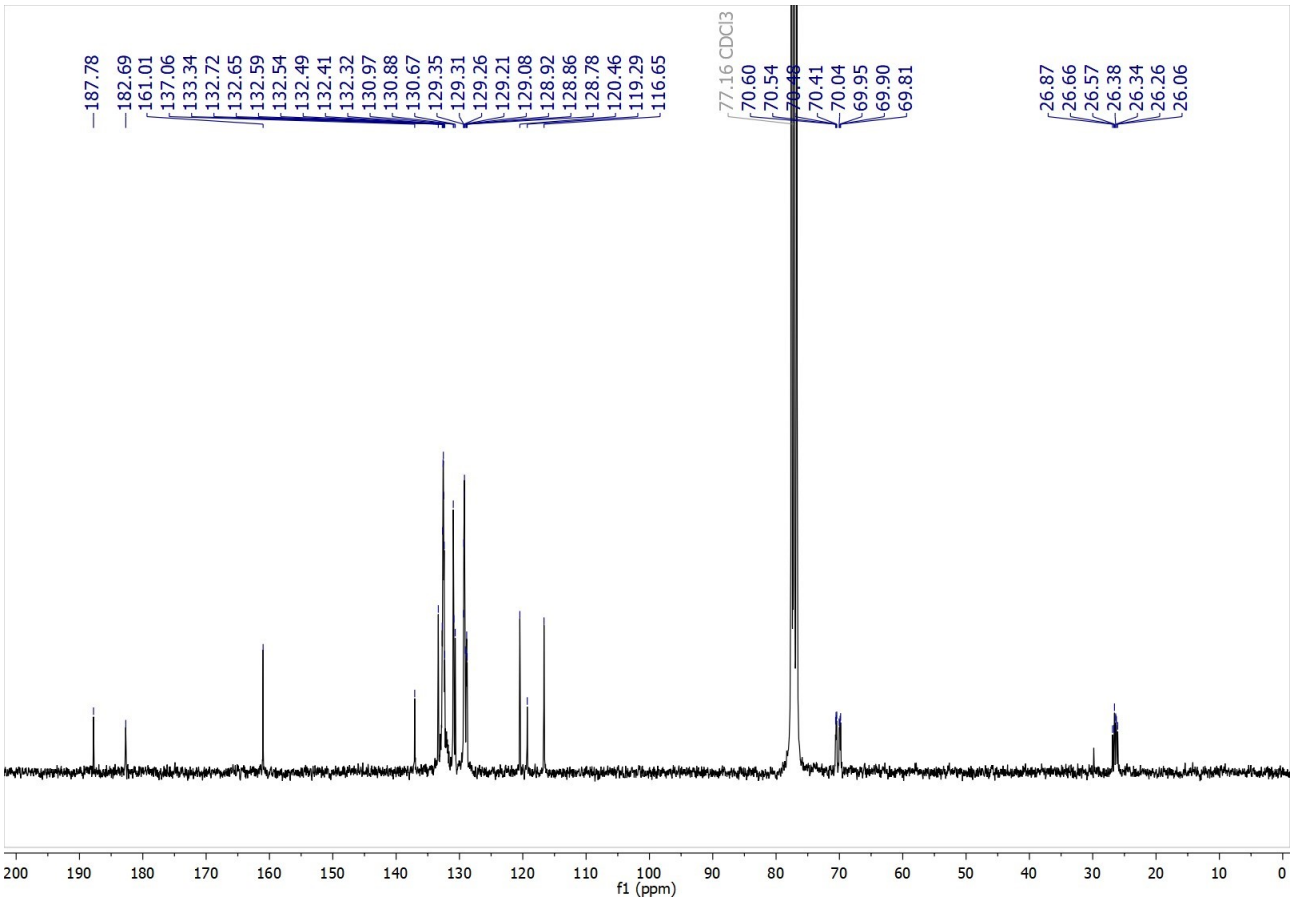

Figure **S5**. $^{13}C\{^{1}H\}$ NMR spectrum of **1** in $CDCl_3$.

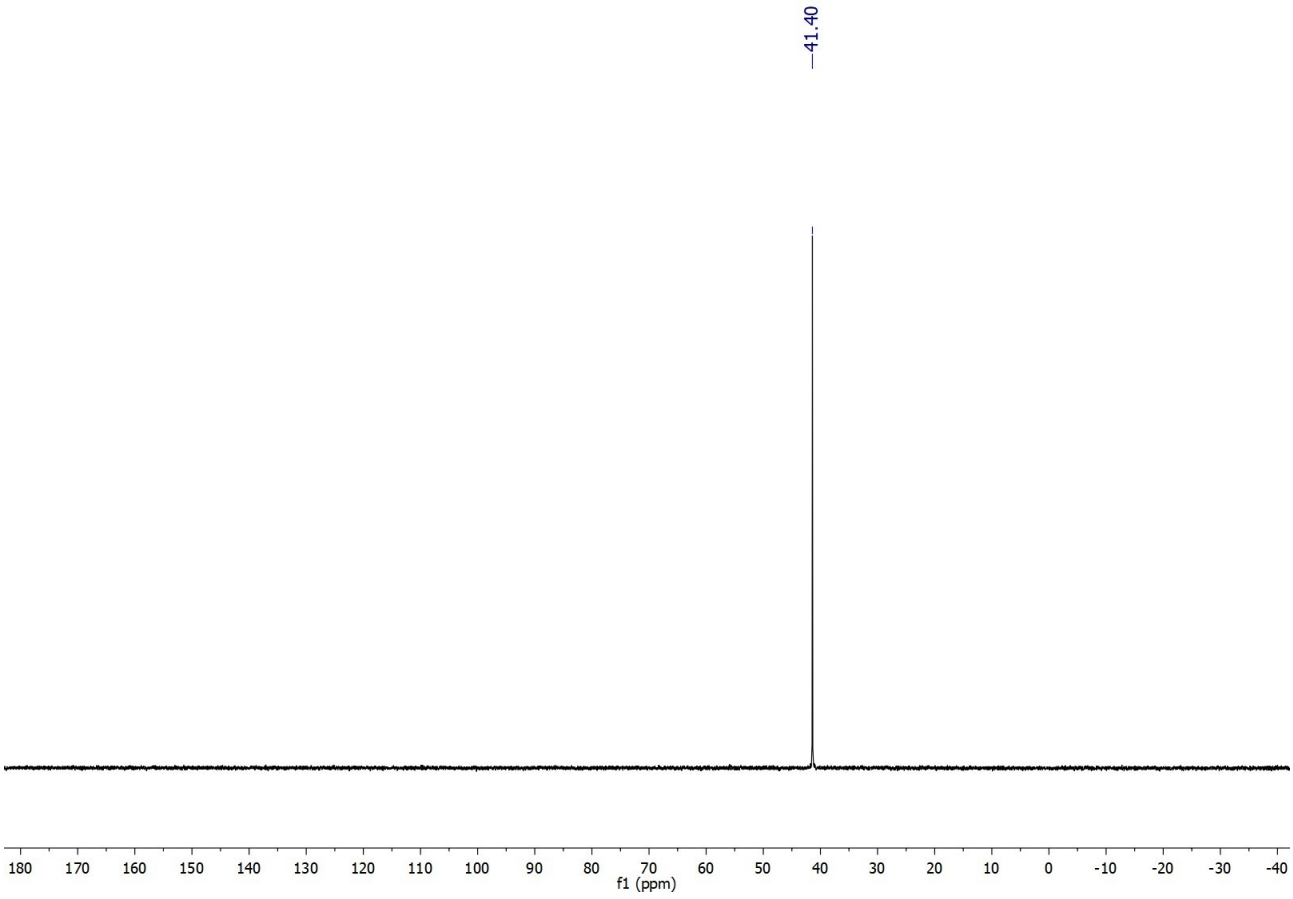

Figure **S6**. $^{31}P\{^{1}H\}$ NMR spectrum of **1** in $CDCl_3$.

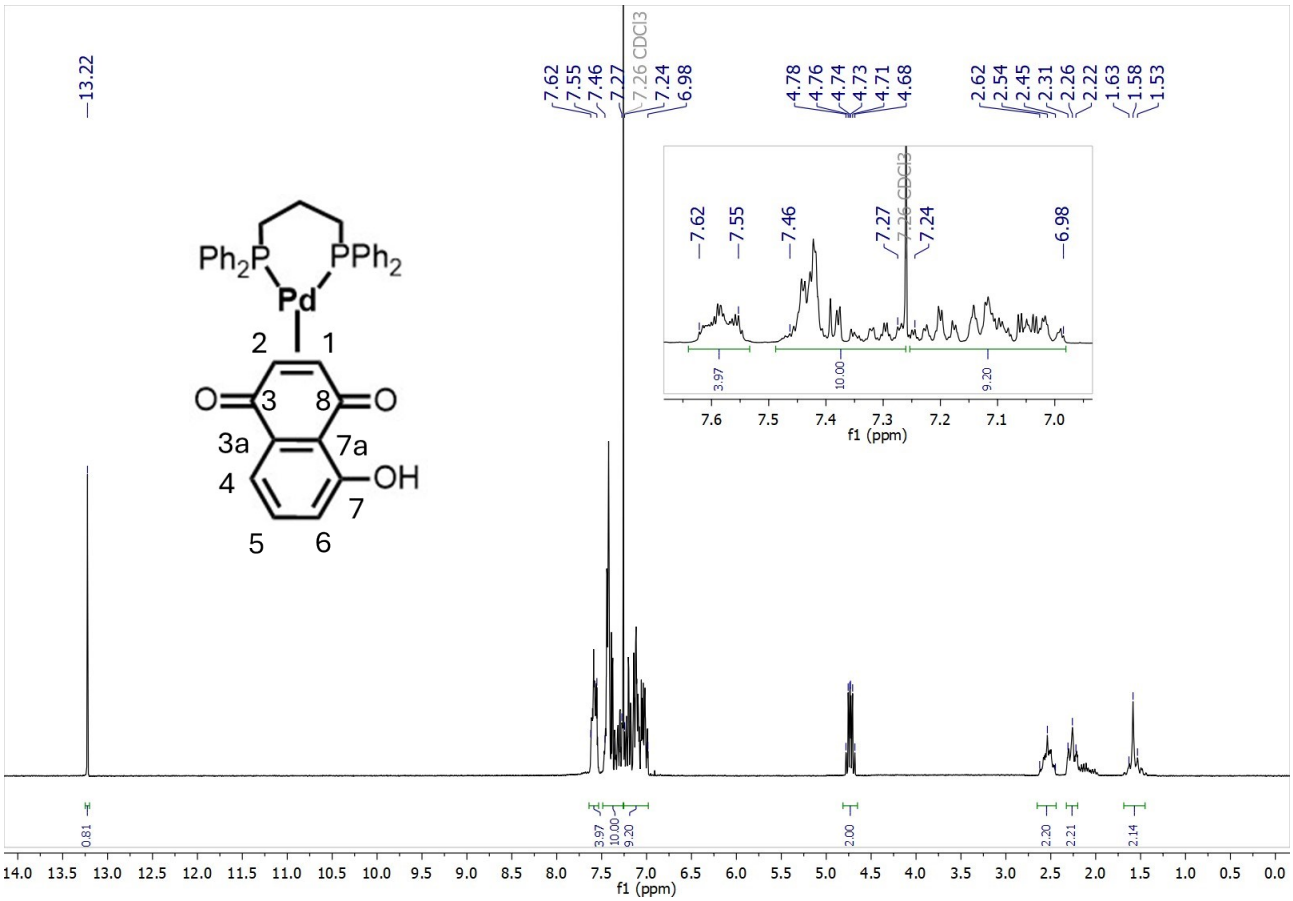

Figure **S7**. ^{1}H NMR spectrum of **2** in $CDCl_3$.

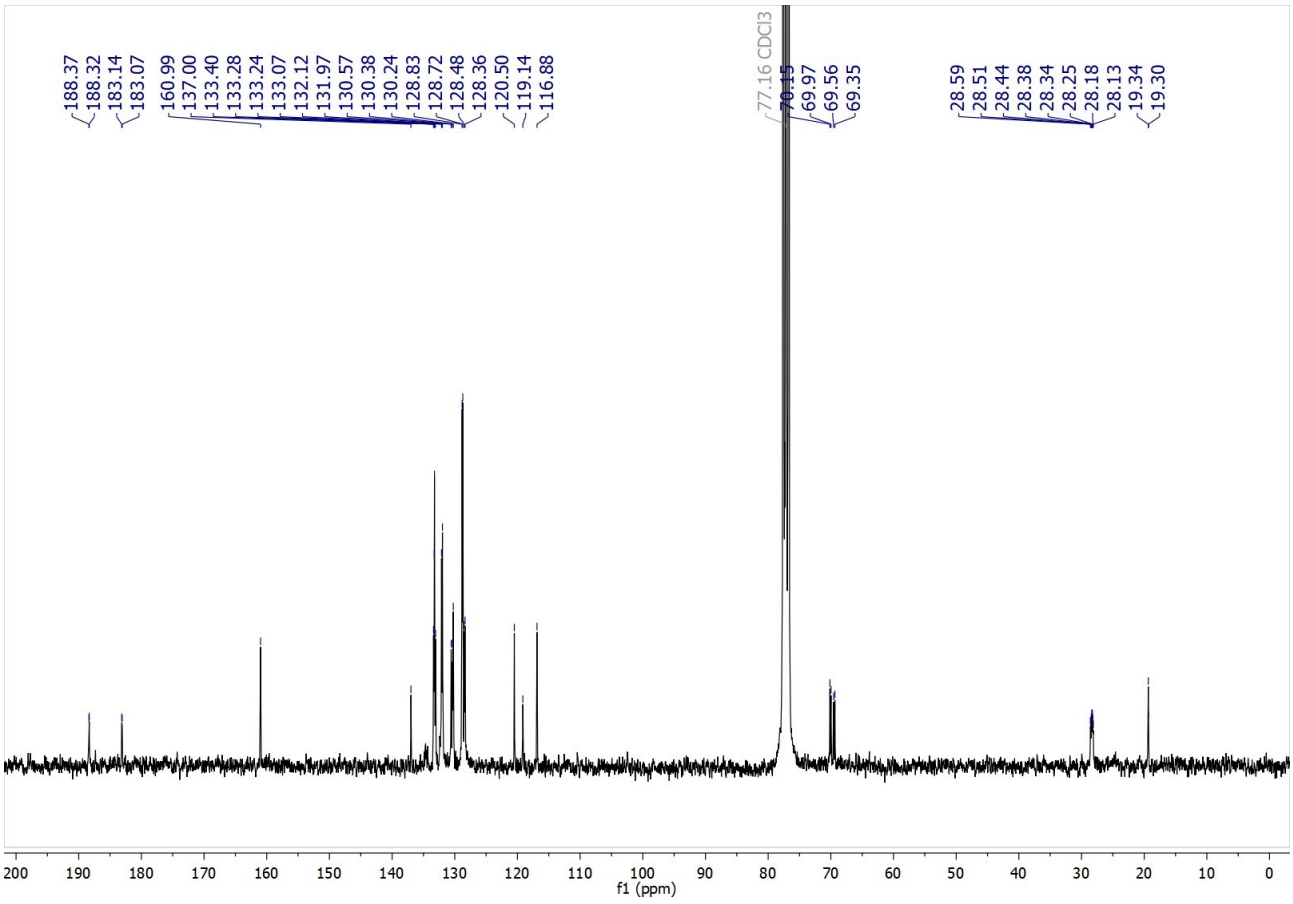

Figure **S8**. $^{13}C\{^{1}H\}$ NMR spectrum of **2** in $CDCl_3$.

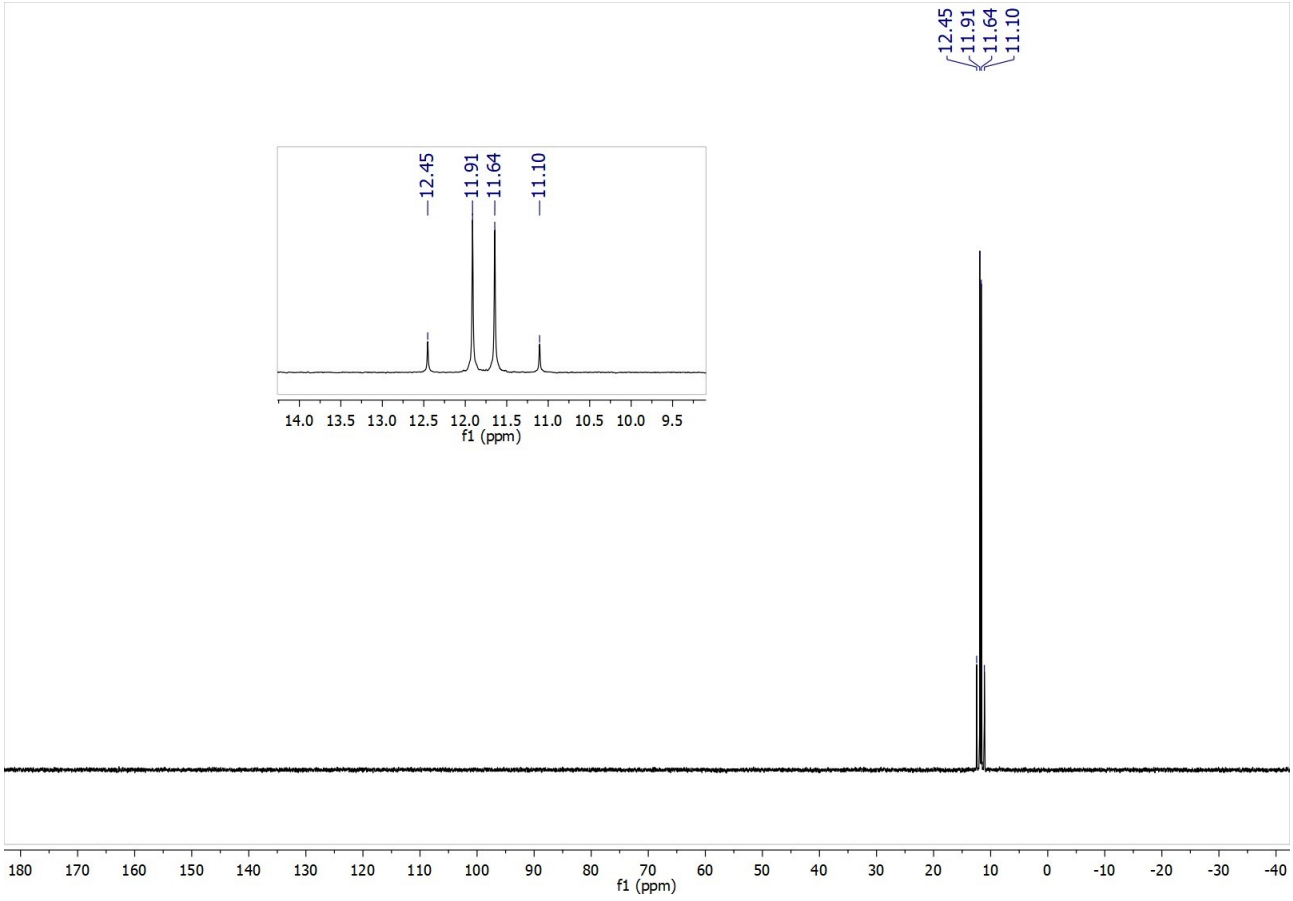

Figure **S9**. $^{31}P\{^{1}H\}$ NMR spectrum of **2** in $CDCl_3$.

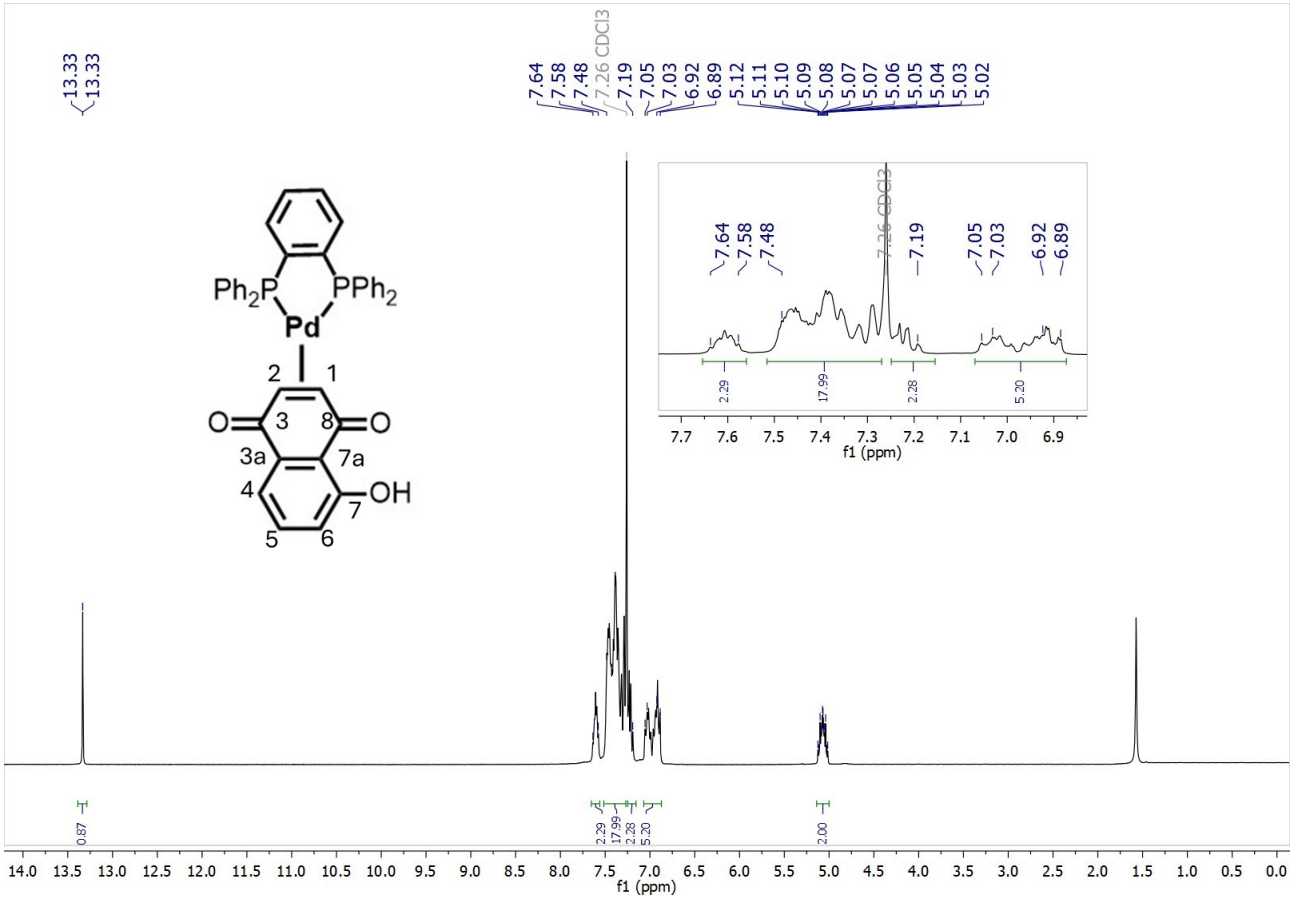

Figure **S10**. ^{1}H NMR spectrum of **3** in $CDCl_3$.

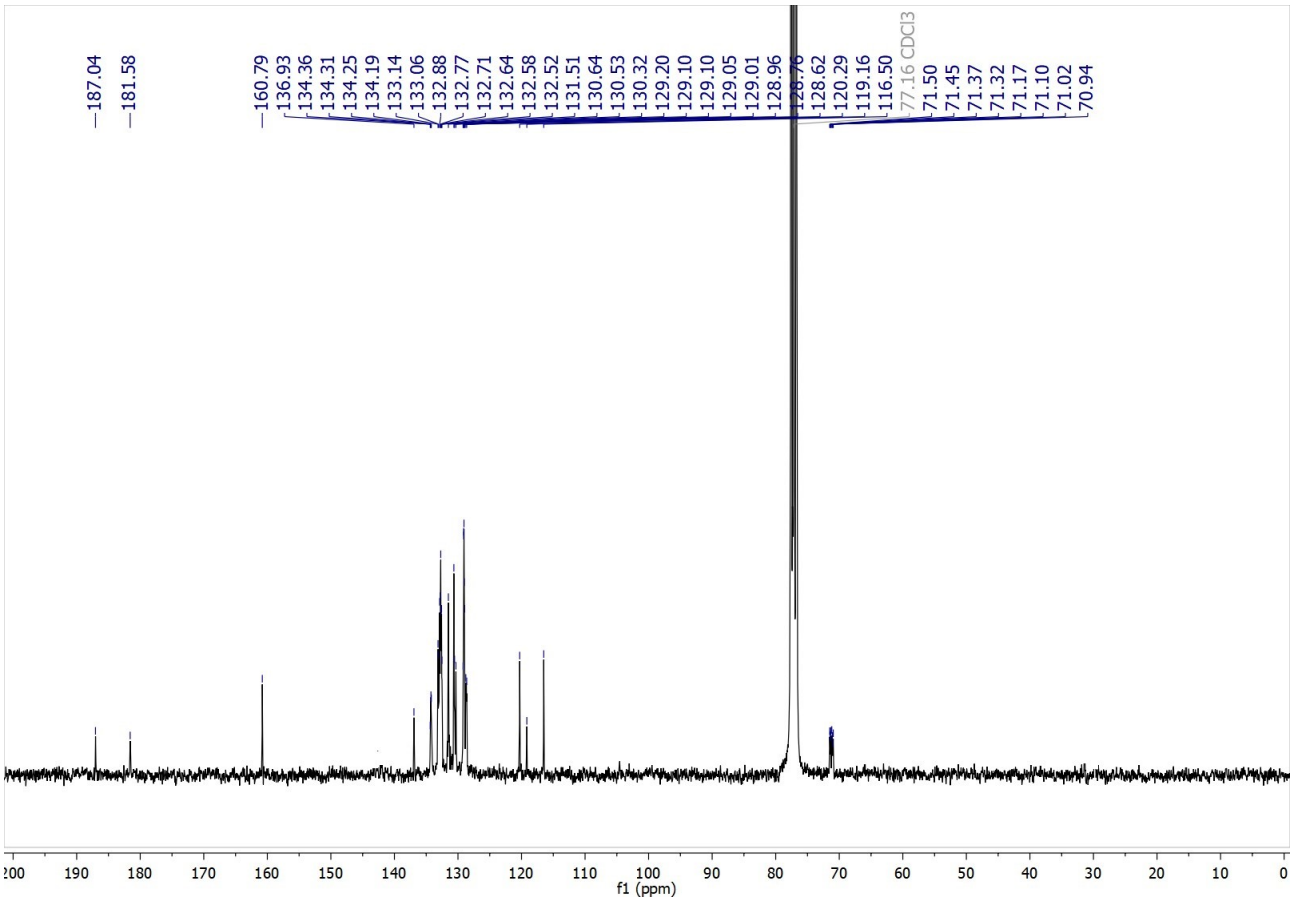

Figure **S11**. $^{13}C\{^{1}H\}$ NMR spectrum of **3** in $CDCl_3$.

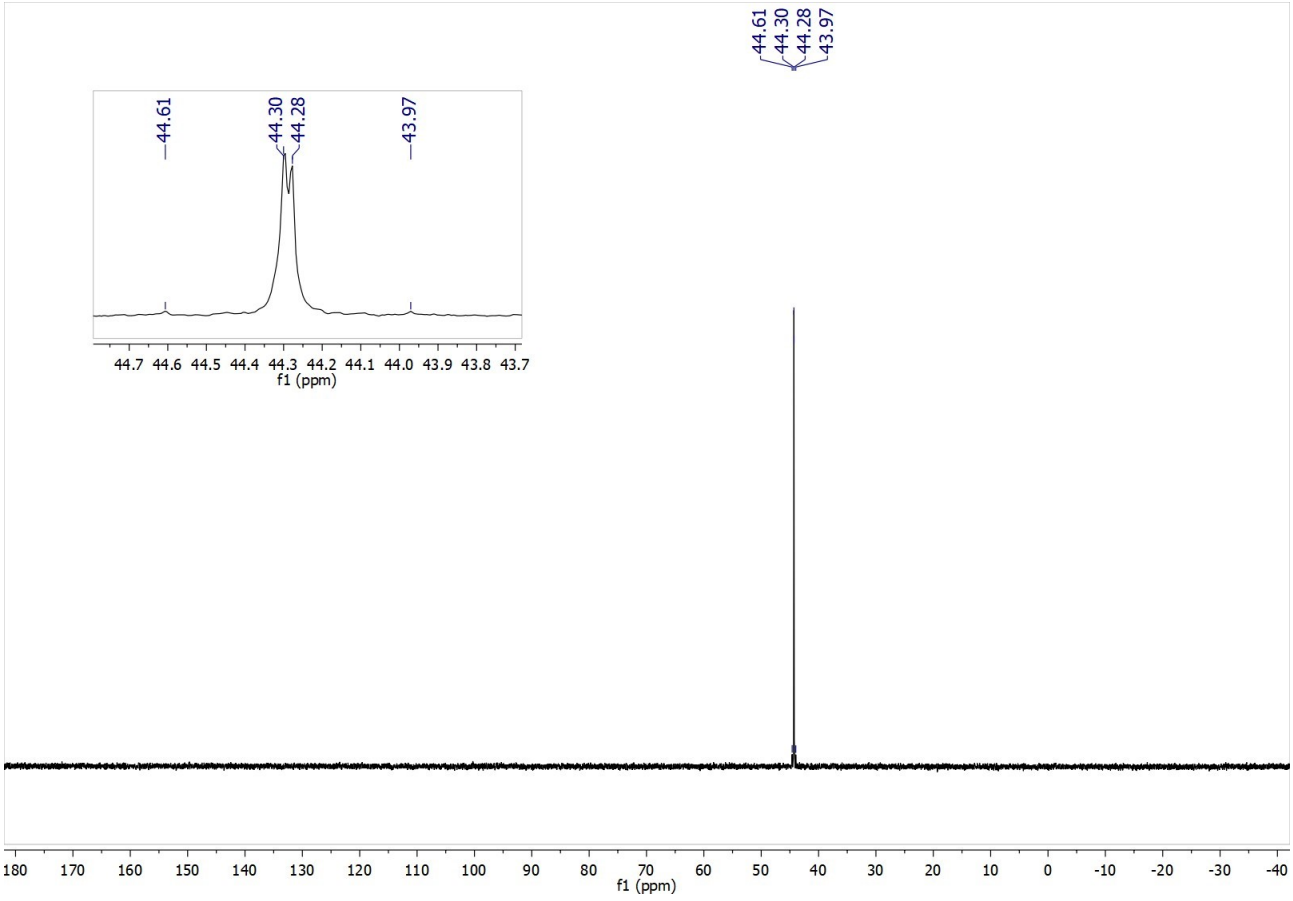

Figure **S12**. $^{31}P\{^{1}H\}$ NMR spectrum of **3** in $CDCl_3$.

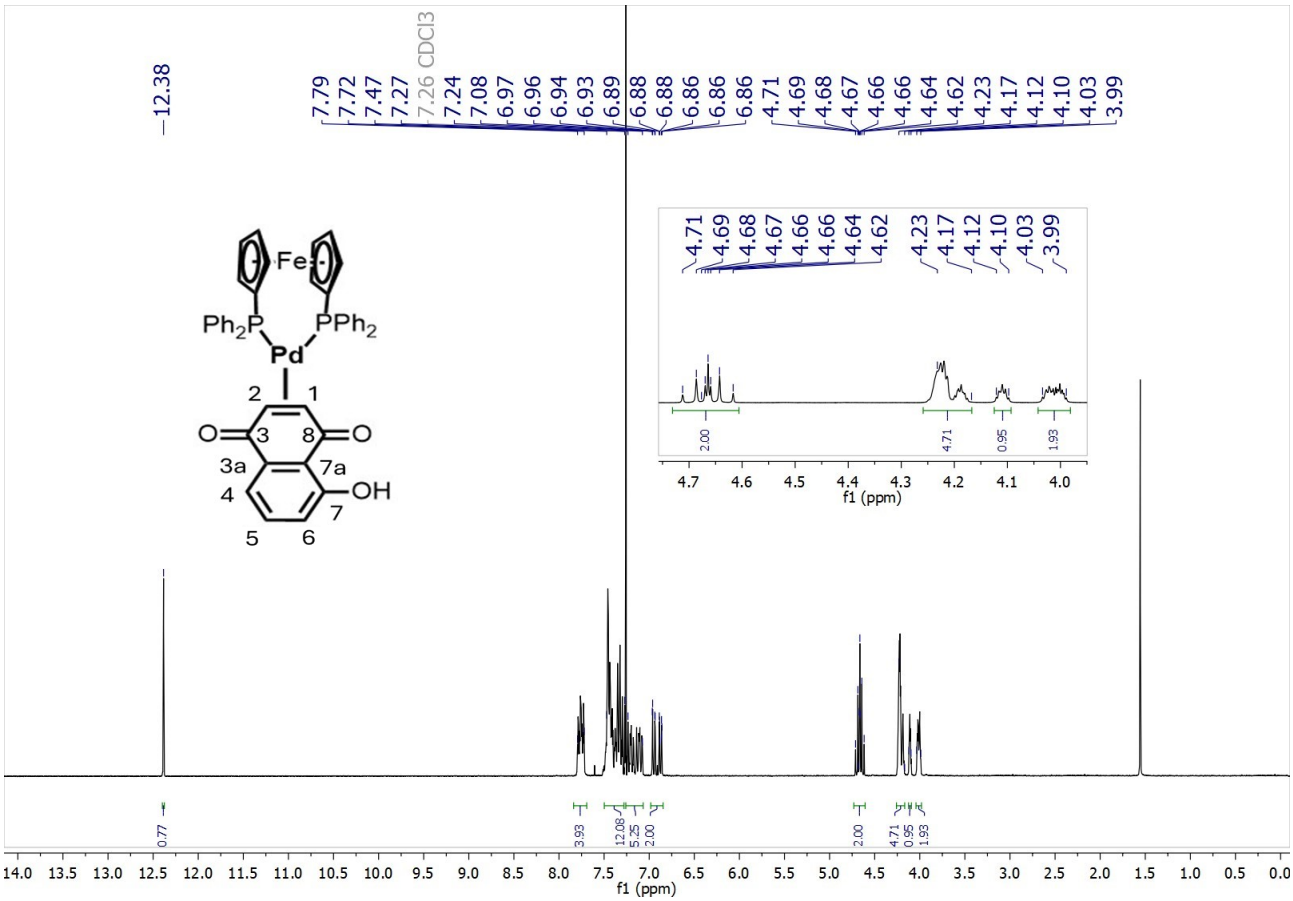

Figure **S13**. ^{1}H NMR spectrum of **4** in $CDCl_3$.

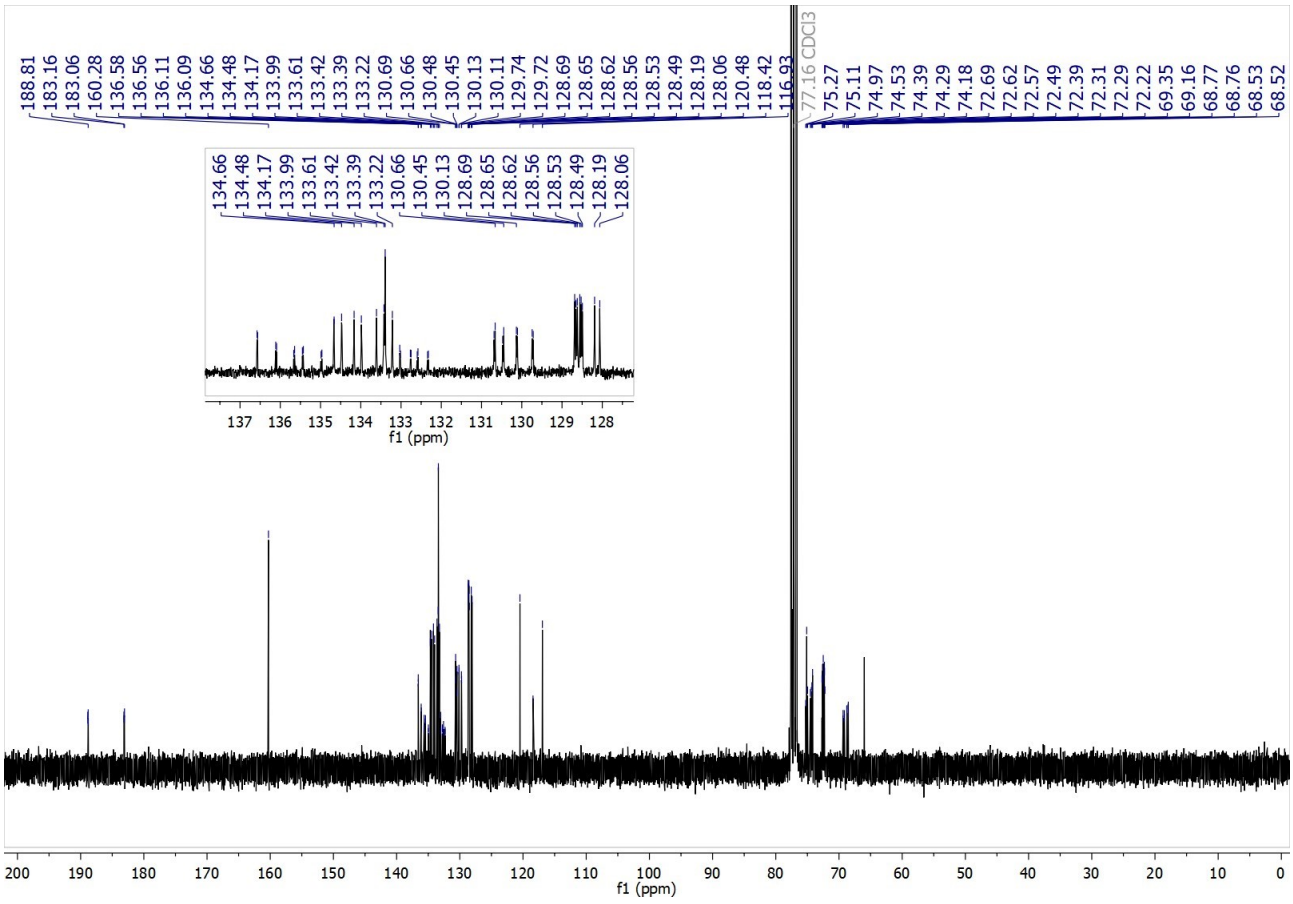

Figure **S14**. $^{13}C\{^{1}H\}$ NMR spectrum of **4** in $CDCl_3$.

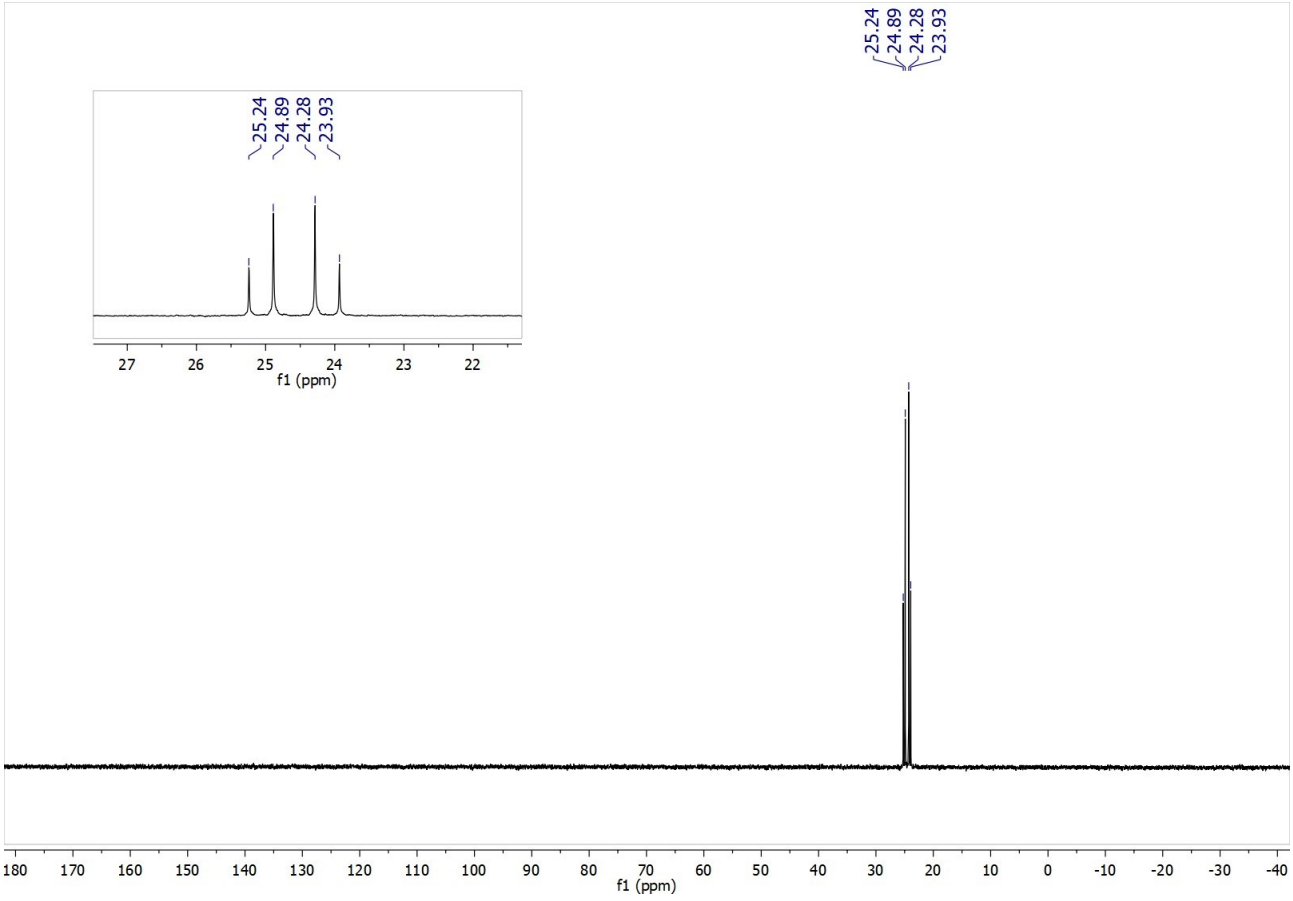

Figure **S15**. $^{31}P\{^{1}H\}$ NMR spectrum of **4** in $CDCl_3$.

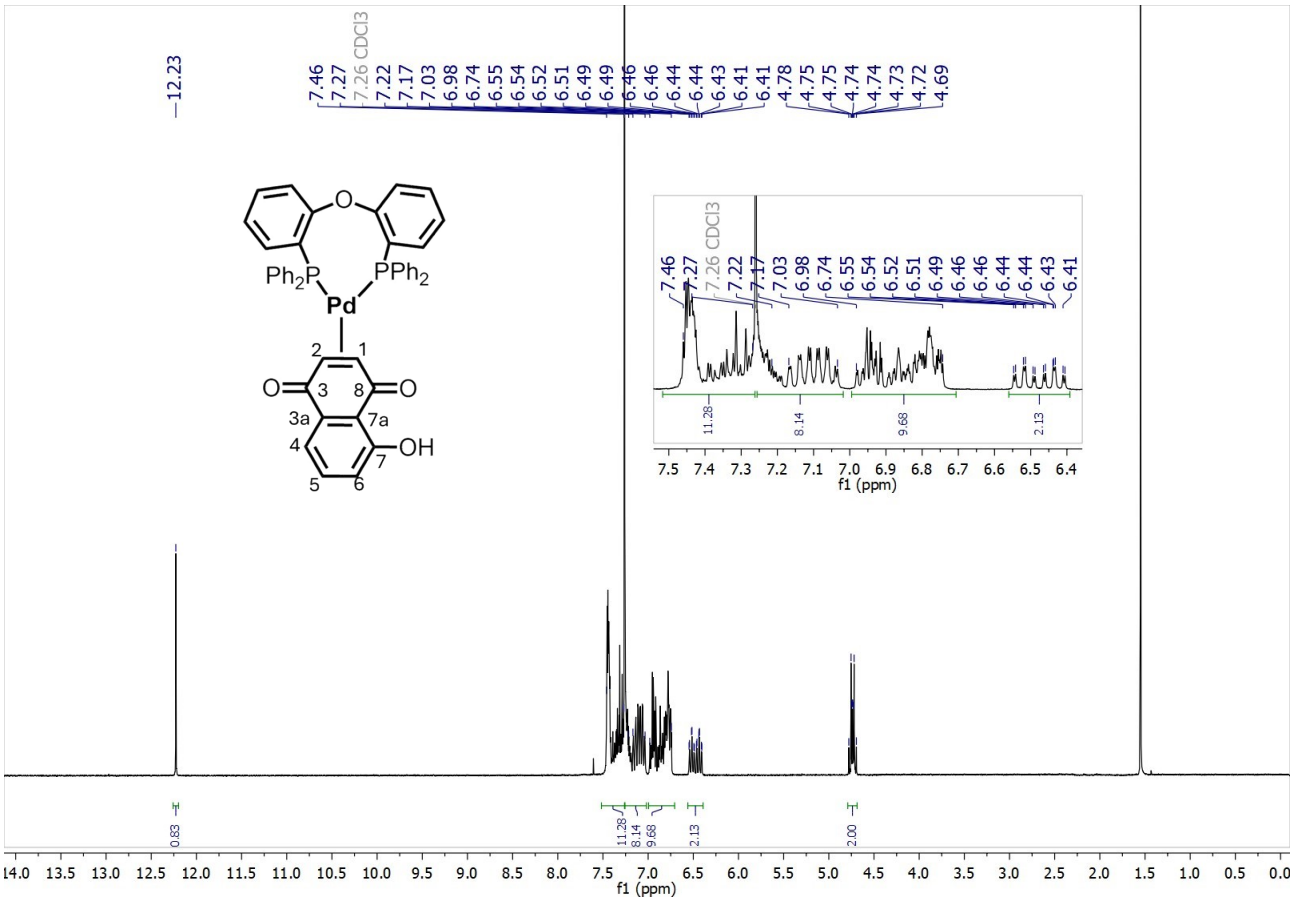

Figure **S16**. ^{1}H NMR spectrum of **5** in $CDCl_3$.

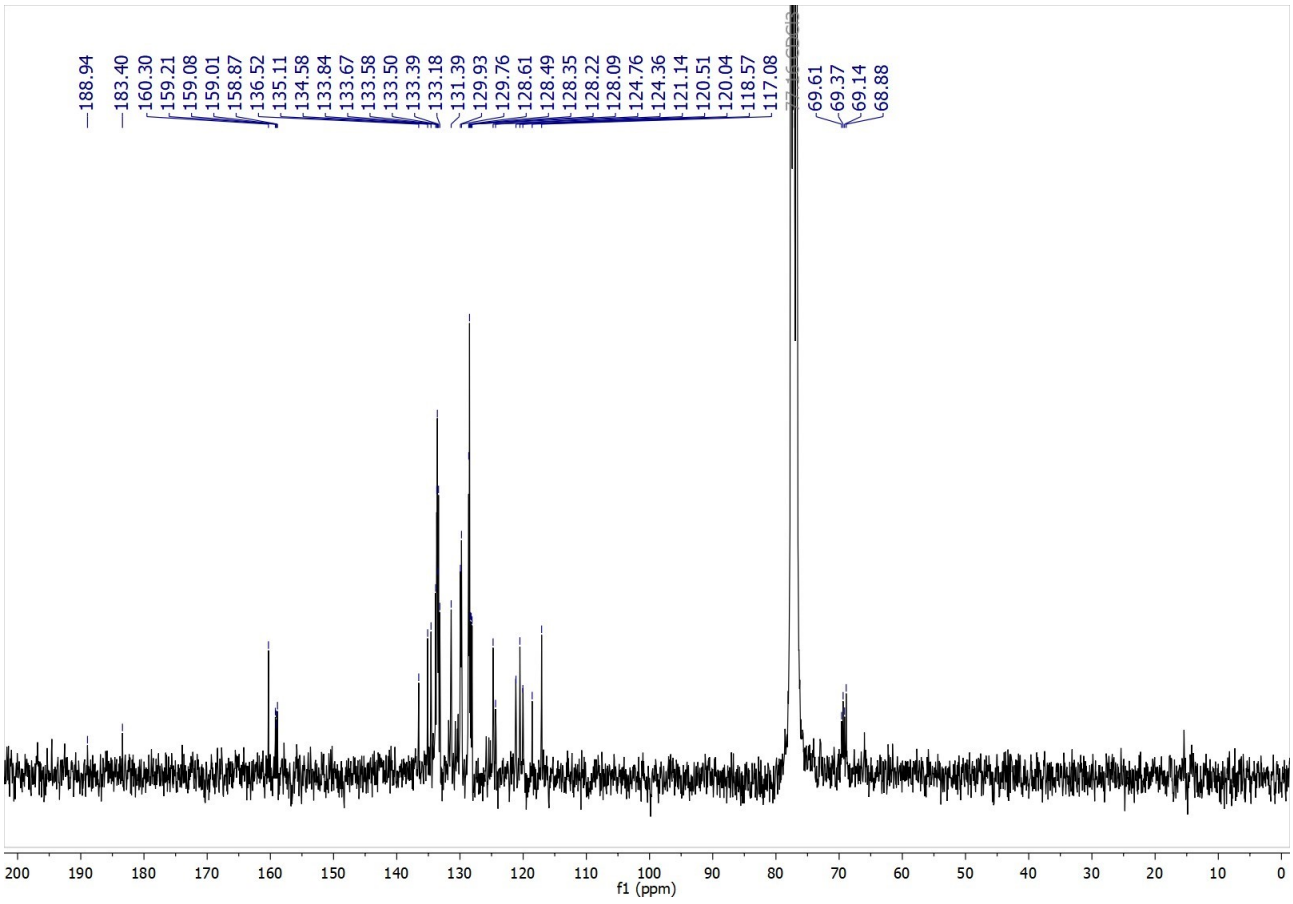

Figure **S17**. $^{13}C\{^{1}H\}$ NMR spectrum of **5** in $CDCl_3$.

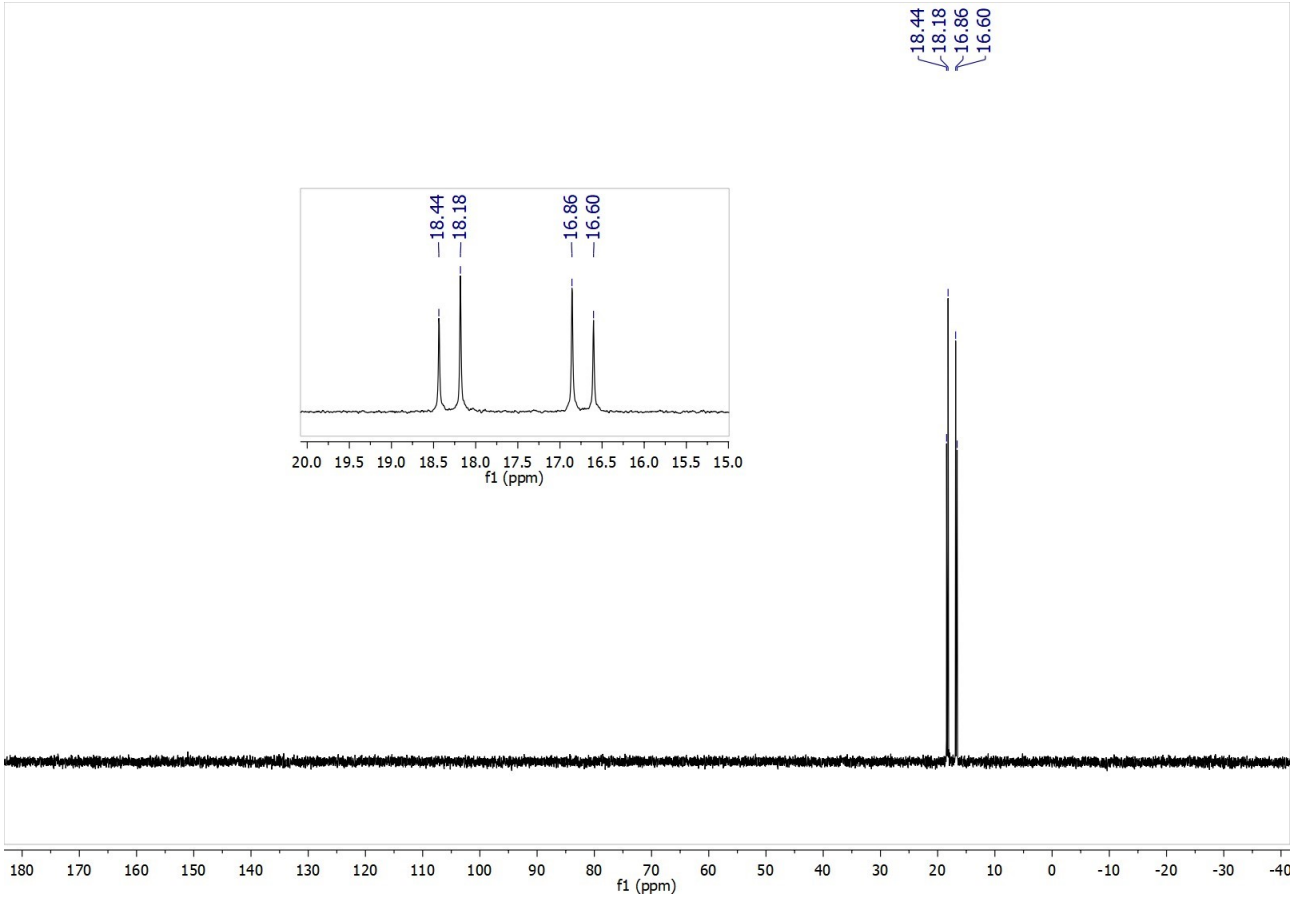

Figure **S18**. $^{31}P\{^{1}H\}$ NMR spectrum of **5** in $CDCl_3$.

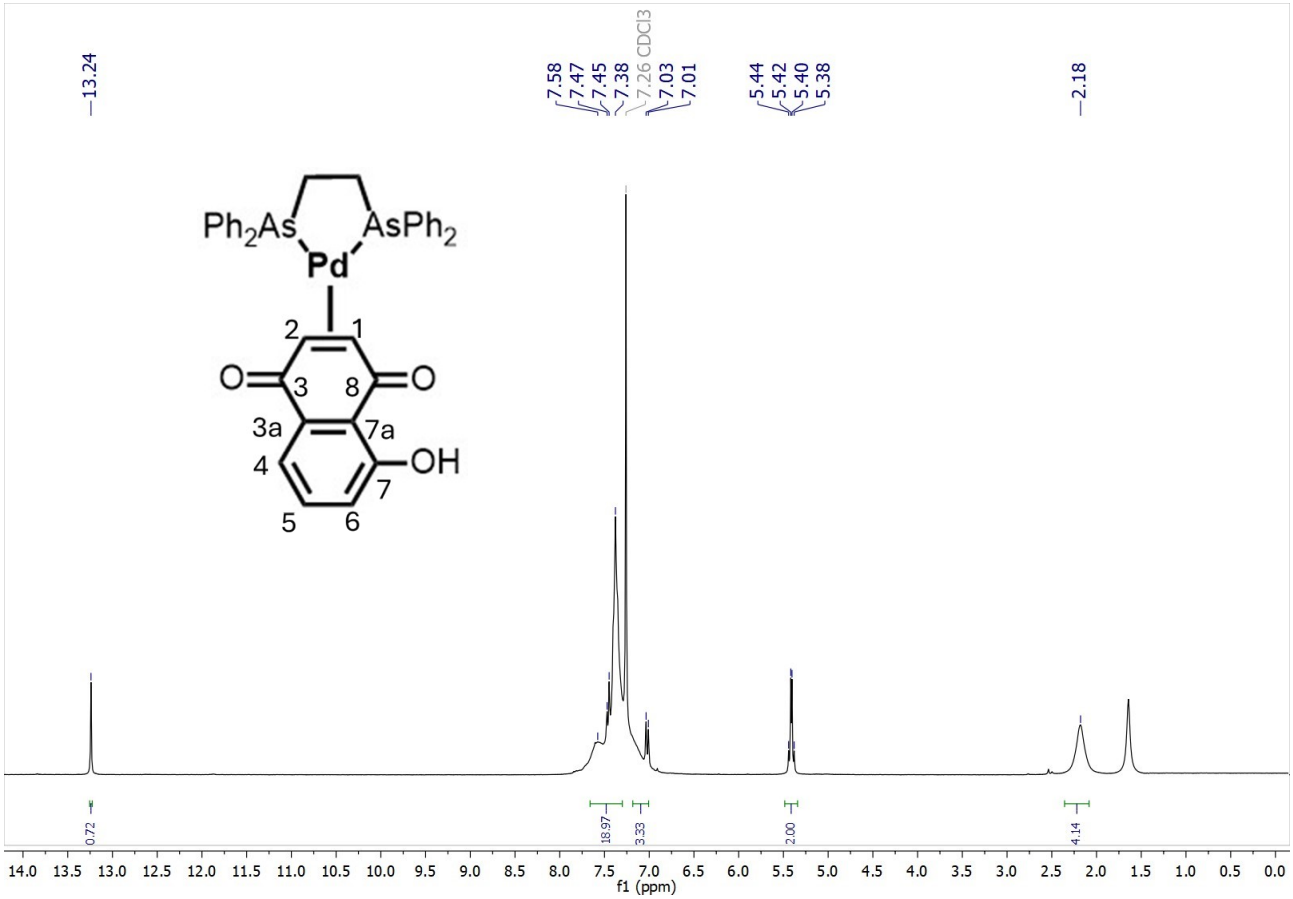

Figure **S19**. ^{1}H NMR spectrum of **6** in $CDCl_3$.

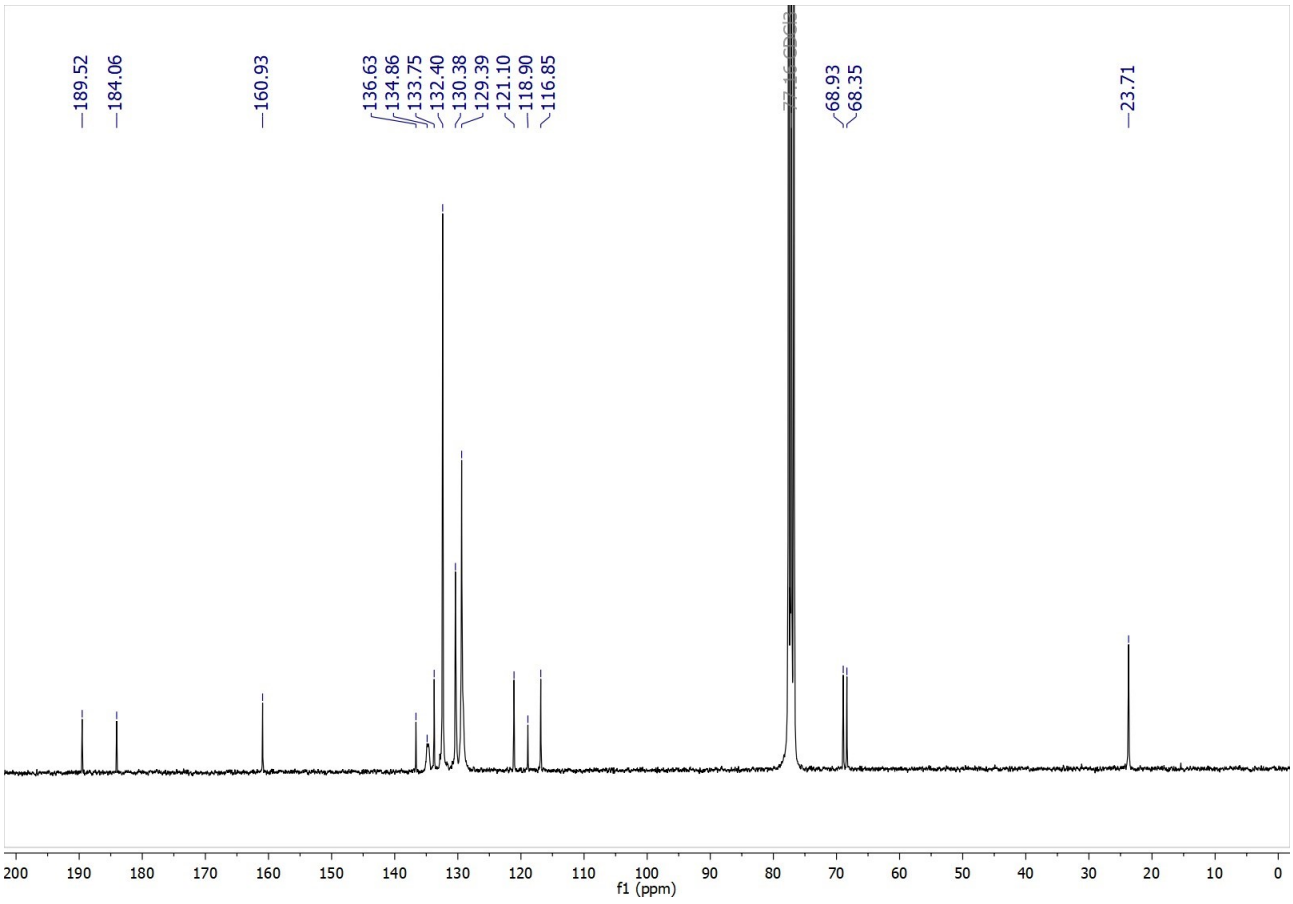

Figure **S20**. $^{13}C\{^{1}H\}$ NMR spectrum of **6** in $CDCl_3$.

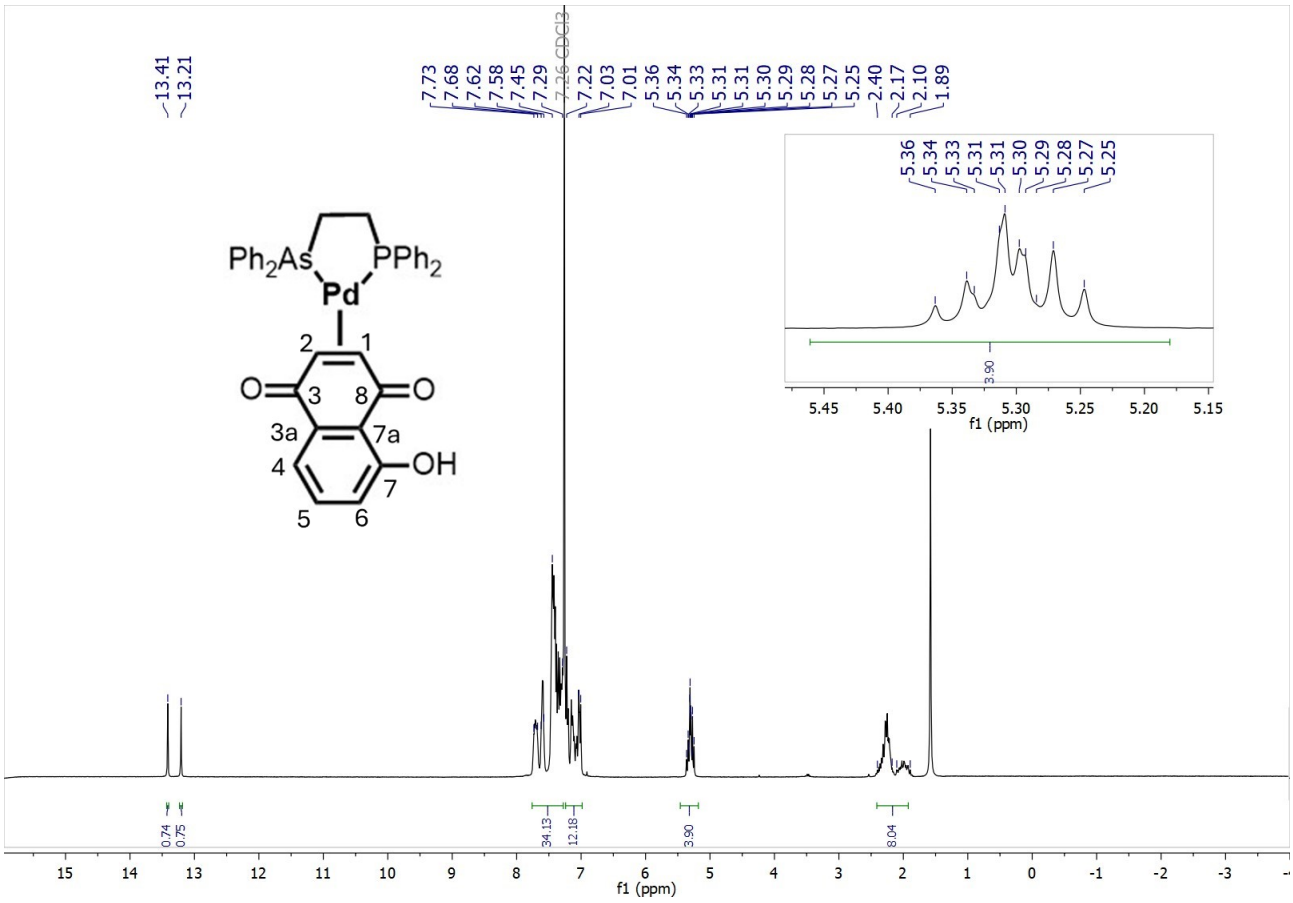

Figure **S21**. ^{1}H NMR spectrum of **7** in $CDCl_3$.

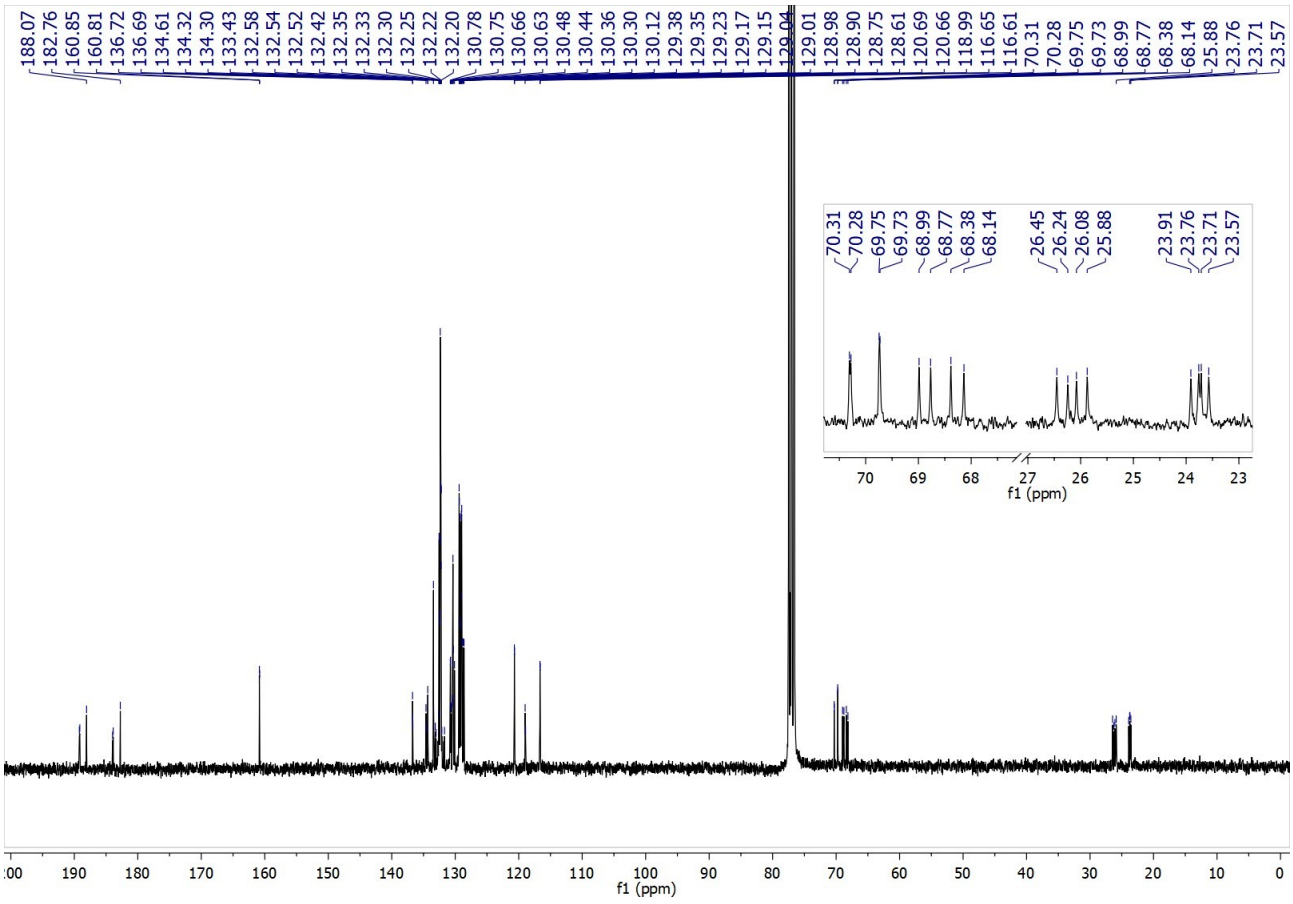

Figure **S22**. $^{13}C\{^{1}H\}$ NMR spectrum of **7** in $CDCl_3$.

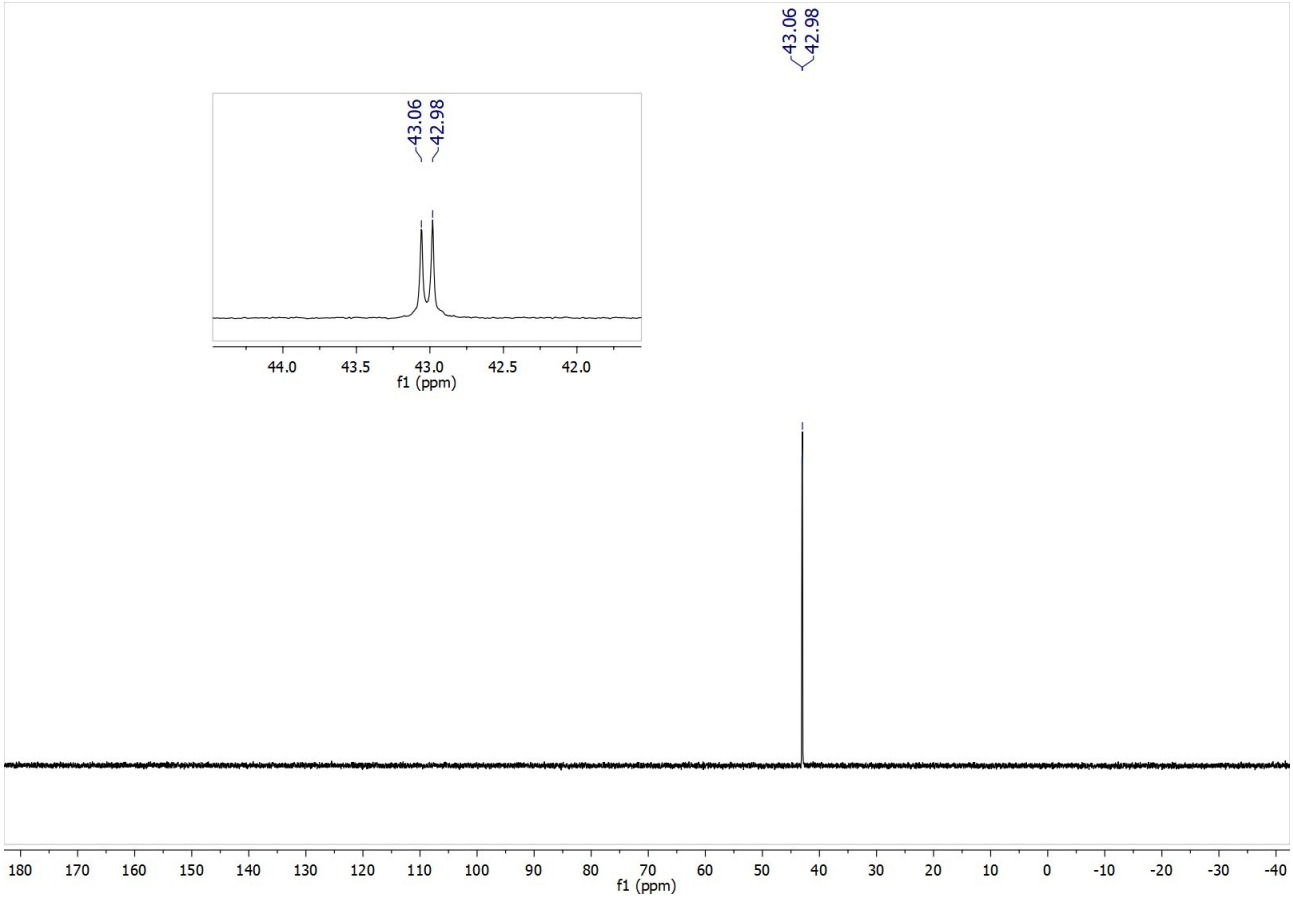

Figure **S23**. $^{31}P\{^{1}H\}$ NMR spectrum of **7** in $CDCl_3$.

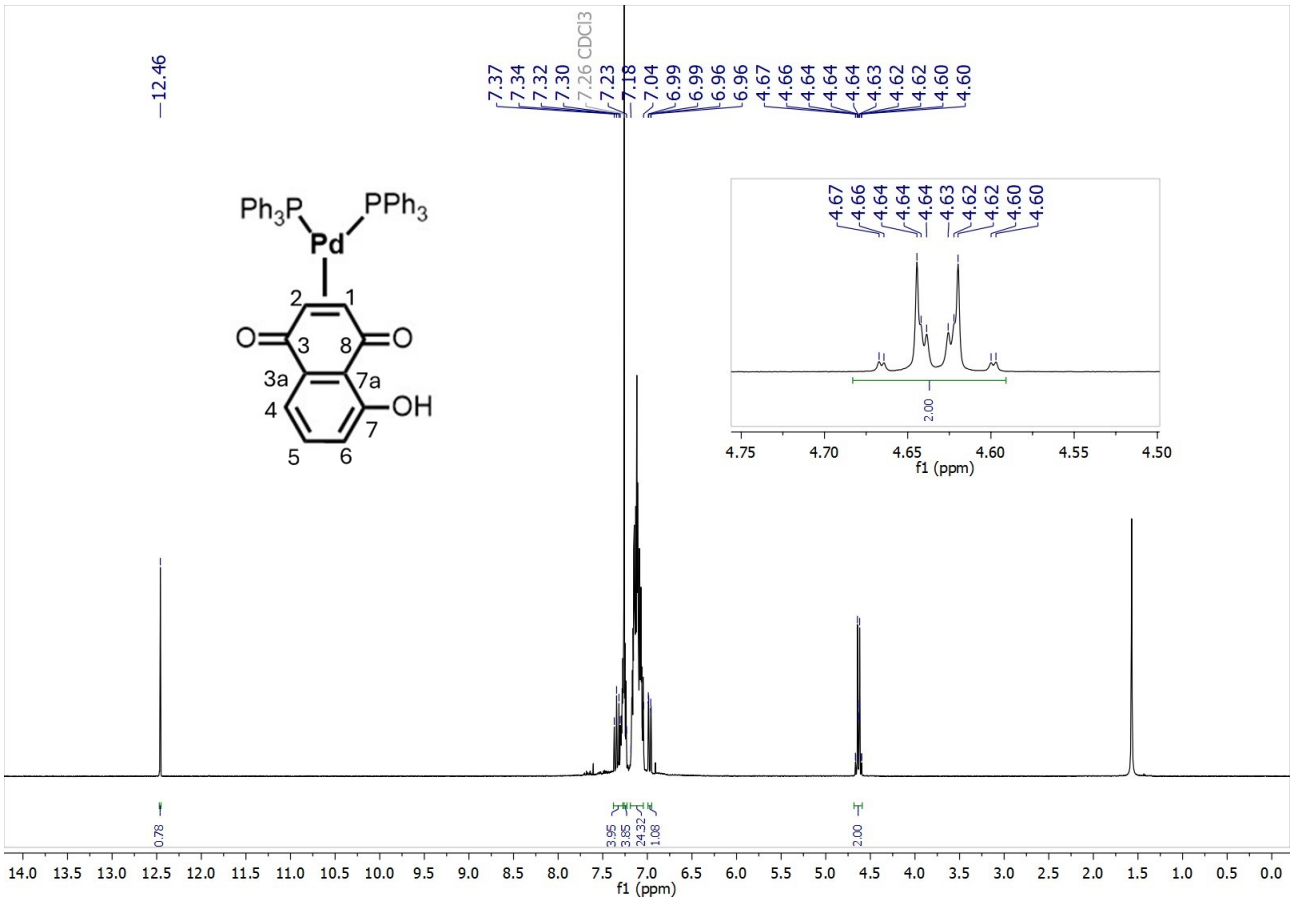

Figure **S24**. ^{1}H NMR spectrum of **8** in $CDCl_3$.

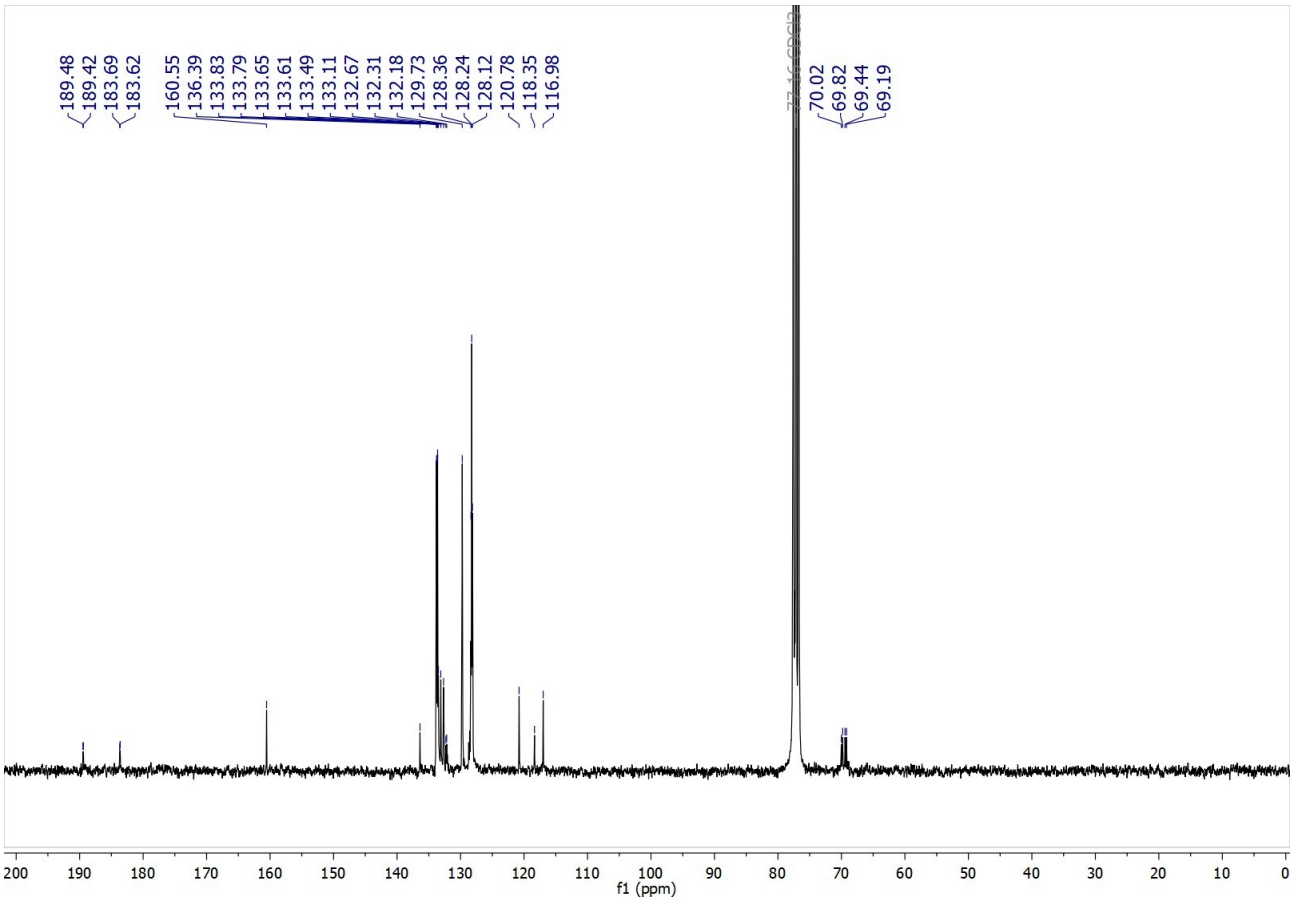

Figure **S25**. $^{13}C\{^{1}H\}$ NMR spectrum of **8** in $CDCl_3$.

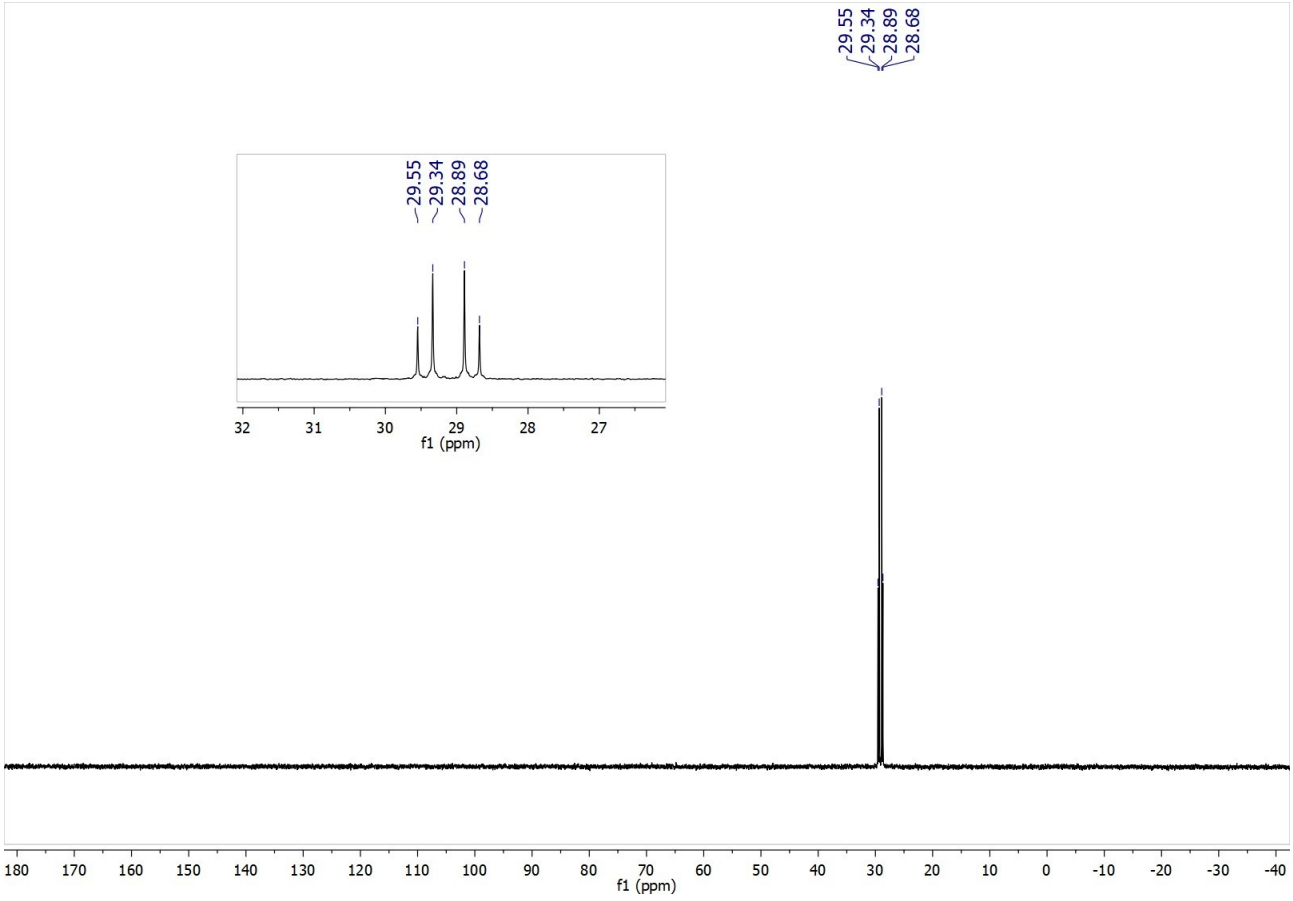

Figure **S26**. $^{31}P\{^{1}H\}$ NMR spectrum of **8** in $CDCl_3$.

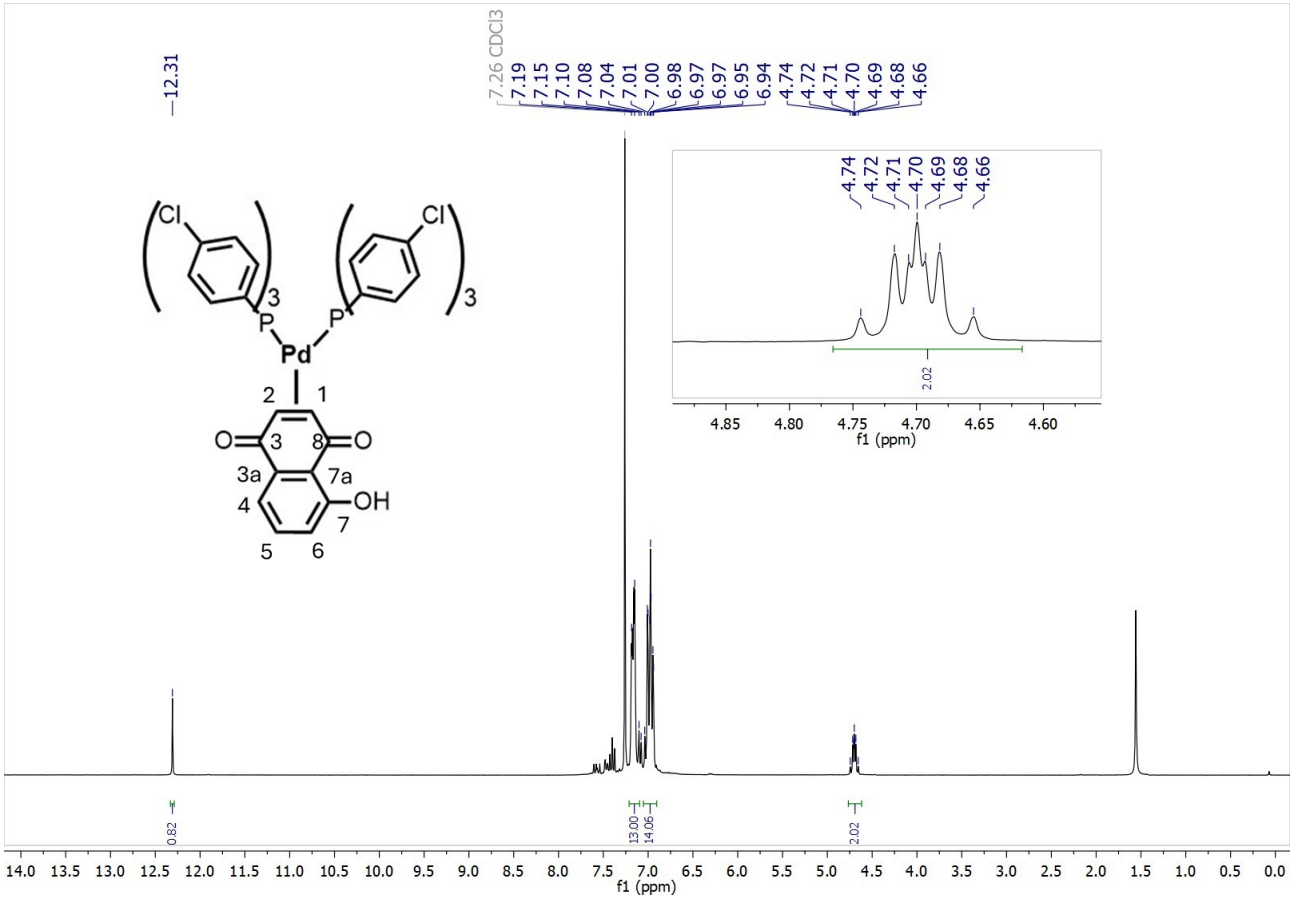

Figure **S27**. ^{1}H NMR spectrum of **9** in $CDCl_3$.

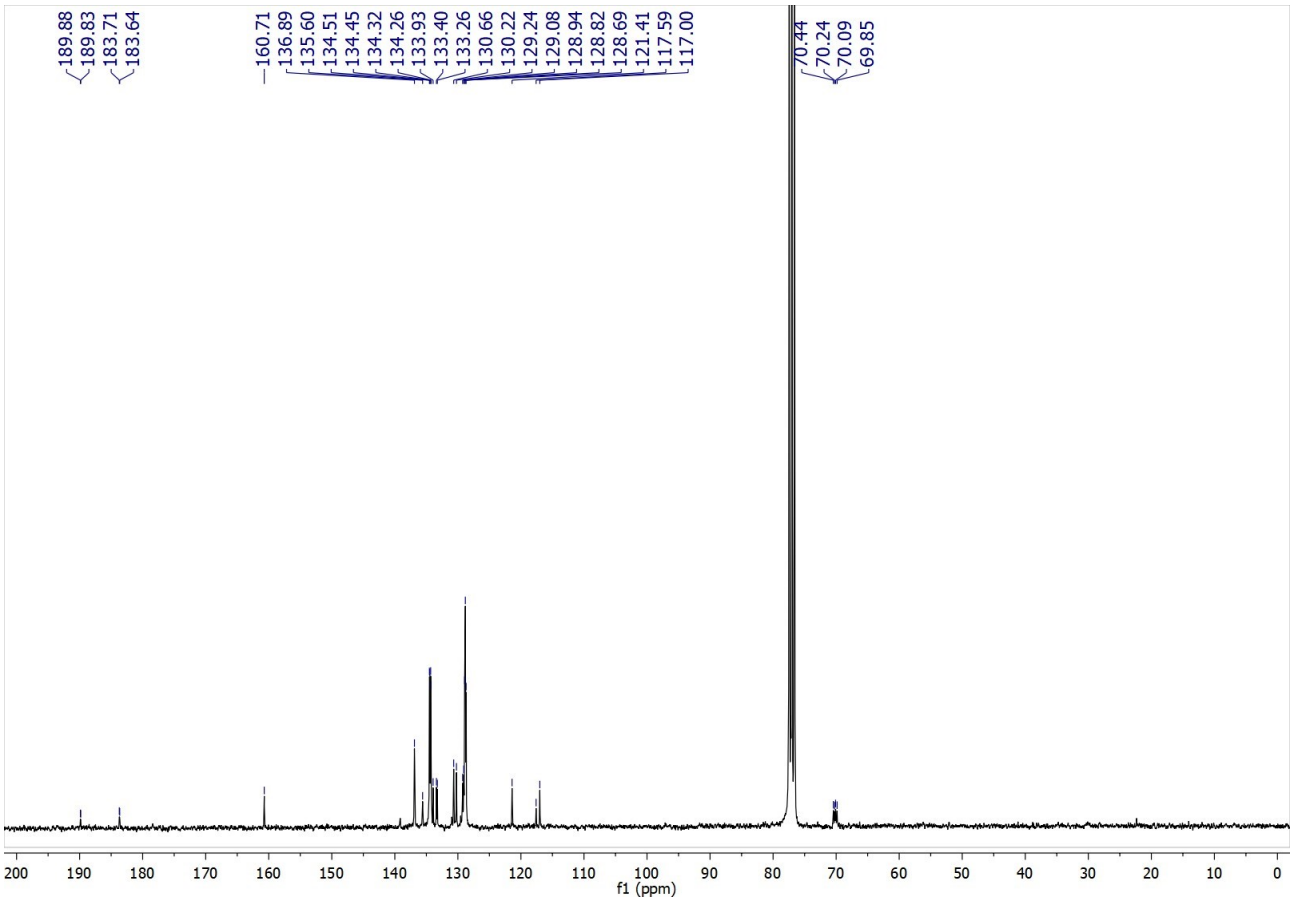

Figure **S28**. $^{13}C\{^{1}H\}$ NMR spectrum of **9** in $CDCl_3$.

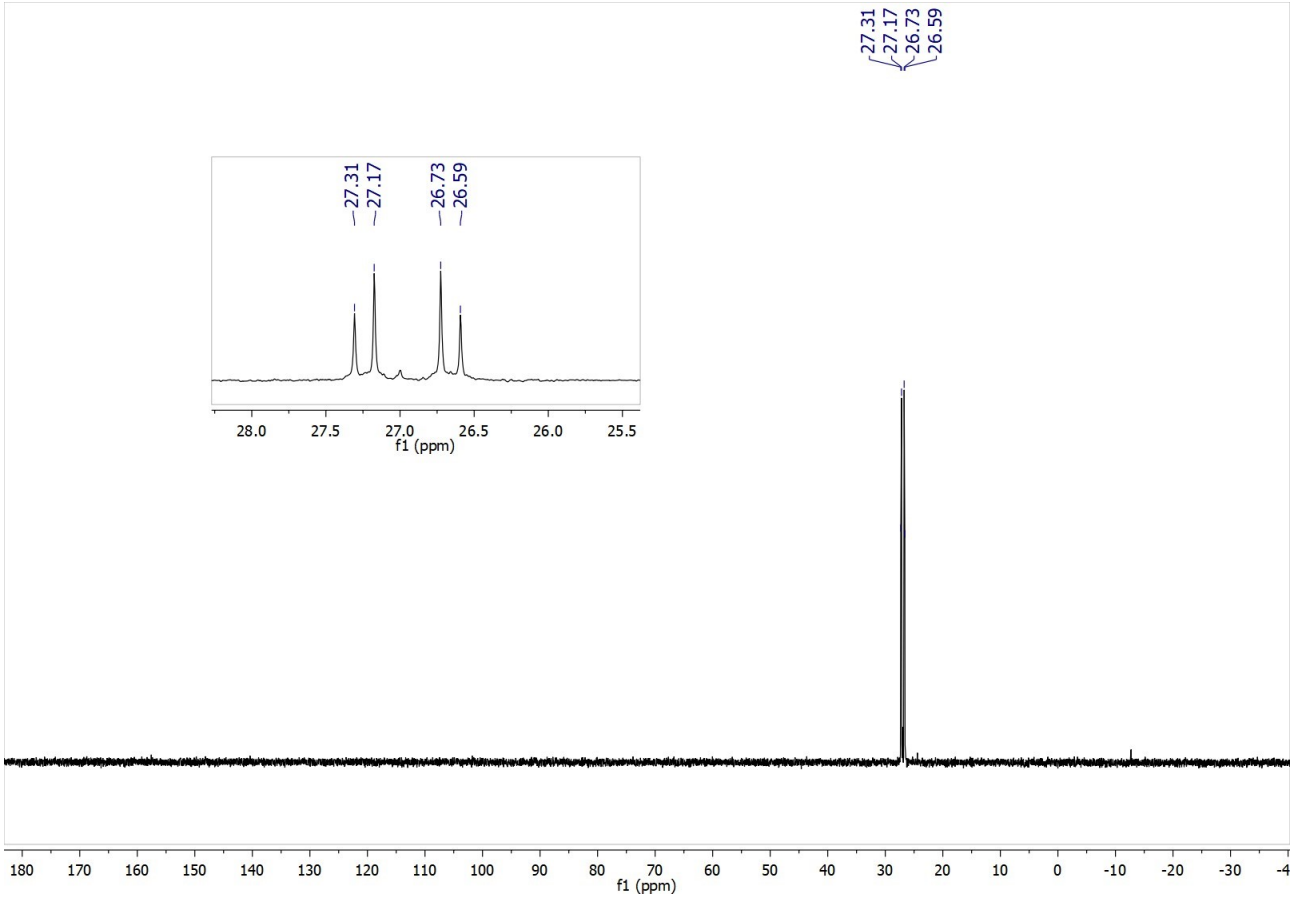

Figure **S29**. $^{31}P\{^{1}H\}$ NMR spectrum of **9** in $CDCl_3$.

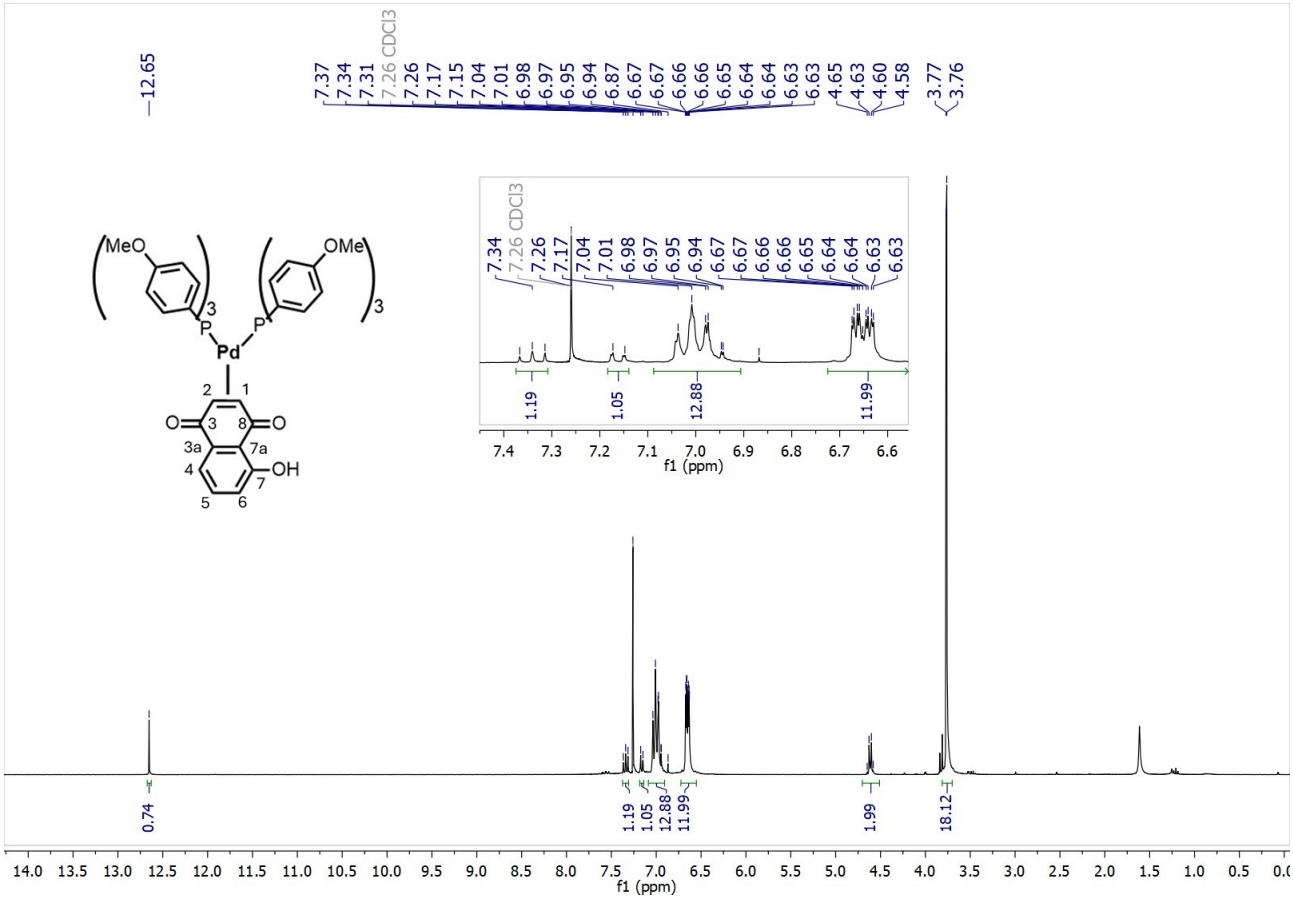

Figure **S30**. ^{1}H NMR spectrum of **10** in $CDCl_3$.

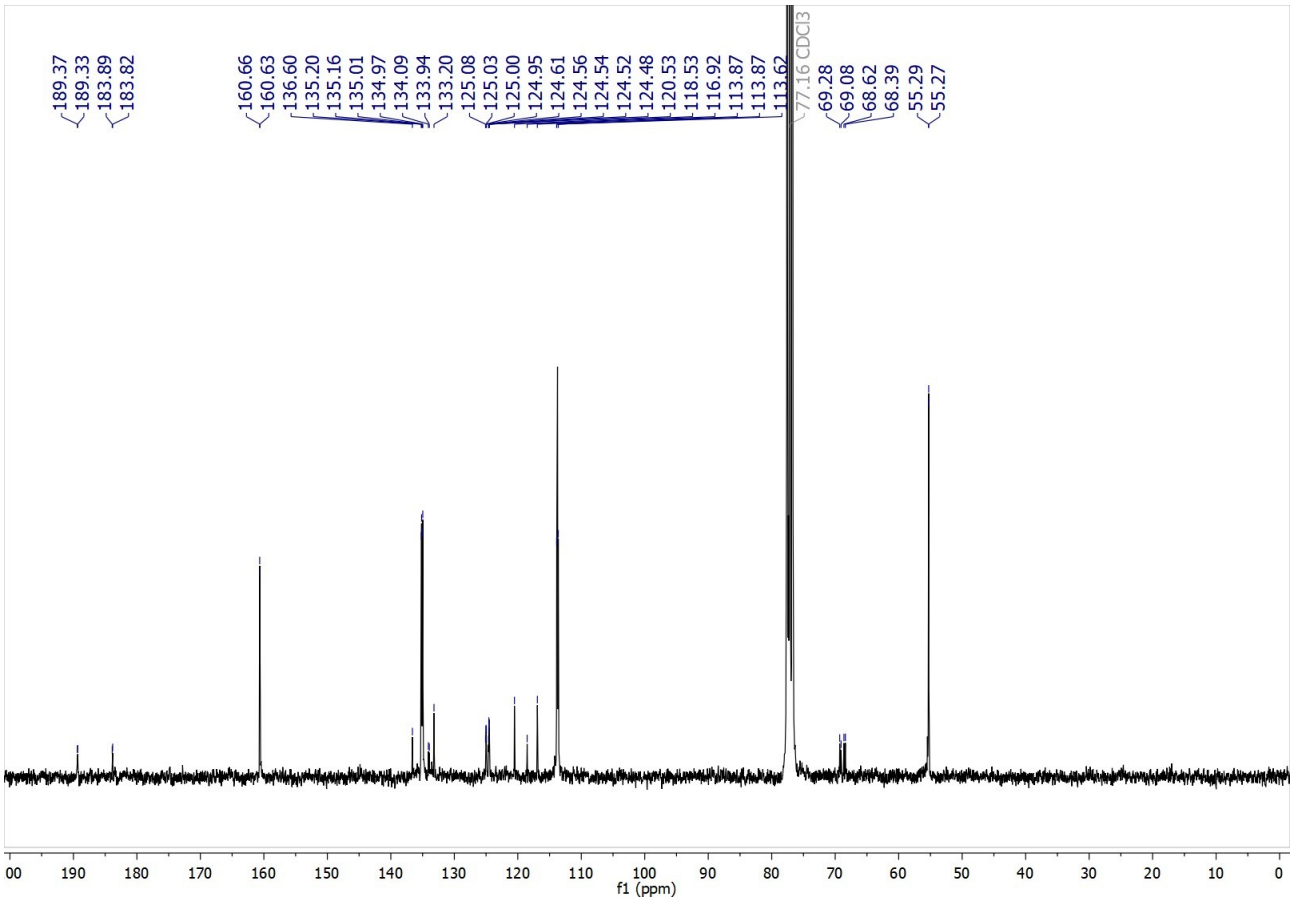

Figure **S31**. $^{13}C\{^{1}H\}$ NMR spectrum of **10** in $CDCl_3$.

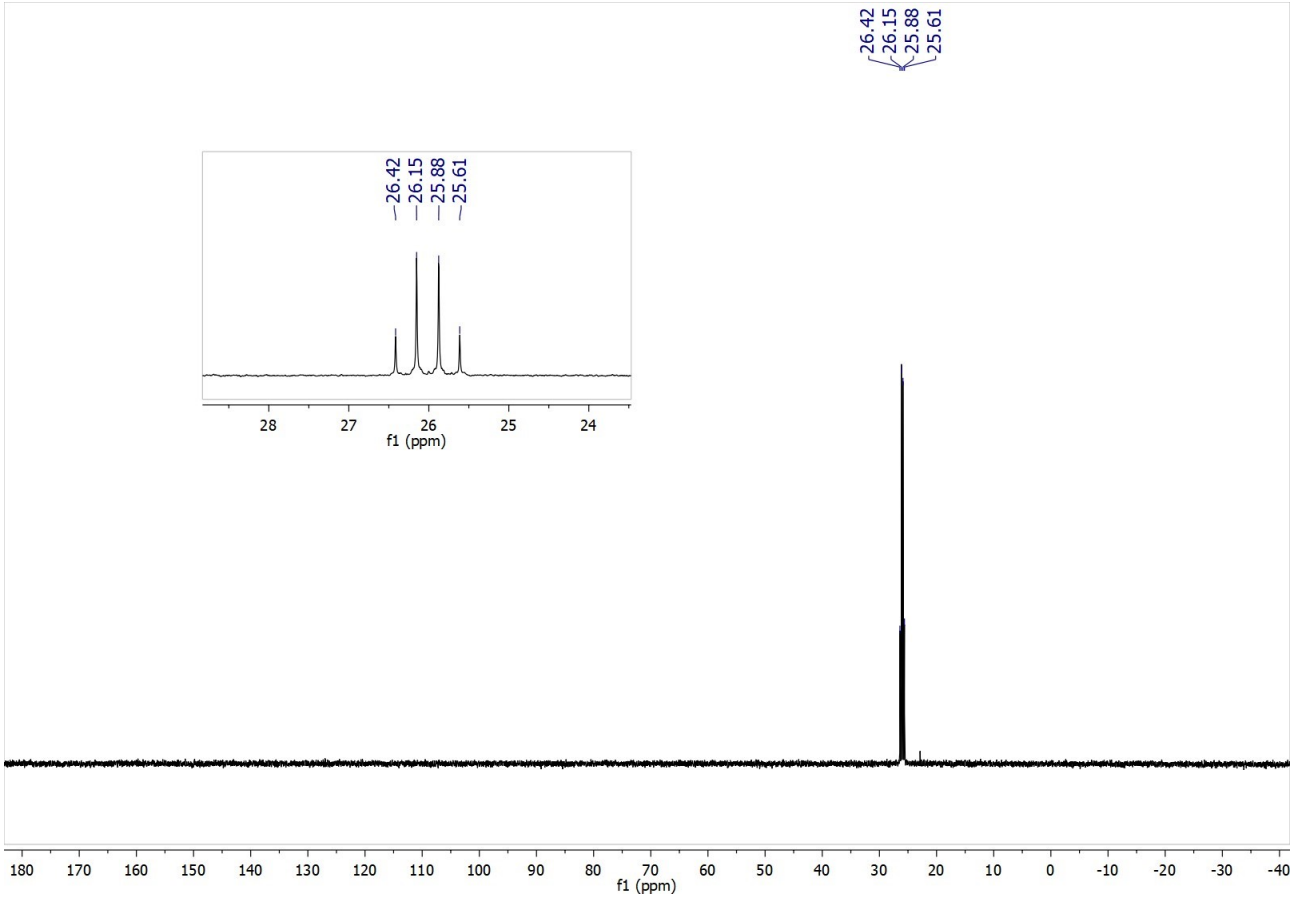

Figure **S32**. $^{31}P\{^{1}H\}$ NMR spectrum of **10** in $CDCl_3$.

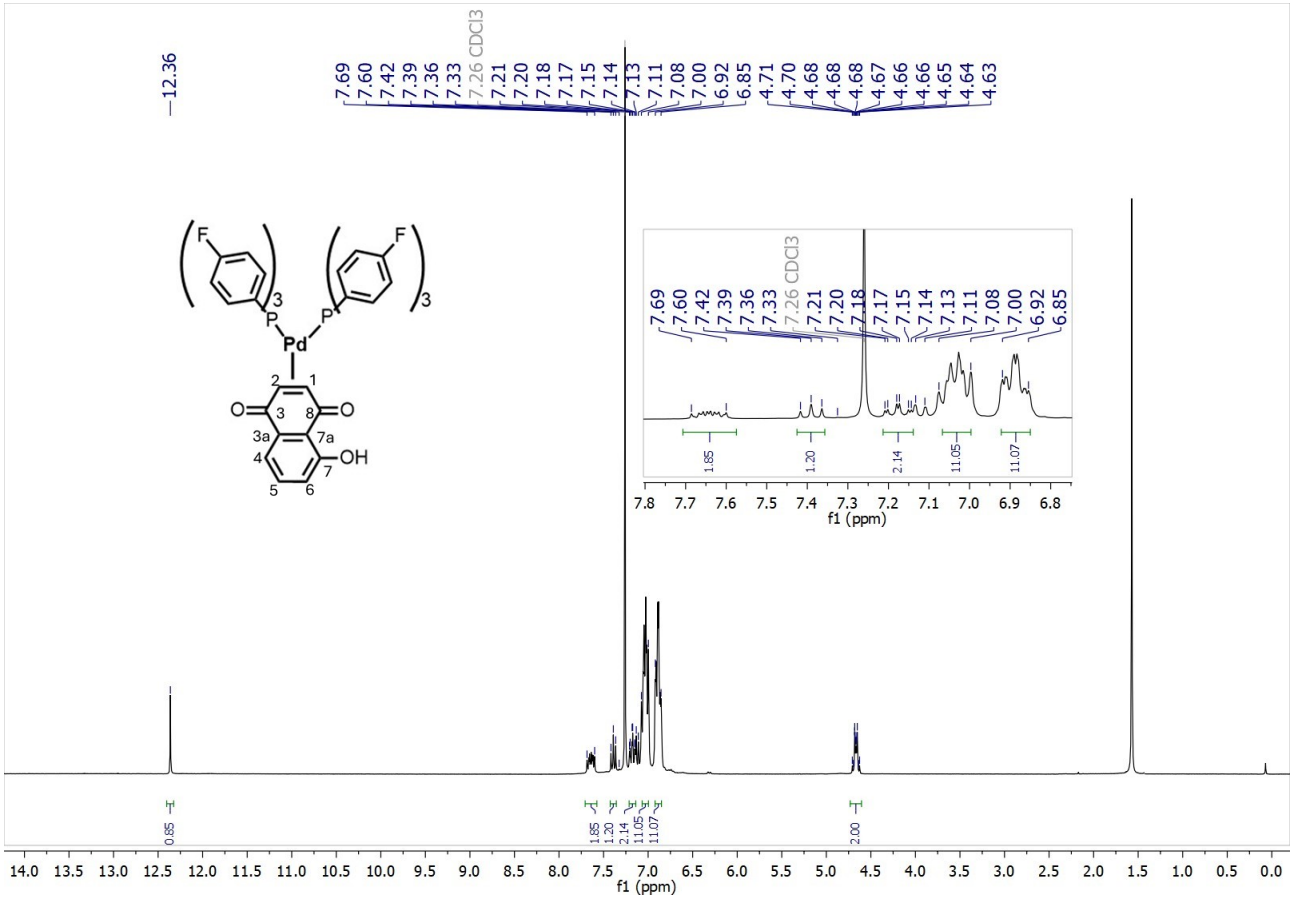

Figure **S33**. ^{1}H NMR spectrum of **11** in $CDCl_3$.

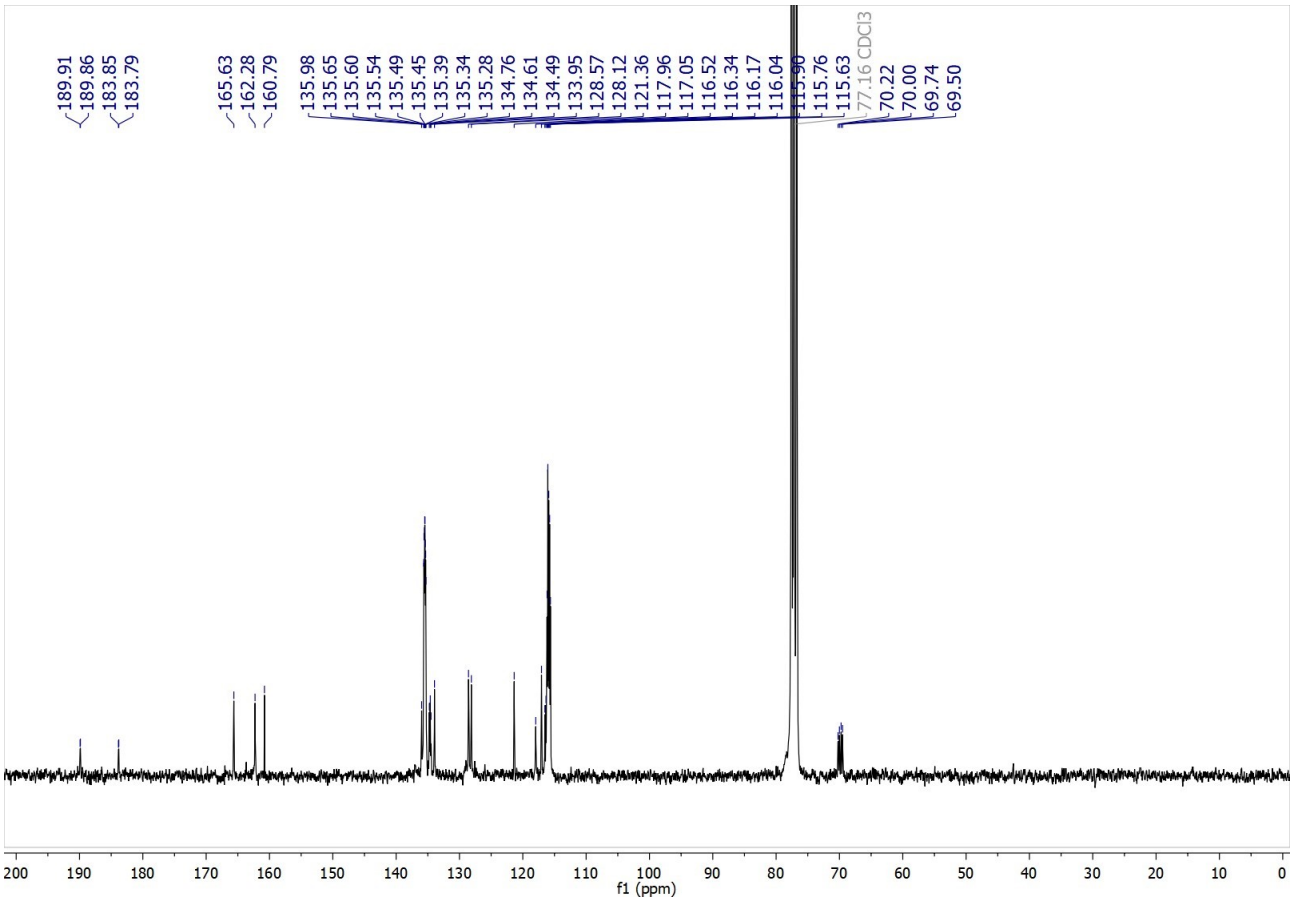

Figure **S34**. $^{13}C\{^{1}H\}$ NMR spectrum of **11** in $CDCl_3$.

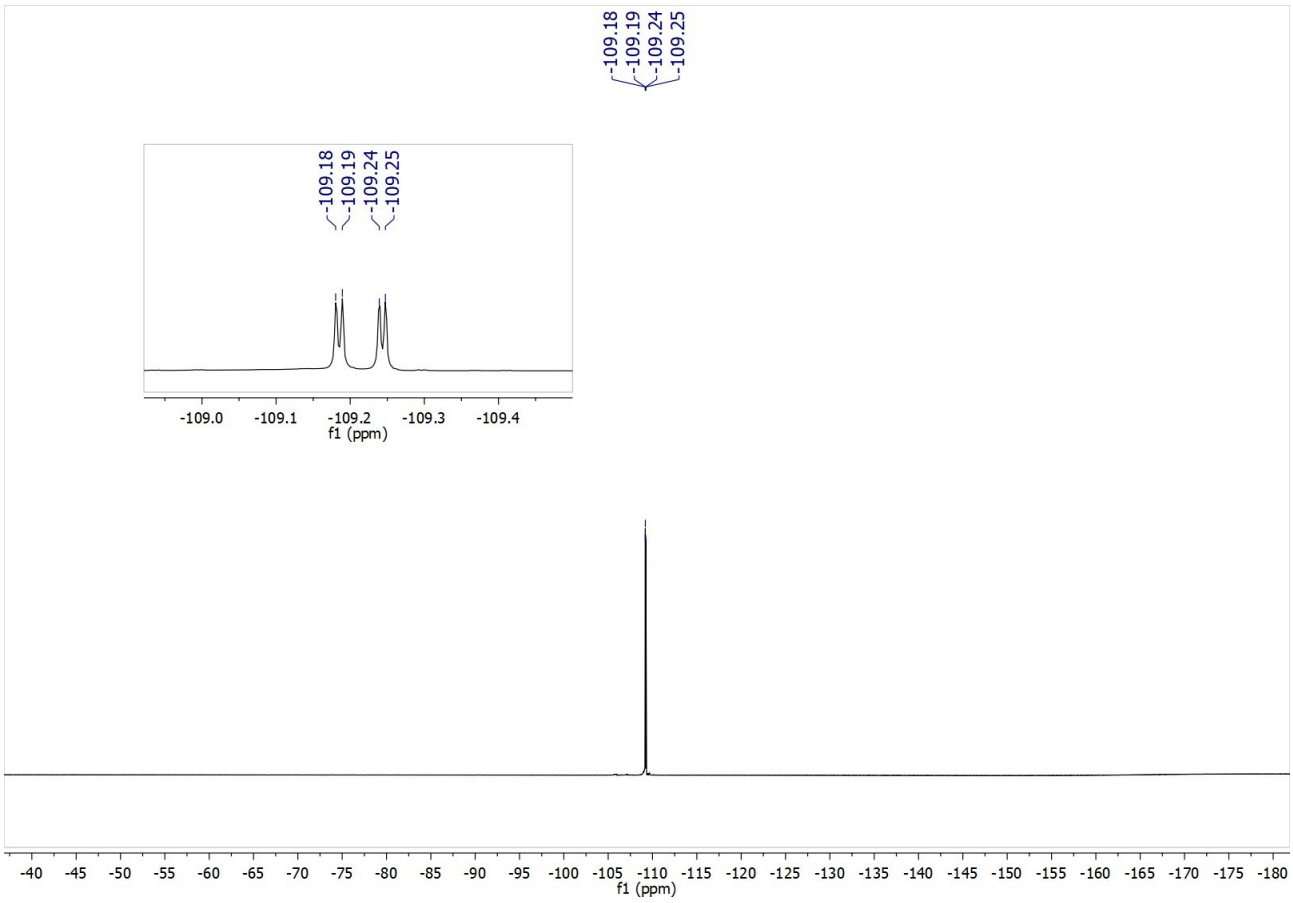

Figure **S35**. $^{31}P\{^{1}H\}$ NMR spectrum of **11** in $CDCl_3$.

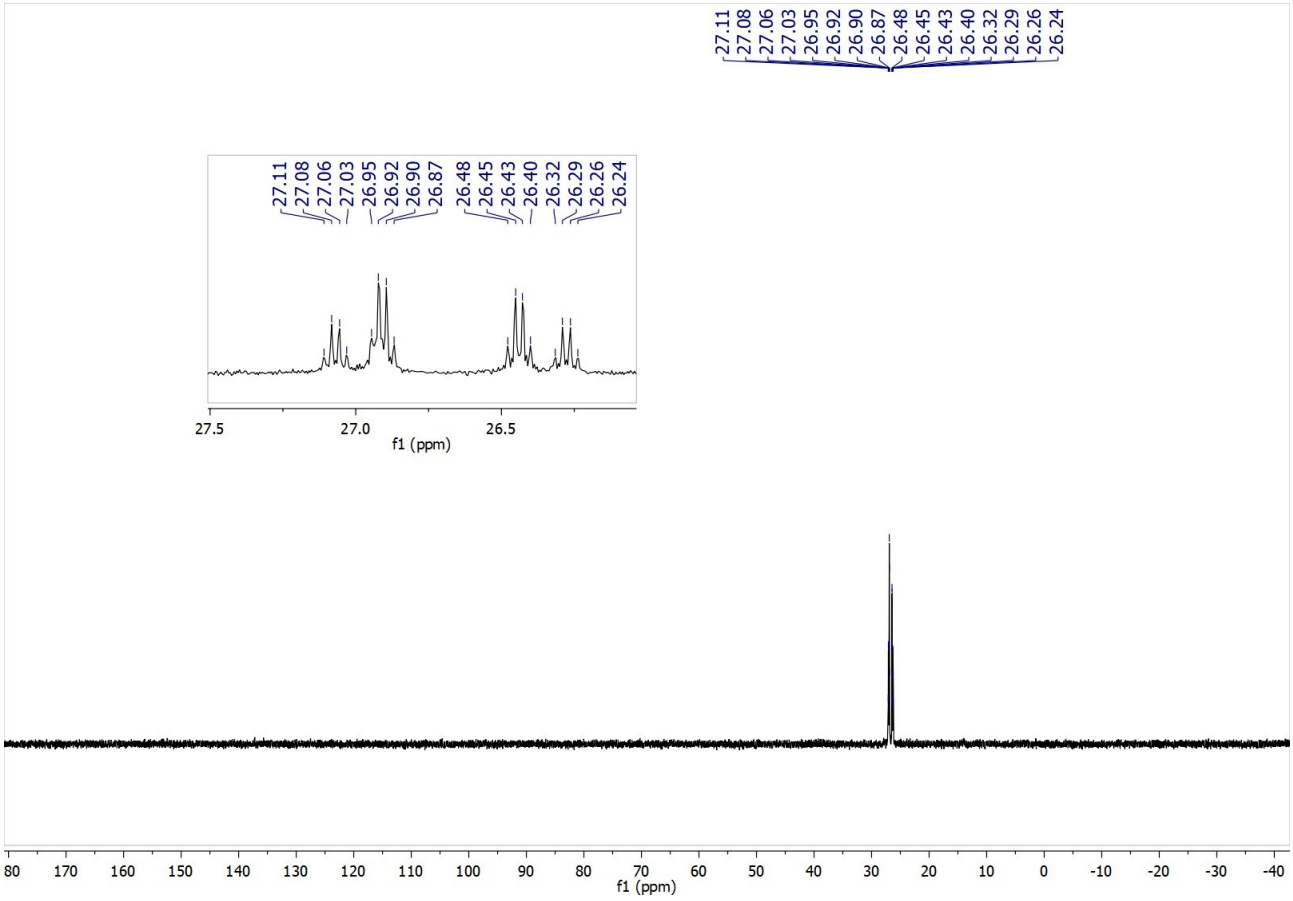

Figure **S36**. $^{19}F\{^{1}H\}$ NMR spectrum of **11** in $CDCl_3$.

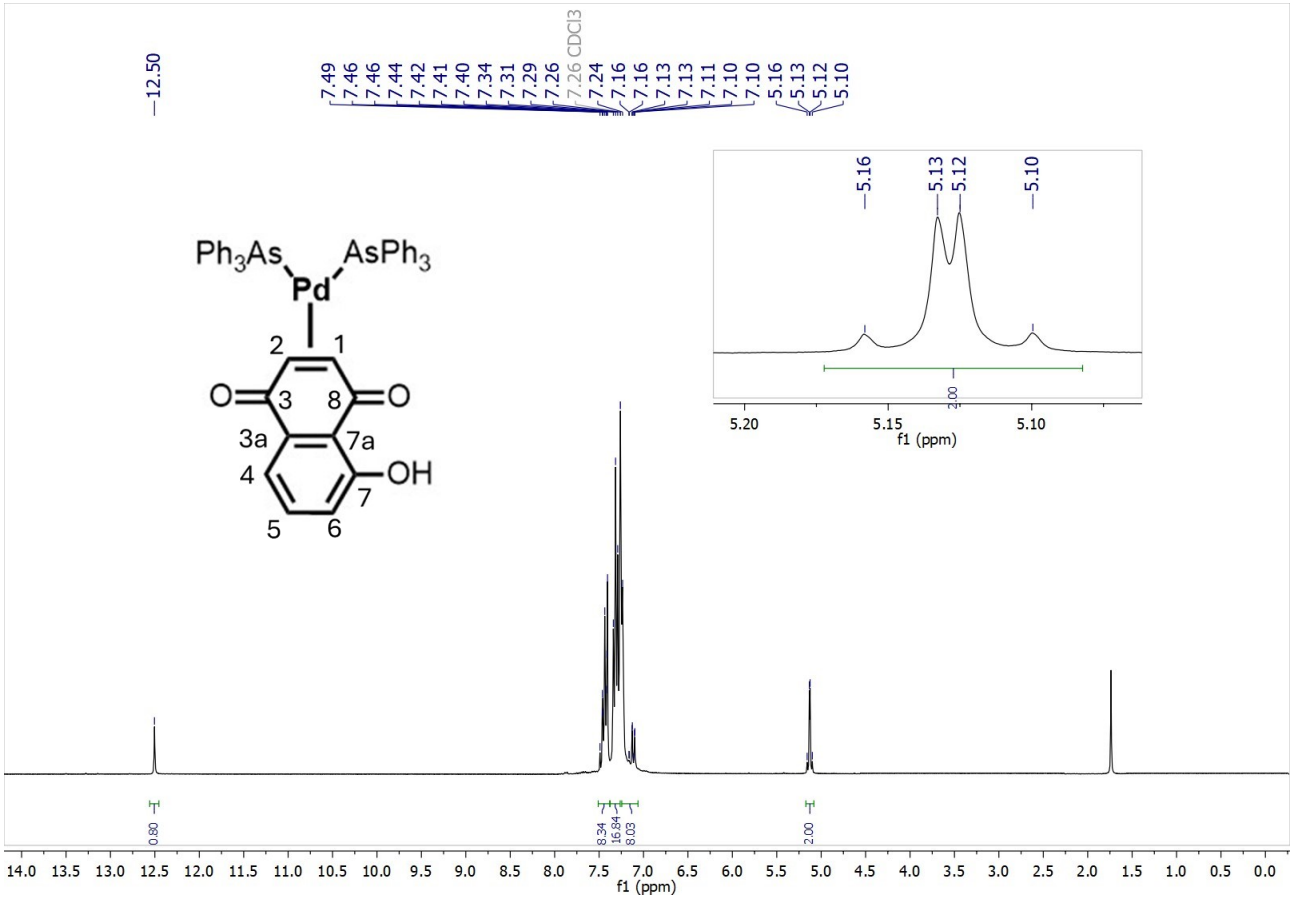

Figure **S37**. ^{1}H NMR spectrum of **12** in $CDCl_3$.

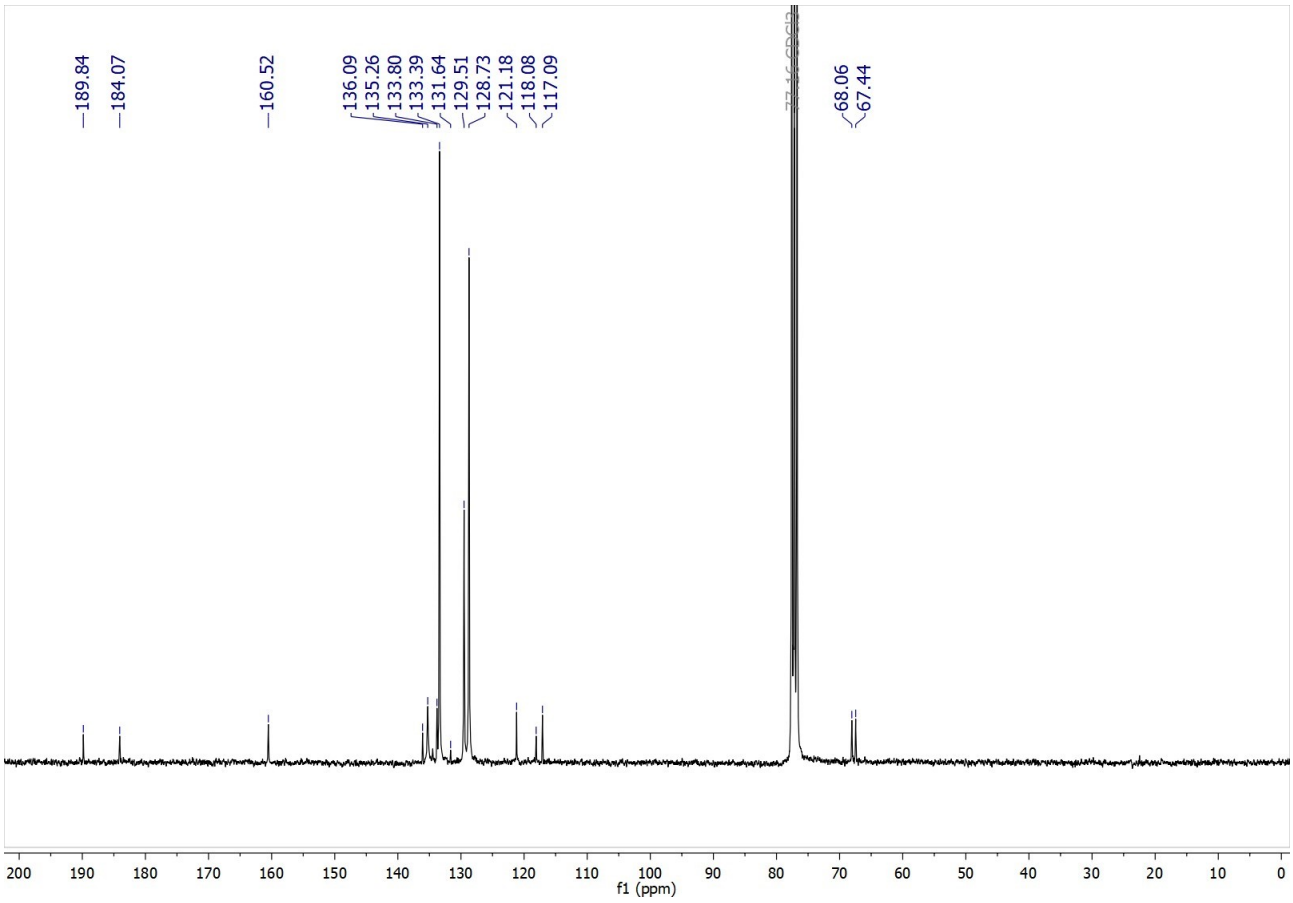

Figure **S38**. $^{13}C\{^{1}H\}$ NMR spectrum of **12** in $CDCl_3$.

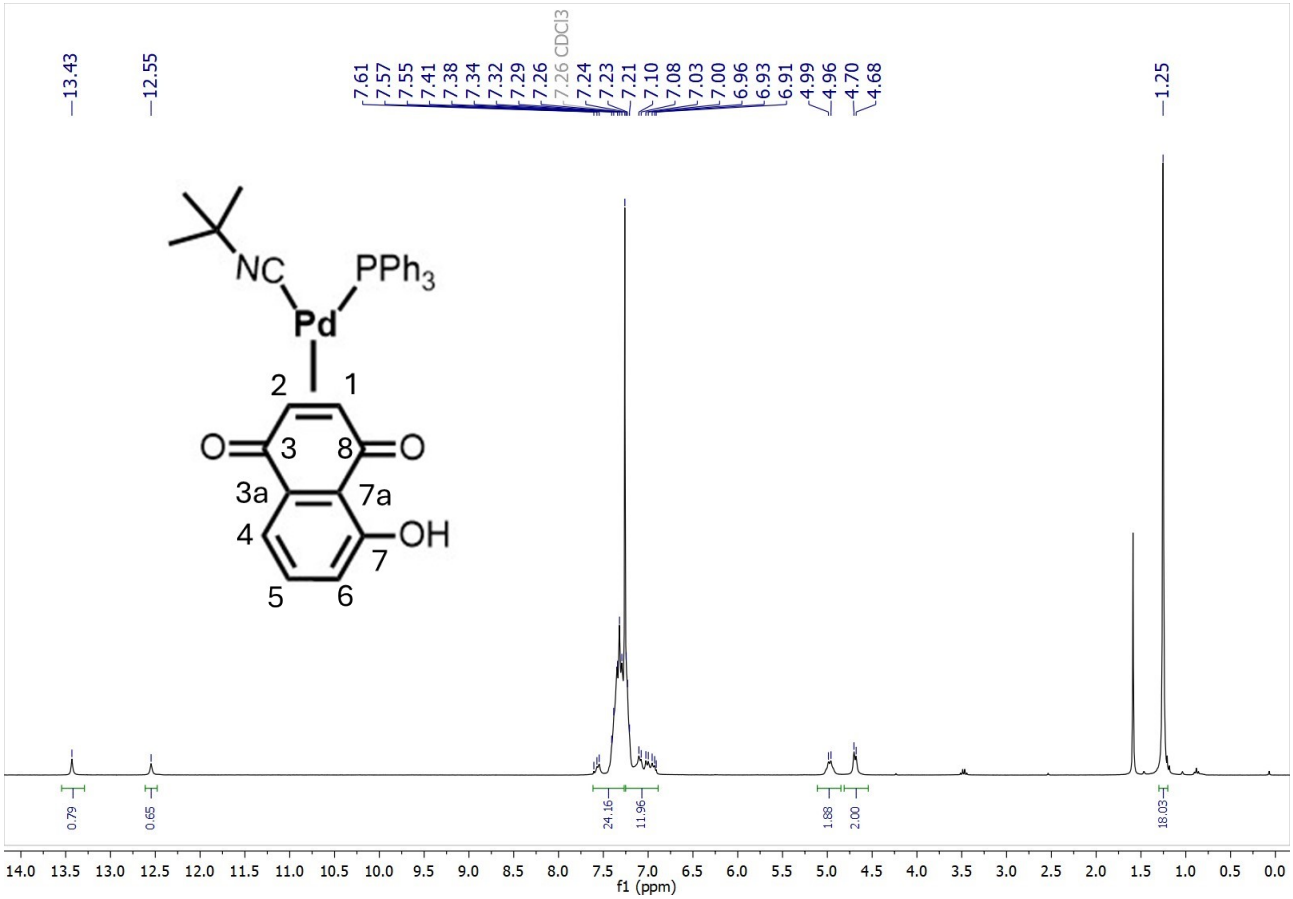

Figure **S39**. ^{1}H NMR spectrum of **13** in $CDCl_3$.

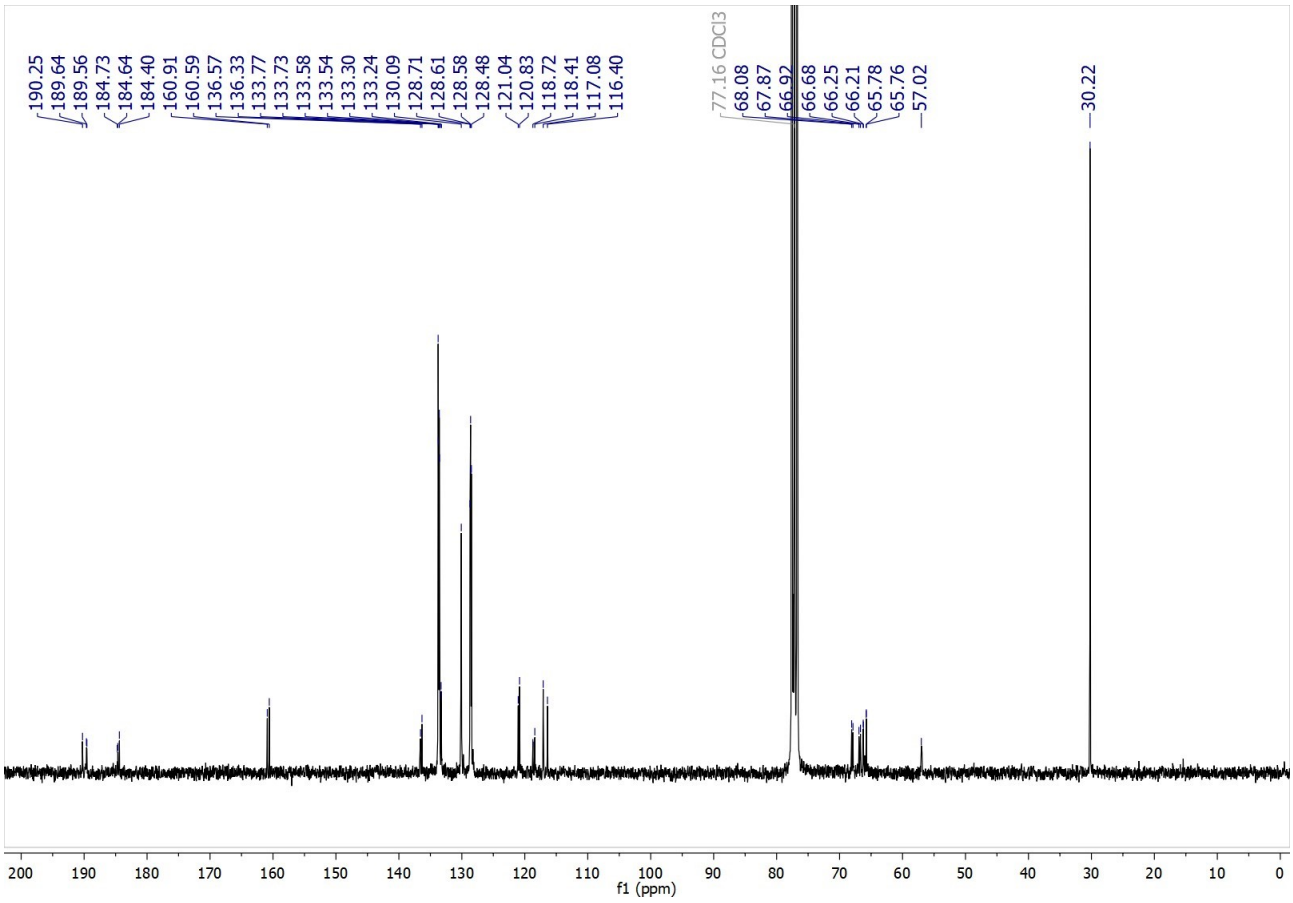

Figure **S40**. $^{13}C\{^{1}H\}$ NMR spectrum of **13** in $CDCl_3$.

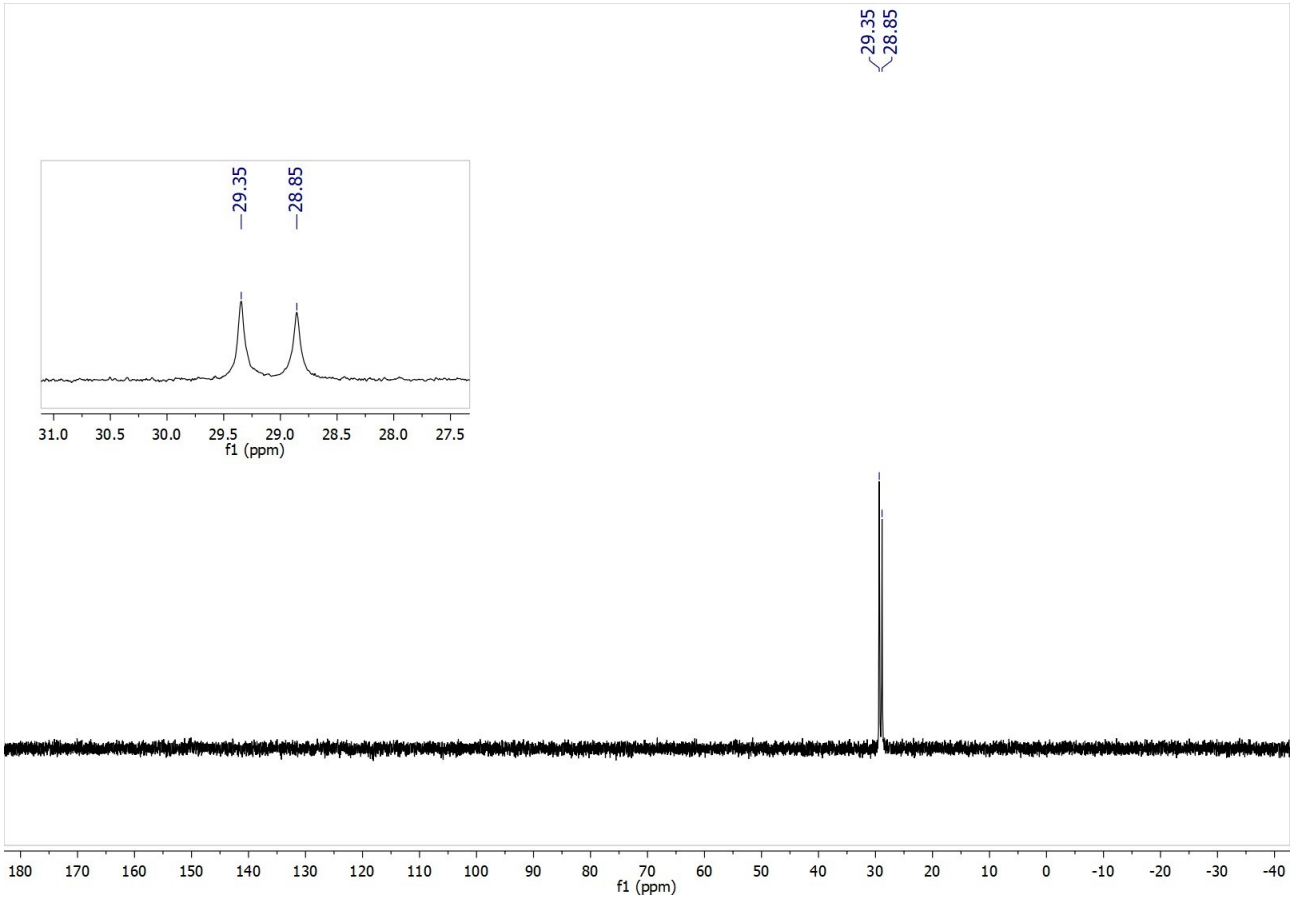

Figure **S41**. $^{31}P\{^{1}H\}$ NMR spectrum of **13** in $CDCl_3$.

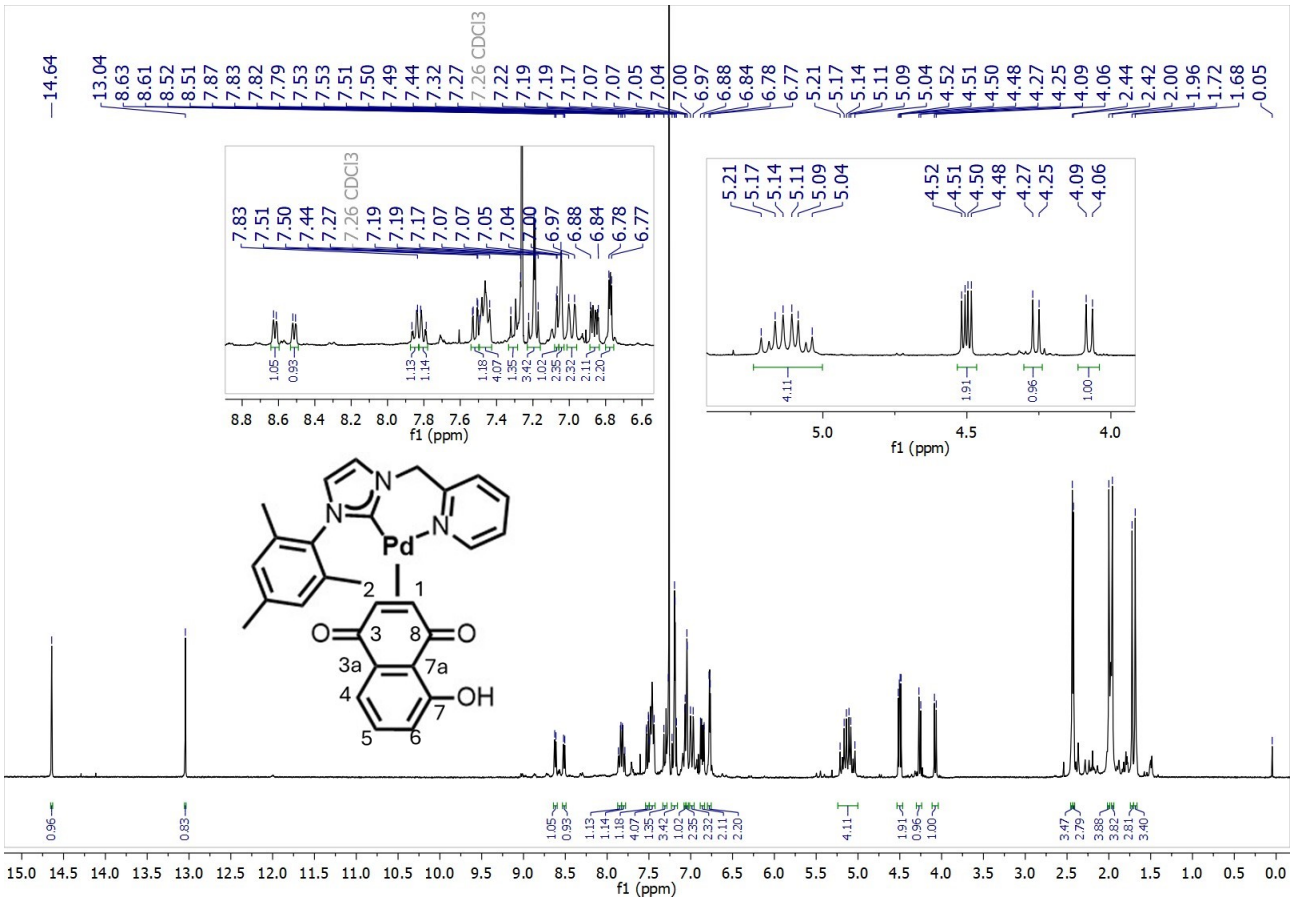

Figure **S42**. ^{1}H NMR spectrum of **14** in $CDCl_3$.

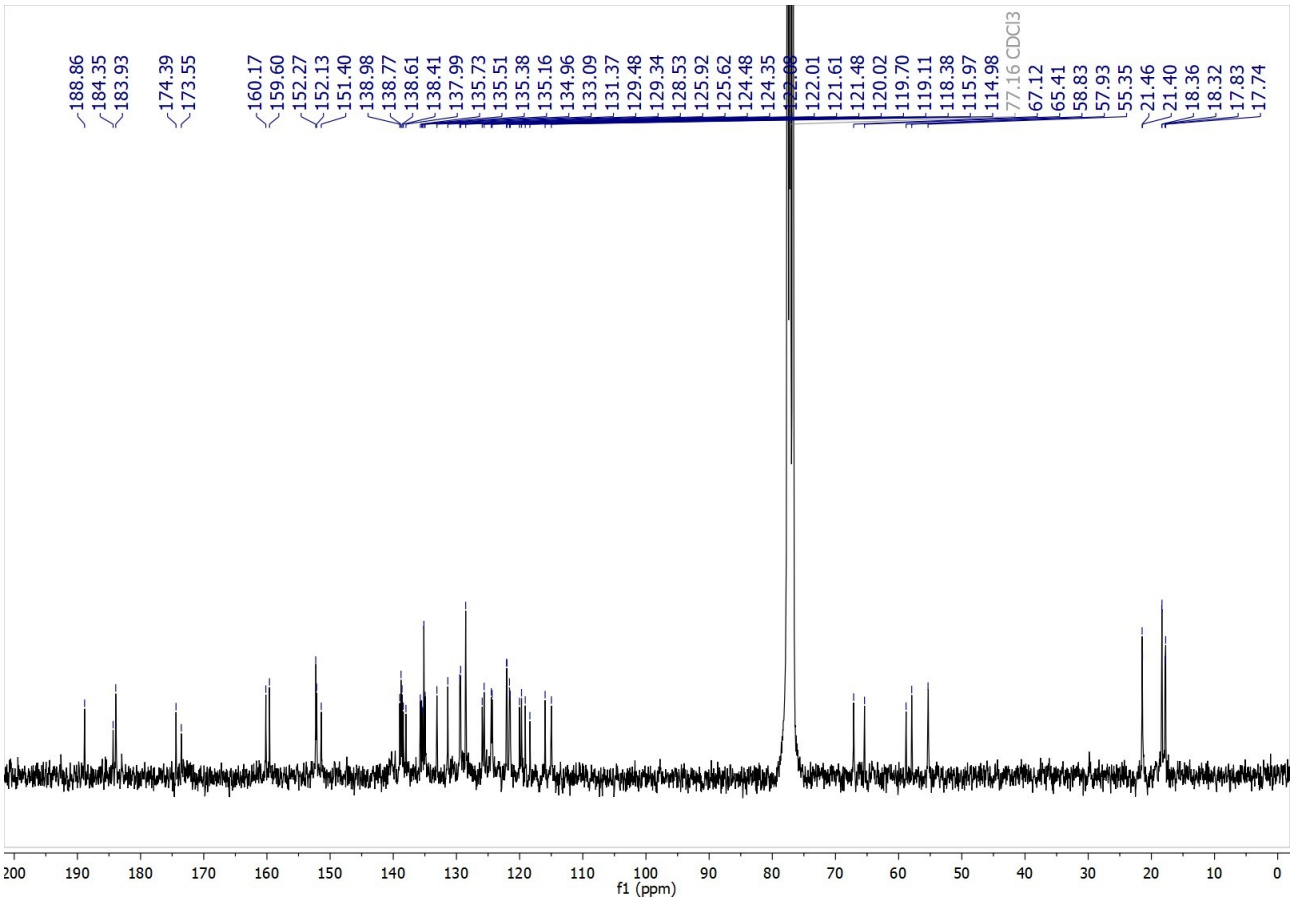

Figure **S43**. $^{13}C\{^{1}H\}$ NMR spectrum of **14** in $CDCl_3$.

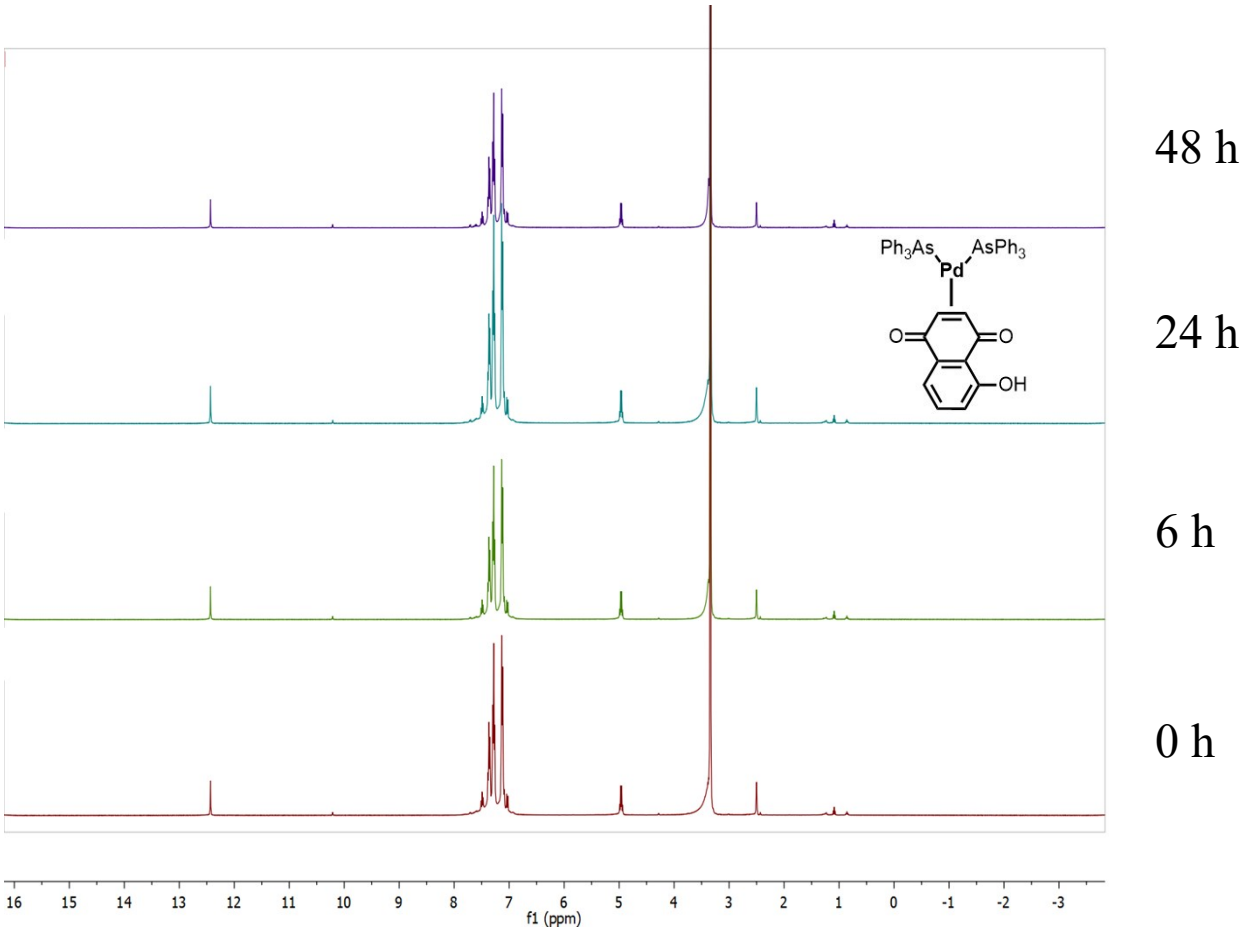

Figure **S44**. ^{1}H spectrum of **12** in a 1:10 DMSO/H_2O solution containing 100 mM NaCl at different time points.

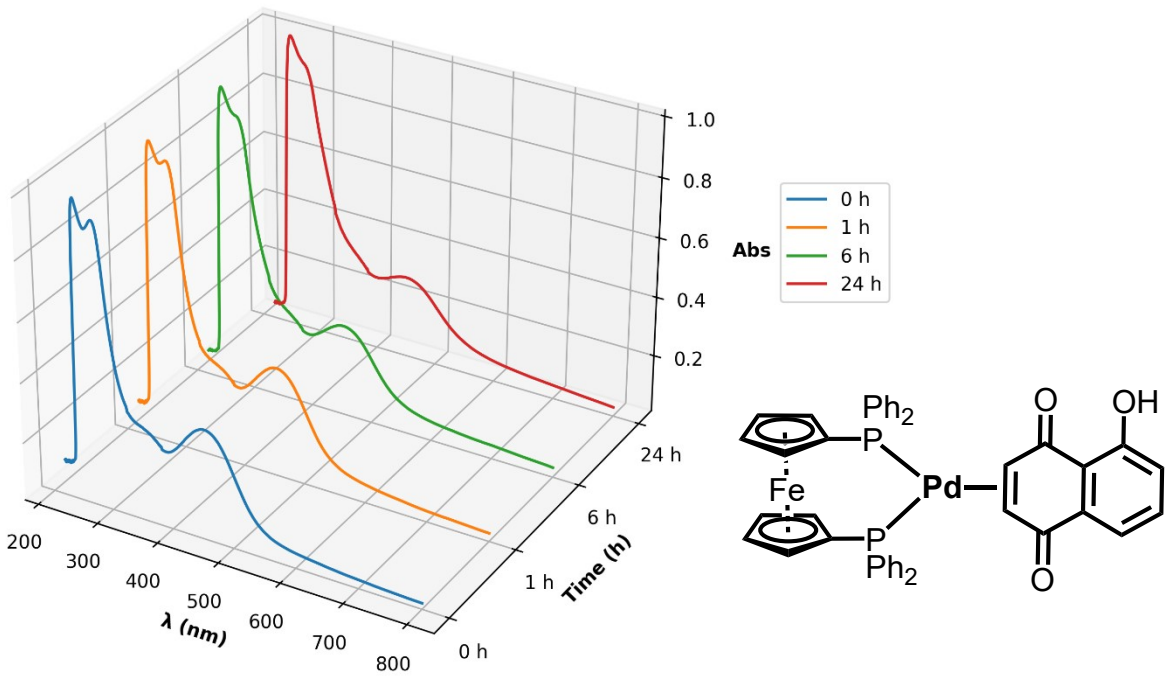

Figure **S45**. UV-VIS spectrum of **4** in DMEM/F12 medium at different time points.

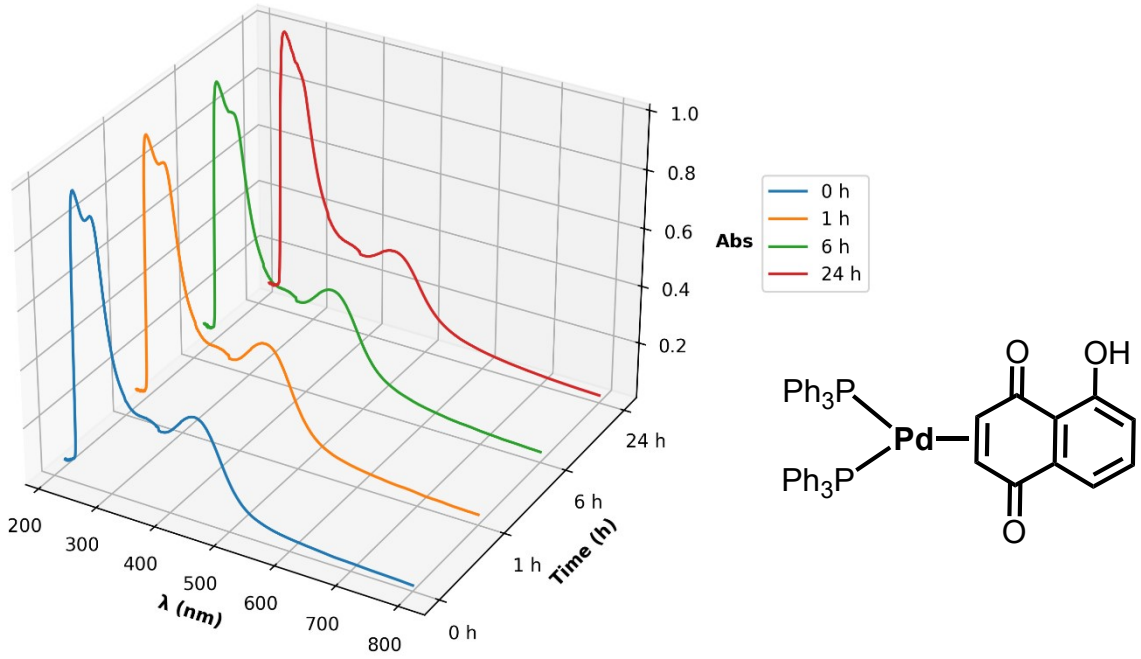

Figure **S46**. UV-VIS spectrum of **8** in DMEM/F12 medium at different time points.

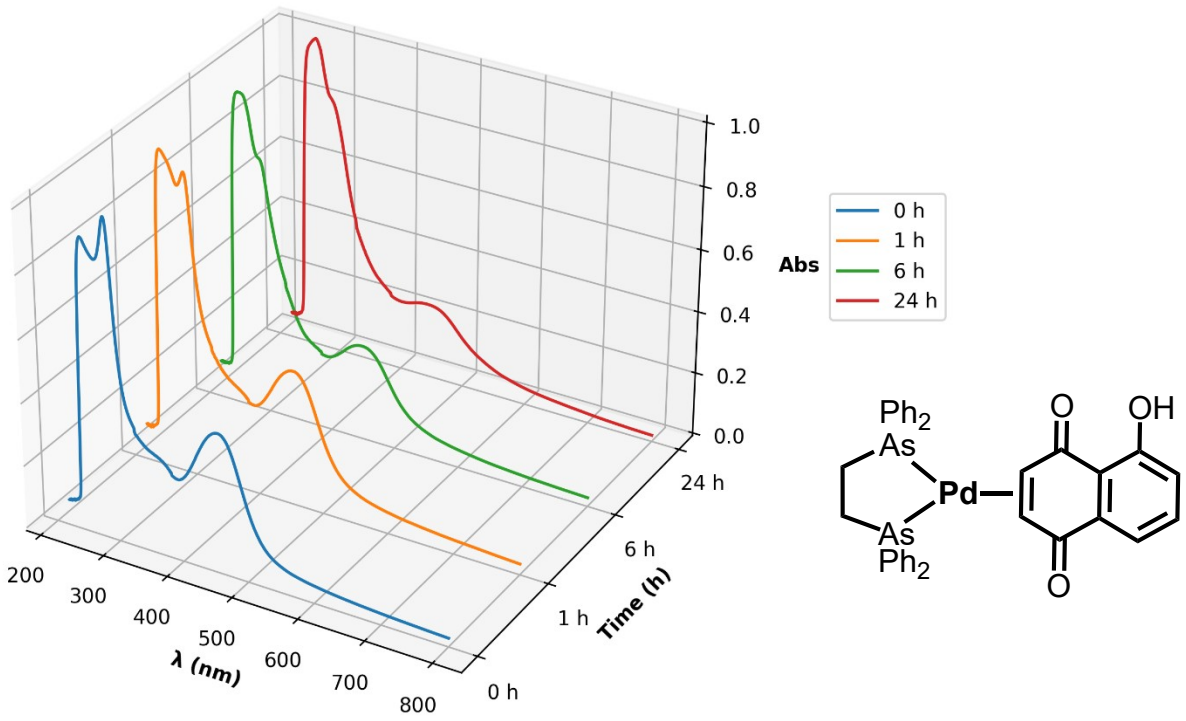

Figure **S47**. UV-VIS spectrum of **6** in DMEM/F12 medium at different time points.

IR SPECTRA

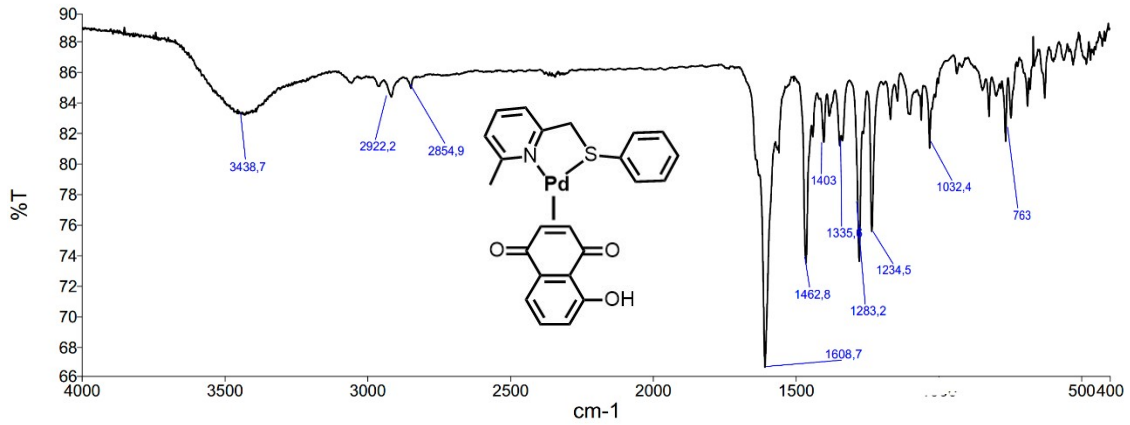

Figure **S48**. IR spectrum (KBr pellet) of **A** at 298K.

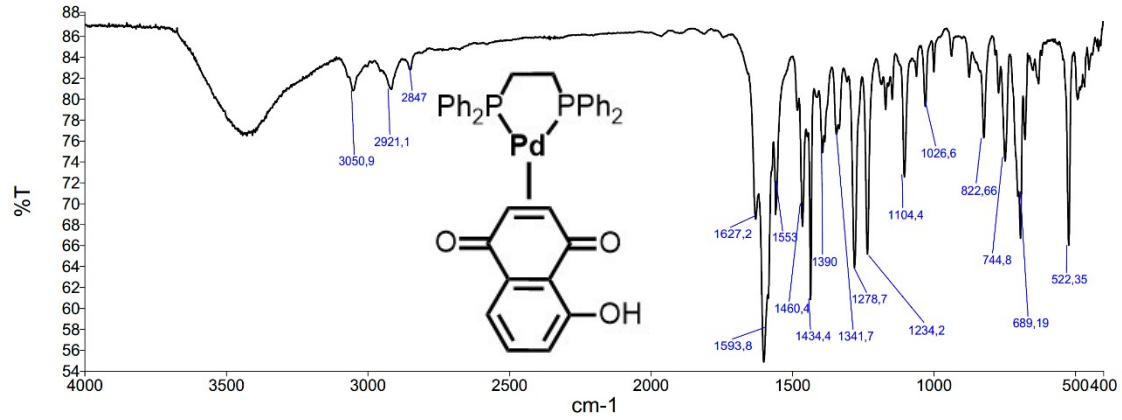

Figure **S49**. IR spectrum (KBr pellet) of **1** at 298 K.

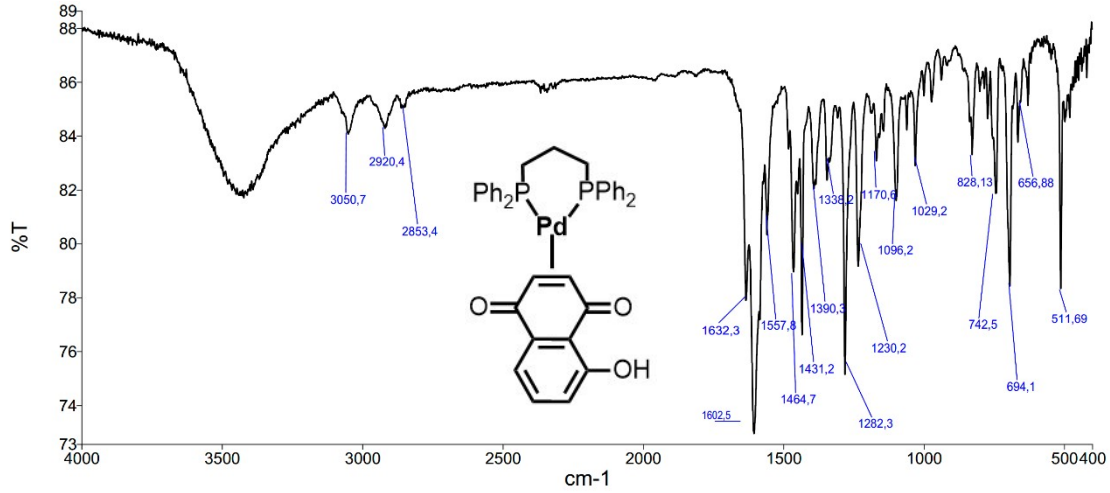

Figure **S50**. IR spectrum (KBr pellet) of **2** at 298 K.

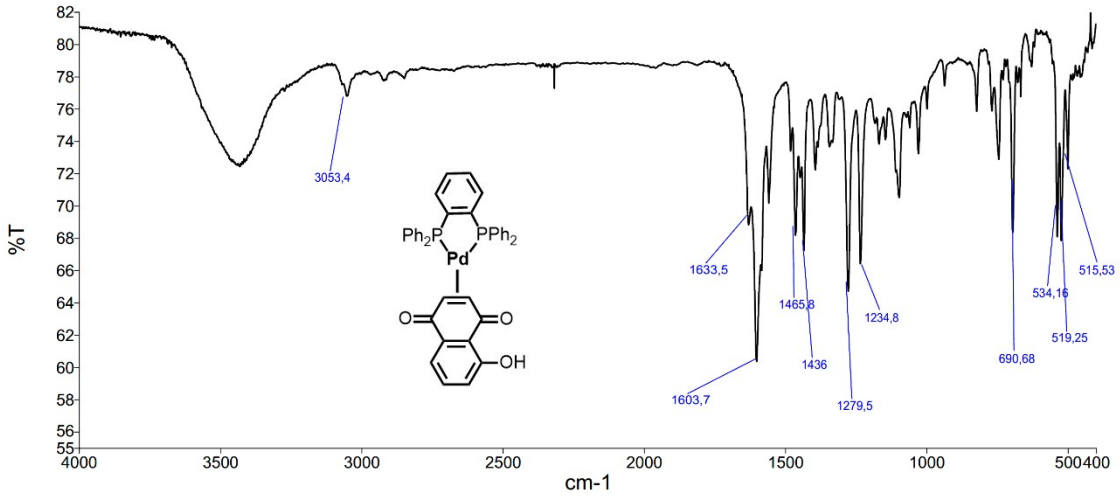

Figure **S51**. IR spectrum (KBr pellet) of **3** at 298 K.

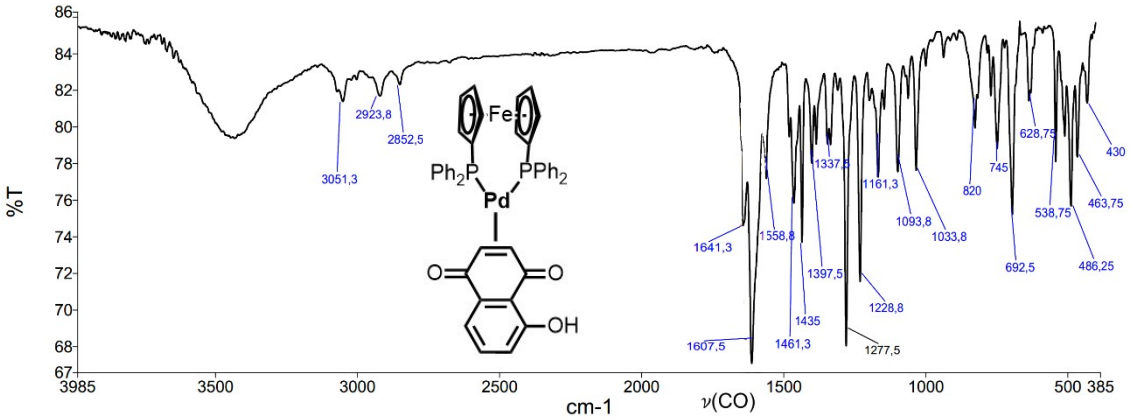

Figure **S52**. IR spectrum (KBr pellet) of **4** at 298 K.

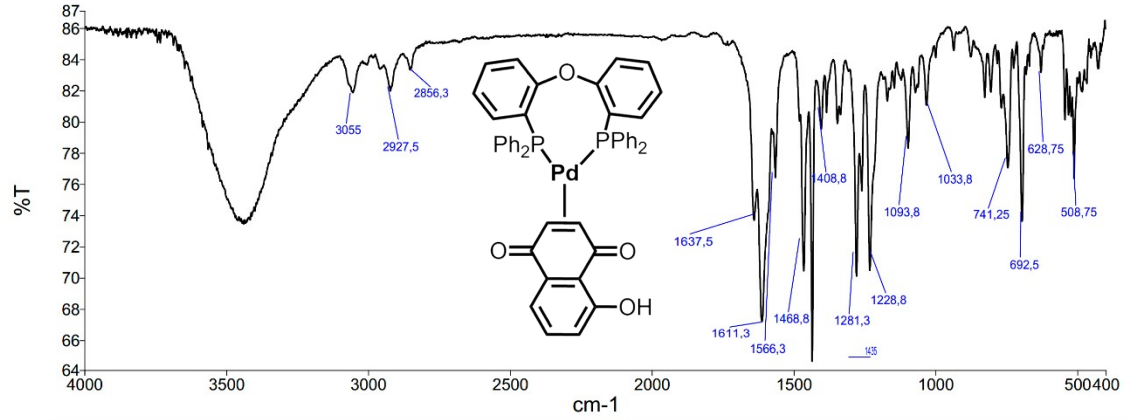

Figure **S53**. IR spectrum (KBr pellet) of **5** at 298 K.

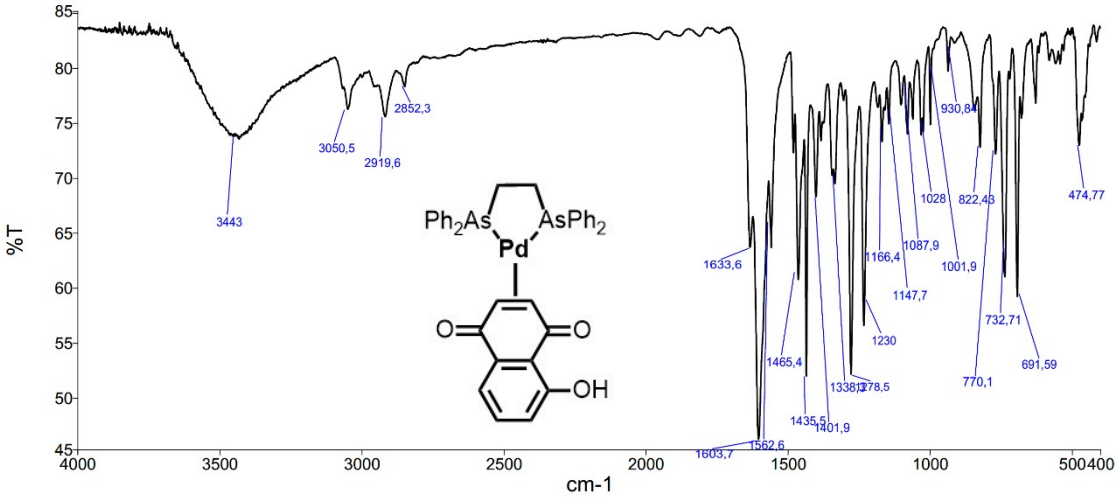

Figure **S54**. IR spectrum (KBr pellet) of **6** at 298 K.

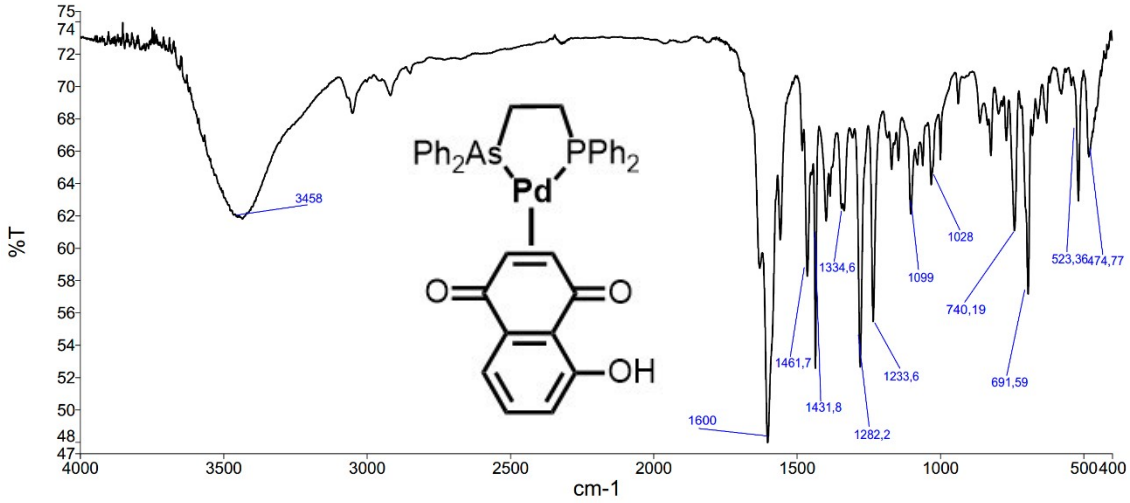

Figure **S55**. IR spectrum (KBr pellet) of **7** at 298 K.

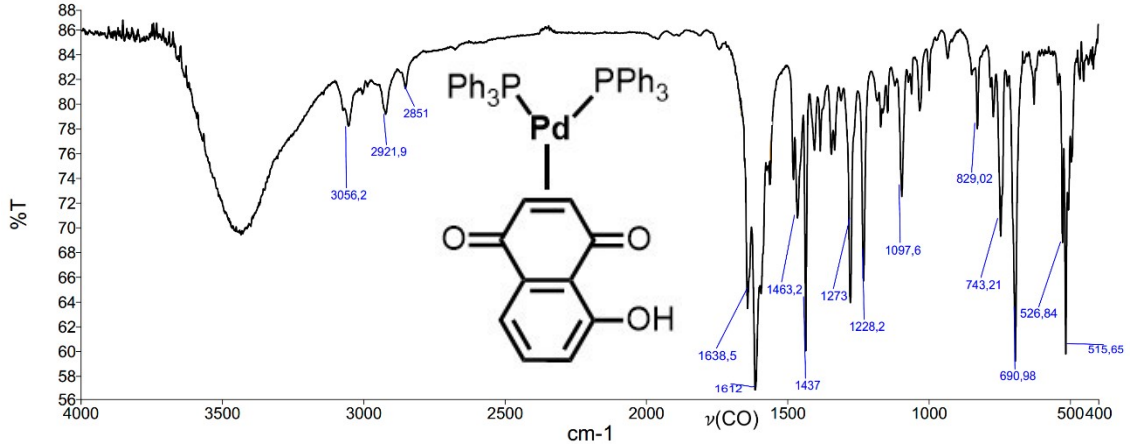

Figure **S56**. IR spectrum (KBr pellet) of **8** at 298 K.

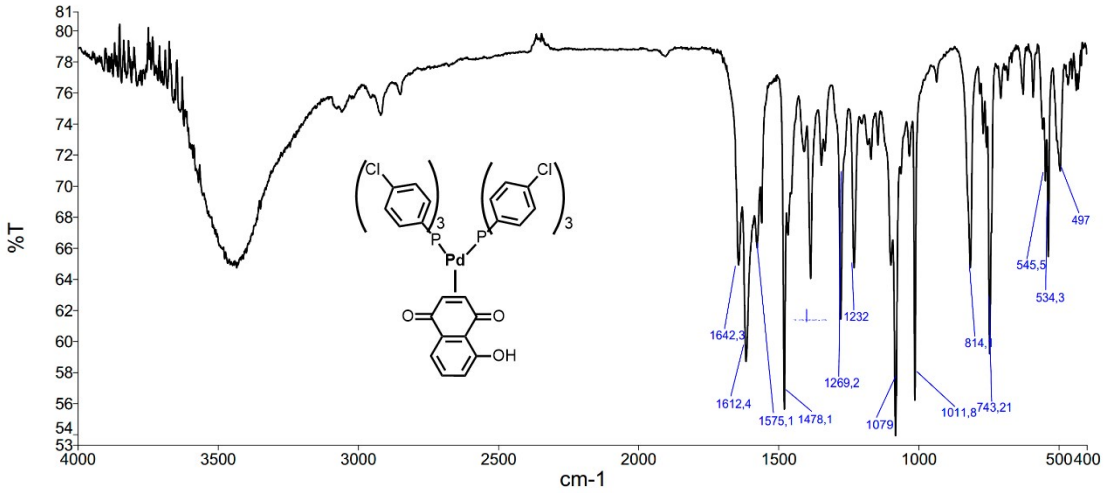

Figure **S57**. IR spectrum (KBr pellet) of **9** at 298 K.

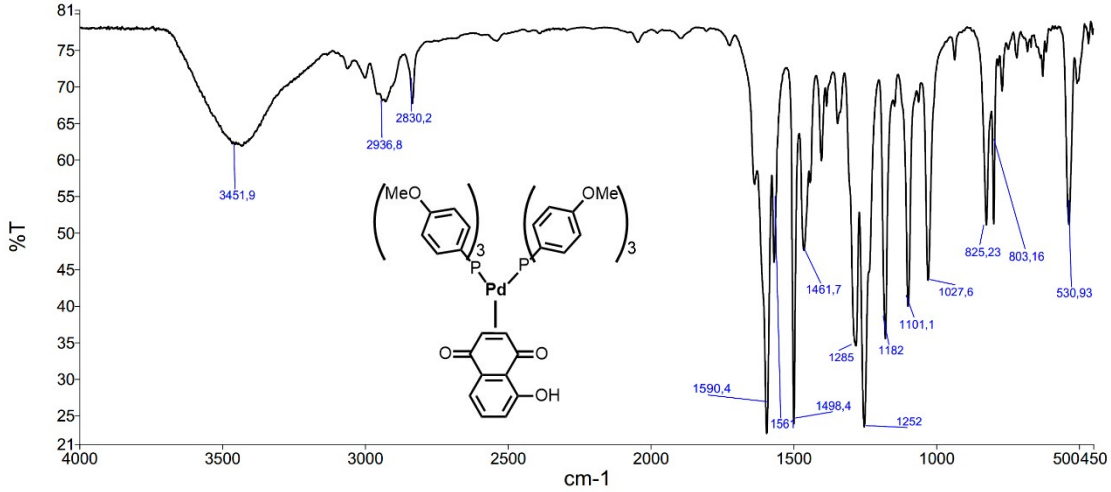

Figure **S58**. IR spectrum (KBr pellet) of **10** at 298 K.

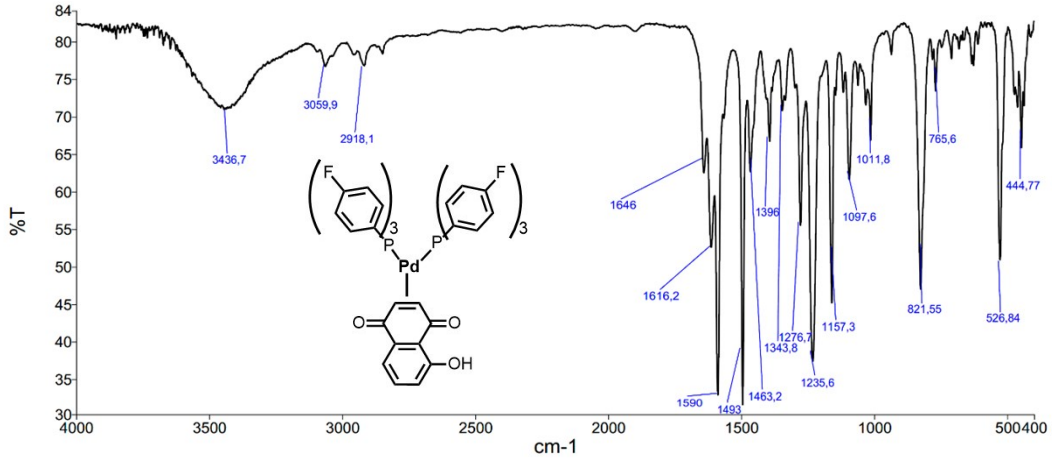

Figure **S59**. IR spectrum (KBr pellet) of **11** at 298 K.

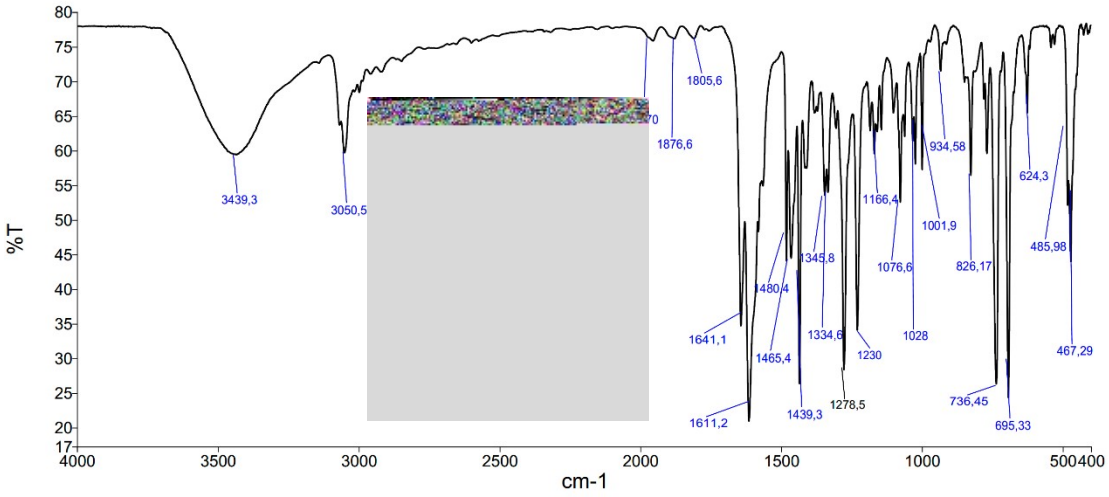

Figure **S60**. IR spectrum (KBr pellet) of **12** at 298 K.

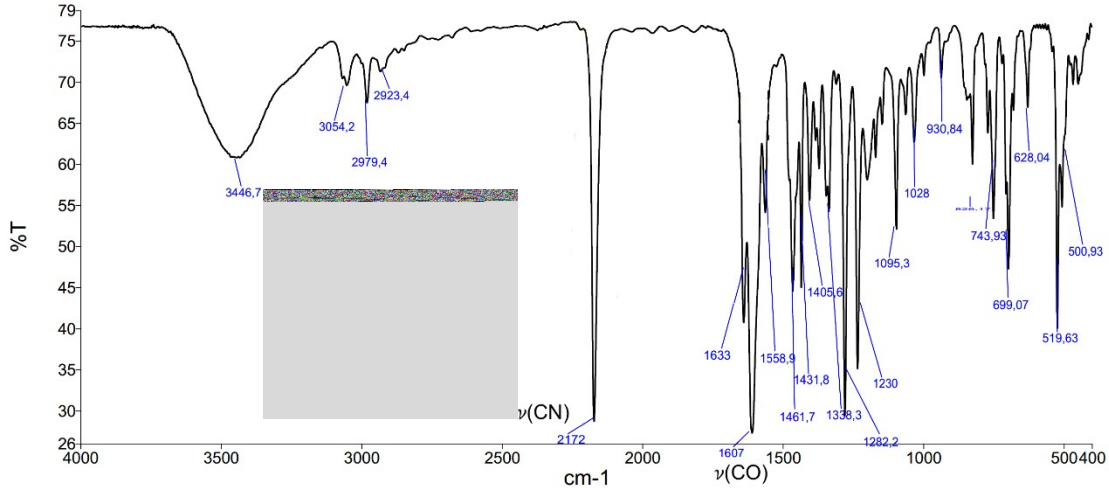

Figure **S61**. IR spectrum (KBr pellet) of **13** at 298 K.

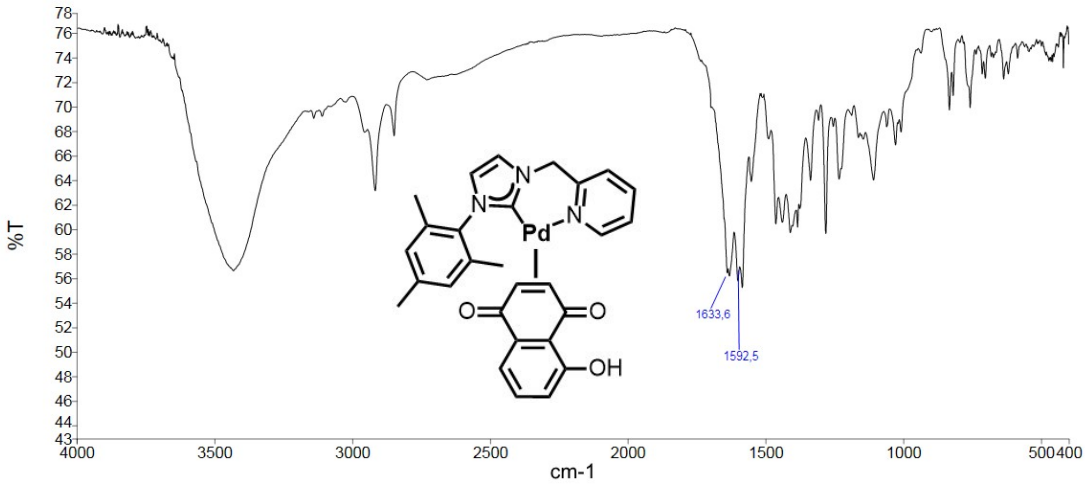

Figure **S62**. IR spectrum (KBr pellet) of **14** at 298 K.

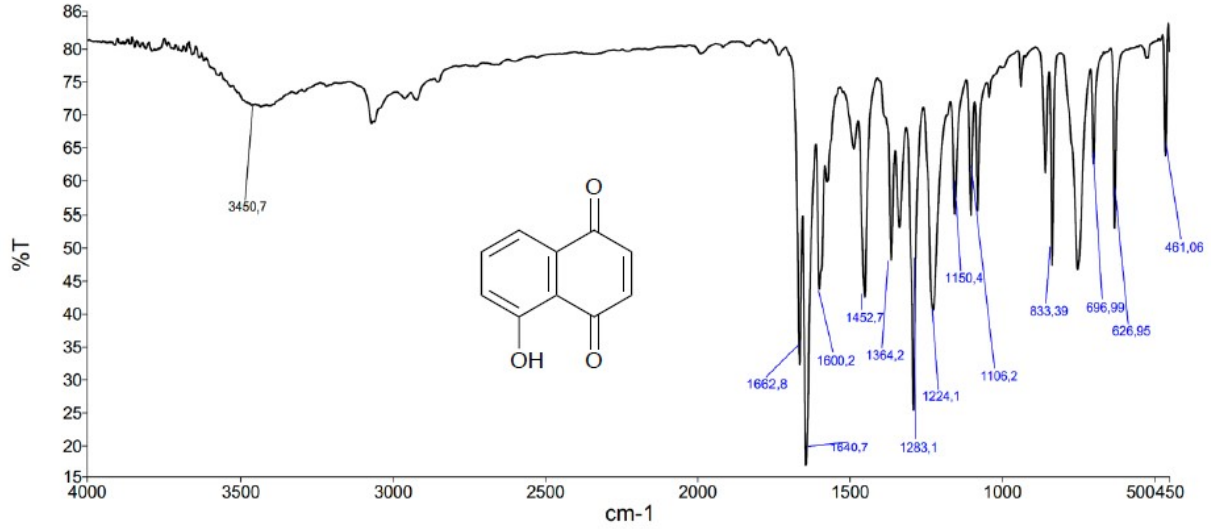

Figure **S63**. IR spectrum (KBr pellet) of **Juglone** at 298 K.

Table 1SI. CO stretching of synthesized complexes.

Complex	ν(CO) (cm^{-1})	ν(CO) Free Juglone (cm^{-1})
A	1609	1640
1	1594	
2	1602	
3	1604	
4	1607	
5	1611	
6	1604	
7	1600	
8	1612	
9	1612	
10	1590	
11	1590	
12	1611	
13	1607	
14	1592	

Table 2SI. Crystallographic data.

Compound	**5@100 K**	**7@100 K**	**13@100 K**	**13@298 K**
Formula	$PdC_{46}H_{34}O_4P_2 \cdot 2CHCl_3$	$PdC_{36}H_{30}AsO_3P \cdot {}^1/_2CHCl_3$	$PdC_{33}H_{30}NO_3P$	$PdC_{33}H_{30}NO_3P$
M/g·mol^{-1}	1057.81	782.57	625.95	625.95
Space group	*P* -1	*P* 2$_1$/*c*	*P bca*	*P bca*
Crystal system	Triclinic	Monoclinic	Orthorhombic	Orthorhombic
a/Å	11.024(2)	38.767(8)	22.714(5)	22.850(5)
b/Å	12.556(3)	9.041(2)	18.484(4)	18.790(4)
c/Å	16.672(3)	18.570(4)	26.741(5)	27.065(5)
α/°	84.30(3)	90	90	90
β/°	80.22(3)	100.26(3)	90	90
γ/°	78.01(3)	90	90	90
V/Å^3	2219.6(8)	6405(2)	11277(4)	11620(4)
Z	2	8	16	16
T/K	100(2)	100(2)	100(2)	100(2)
D_c/g·cm^{-3}	1.583	1.623	1.481	1.431
F(000)	1068	3144	5120	5120
μ/mm^{-1}	0.608	1.251	0.518	0.501
Measured Reflections	104700	72954	264364	199826
Unique Reflections	19342	21164	24860	25755
R_{int}	0.0387	0.1205	0.0743	0.0467
Obs. Refl.ns [I≥2σ(I)]	18504	8556	20807	15915
θ_{min}- θ_{max}/°	1.08 – 31.10	0.93 – 27.11	1.33 – 31.10	1.31 – 31.10
hkl ranges	-16,16; -20,20; -25,25	-56,56; -13,13; -25,27	-33,33; -30,30; -40,40	-33,33; -30,30; -39,41
R(F^2) (Obs.Refl.ns)	0.0303	0.0832	0.0367	0.04607
wR(F^2) (All Refl.ns)	0.0802	0.2656	0.0986	0.1479
No. Variables	616	792	711	711
Goodness of fit	1.047	0.955	1.024	1.012
$\Delta\rho_{max}$; $\Delta\rho_{min}$/e·Å^{-3}	2.28; -1.17	1.80; -0.89	1.71; -1.73	1.21; -0.40
CCDC Deposition N.	2441626	2441623	2441624	2441625

Table 3SI. Selected palladium distances and angles for **5** at 100 K.

5 (100 K) – $PdC_{46}H_{34}O_4P_2$

Distances (Å)		Angles	(°)
Pd_1-C2_2	2.156(1)	C2_2-Pd_1-C3_2	38.61(4)
Pd_1-C3_2	2.145(2)	P10_3-Pd_1-C3_2	105.96(3)
Pd_1-C1_2	2.845(2)	P10_3-Pd_1-P30_3	105.94(1)
Pd_1-C4_2	2.822(2)	P30_3-Pd_1- C2_2	109.76(3)
Pd_1-P10_3	2.313(1)	Pd-Juglone Ave Plane[a]	85.55(2)
Pd_1-P30_3	2.332(1)	Juglone Ave Plane[b]	3.84(4)

[a]Average angle between the mean metal coordination plane and the mean juglone plane; [b]Average angle between quinone and phenolic rings in juglone

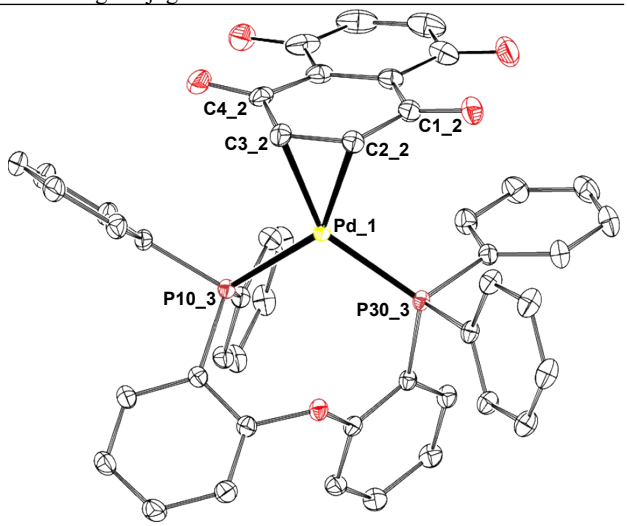

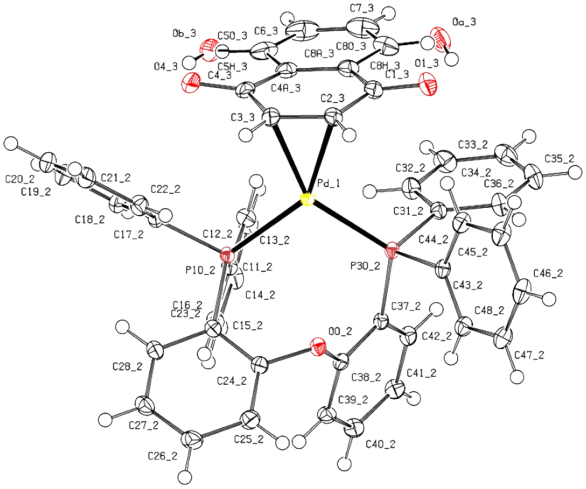

Table 4SI. Selected palladium distances and angles for **7** at 100 K. Associated molecular representations omit disorder for clarity.

7 (100 K) – $PdC_{36}H_{30}AsO_3P$					
ASU Molecule 1				**ASU Molecule 2**	
Distances	(Å)	**Angles**	**(°)**	**Distances**	(Å)	**Angles**	**(°)**
Pd_1-C2_2	2.151(9)	C2_2-Pd_1-C3_2	38.3(3)	Pd_1-C2_2	2.160(10)	C2_2-Pd_1-C3_2	38.2(4)
Pd_1-C3_2	2.141(8)	P_3-Pd_1-C_2[a]	119.3(3)	Pd_1-C3_2	2.160(10)	P_3-Pd_1-C_2[a]	117.9(3)
Pd_1-C1_2	2.750(10)	P_3-Pd_1-As_3	87.2(2)	Pd_1-C1_2	2.780(10)	P_3-Pd_1-As_3	85.8(2)
Pd_1-C4_2	2.750(10)	As_3-Pd_1- C_2[a]	119.4(2)	Pd_1-C4_2	2.780(10)	As_3-Pd_1- C_2[a]	117.9(3)
Pd_1-P_3	2.338(7)	Pd-Juglone Ave Plane[a]	87.1(2)	Pd_1-P_3	2.332(6)	Pd-Juglone Ave Plane[b]	88.9(2)
Pd_1-As_3	2.332(3)	Juglone Ave Plane[b]	5.5(3)	Pd_1-As_3	2.339(3)	Juglone Ave Plane[c]	3.7(4)

[a]Average angle with closer C; [b]Average angle between the mean metal coordination plane and the mean juglone plane; [c]Average angle between quinone and phenolic rings in juglone

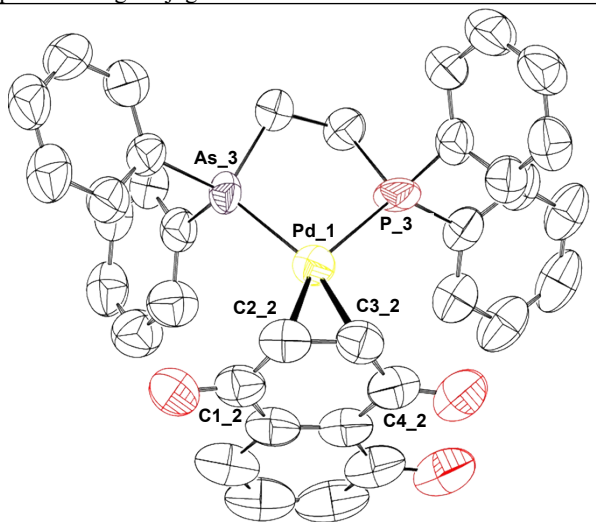

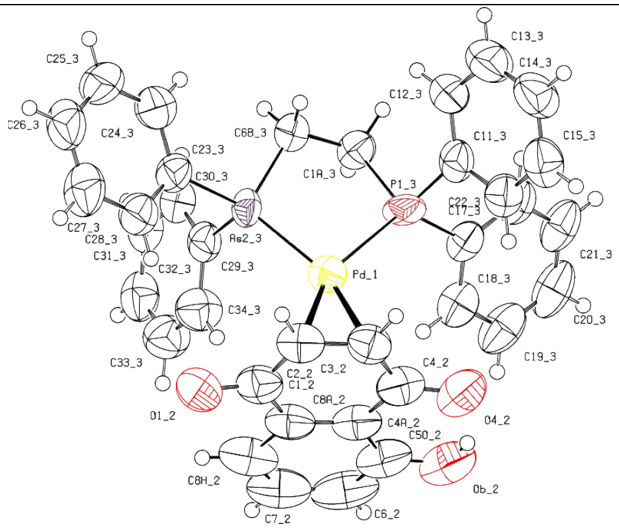

Table 5SI. Selected palladium distances and angles for **13** at 100 K and 298 K.

13 (100 K) – $PdC_{33}H_{30}NO_3P$							
ASU Molecule 'A'				**ASU Molecule 'B'**			
Distances	(Å)	**Angles**	**(°)**	**Distances**	(Å)	**Angles**	**(°)**
Pd_1-C2_2	2.147(2)	C2_2-Pd_1-C3_2	38.50(6)	Pd_1-C2_2	2.153(2)	C2_2-Pd_1-C3_2	38.73(6)
Pd_1-C3_2	2.144(2)	P_3-Pd_1-C3_2	111.11(5)	Pd_1-C3_2	2.122(2)	P_3-Pd_1-C3_2	109.40(5)
Pd_1-C1_2	2.696(2)	P_3-Pd_1-C_4	103.41(5)	Pd_1-C1_2	2.796(2)	P_3-Pd_1-C_4	99.02(5)
Pd_1-C4_2	2.809(2)	C_4-Pd_1- C2_2	106.96(7)	Pd_1-C4_2	2.856(2)	C_4-Pd_1- C2_2	112.83(7)
Pd_1-P_3	2.312(1)	Pd-Juglone Ave Plane[a]	80.32(3)	Pd_1-P_3	2.312(1)	Pd-Juglone Ave Plane[a]	87.83(3)
Pd_1-C_4	2.001(2)	Juglone Ave Plane[b]	8.14(5)	Pd_1-C_4	2.012(2)	Juglone Ave Plane[b]	5.48(6)

[a]Average angle between the mean metal coordination plane and the mean juglone plane; [b]Average angle between quinone and phenolic rings in juglone

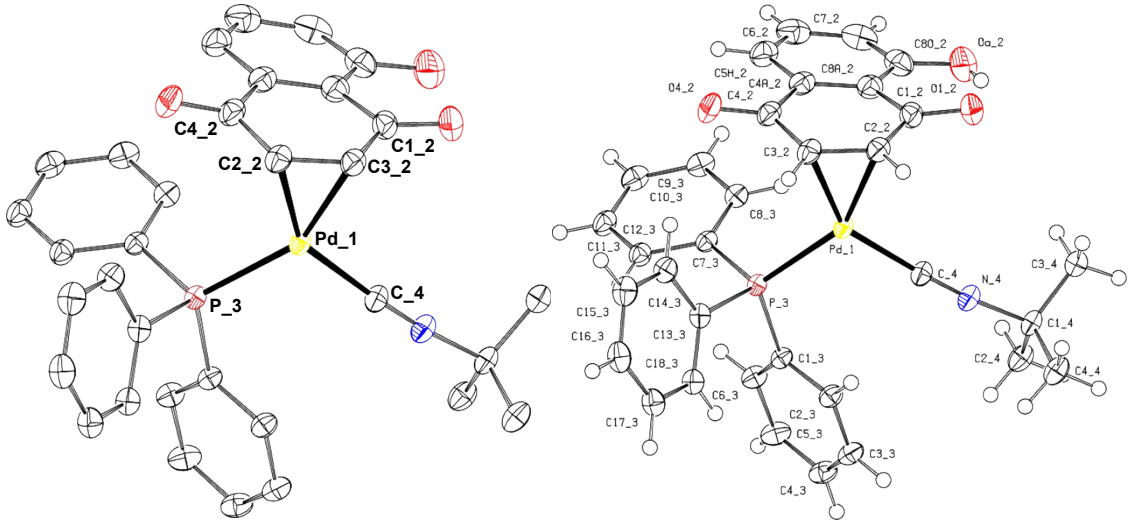

13 (298 K) – $PdC_{33}H_{30}NO_3P$							
ASU Molecule 'A'				**ASU Molecule 'B'**			
Distances	(Å)	**Angles**	**(°)**	**Distances**	(Å)	**Angles**	**(°)**
Pd_1-C2_2	2.144(3)	C2_2-Pd_1-C3_2	38.30(10)	Pd_1-C2_2	2.156(3)	C2_2-Pd_1-C3_2	38.38(9)
Pd_1-C3_2	2.141(3)	P_3-Pd_1-C3_2	111.20(8)	Pd_1-C3_2	2.123(2)	P_3-Pd_1-C3_2	109.71(7)
Pd_1-C1_2	2.706(3)	P_3-Pd_1-C_4	104.15(8)	Pd_1-C1_2	2.811(3)	P_3-Pd_1-C_4	99.25(7)
Pd_1-C4_2	2.807(3)	C_4-Pd_1- C2_2	106.30(10)	Pd_1-C4_2	2.851(3)	C_4-Pd_1- C2_2	112.70(10)
Pd_1-P_3	2.318(1)	Pd-Juglone Ave Plane[a]	82.11(4)	Pd_1-P_3	2.318(1)	Pd-Juglone Ave Plane[a]	89.54(5)
Pd_1-C_4	2.004(2)	Juglone Ave Plane[b]	7.65(9)	Pd_1-C_4	2.016(2)	Juglone Ave Plane[b]	4.44(8)

[a]Average angle between the mean metal coordination plane and the mean juglone plane; [b]Average angle between quinone and phenolic rings in juglone

Structural characterization of 5, 7 and 13.

5, **7** and **13** molecules have been crystallized by slow diffusion of diethyl ether in a dichloromethane solution of complex. The characterization through XRD and show square planar Palladium coordination spheres (**Tables 2SI-5SI**). Bite angle differences in phosphine ligands impact the complex geometries with minor effect on Juglone binding as shown in **Figure S2**. A η^2-coordination has been detected in all the systems as previously reported for Pd-ethylene- or quinone-based phosphine complexes.[1S, 2S] Steric hindrance of ligands control binding of juglone which is disordered when the bidentate phosphine/arsine bears two almost equivalent binding groups. Some planarity distorsion of juglone naphthalene core has been detected and it is more prominent in the asymmetric coordination environment of **13**.
Crystal packing shows hydrophobic contacts among neighbour molecules, involving weak intermolecular $\pi\cdots\pi$ and $CH\cdots\pi$ interactions, involving aromatic rings in close contacts. Solvent molecules have been found in the crystal packing of **5** and **7** (*i.e.* heavily disordered chloroform). Minor cell volume contraction has been found in **13** (~3%) upon cooling, with no significant packing rearrangements.

[1S] Wang J. Y., Strom A. E., Hartwig J. F. (2018). Mechanistic Studies of Palladium-Catalyzed Aminocarbonylation of Aryl Chlorides with Carbon Monoxide and Ammonia. JACS, 140(25), 7979-7993. https://doi.org/10.1021/jacs.8b04073

[2S] Clegg W., Eastham G. R., Elsegood M. R. J., Heaton B. T., Iggo J. A., Tooze R. P., Whyman R., Zacchini S. (2002) Synthesis and reactivity of palladium hydrido-solvento complexes, including a key intermediate in the catalytic methoxycarbonylation of ethene to methyl propanoate. J. Chem. Soc., Dalton Trans., 3300-3308. https://doi.org/10.1039/B202372P

Figure S64. Ortep representations of asymmetric unit contents for **5** at 100 K (A), **7** at 100 K (B), **13** at 100 K (C) and **13** at 298 K (D). Ellipsoids correspond to 50% probability.

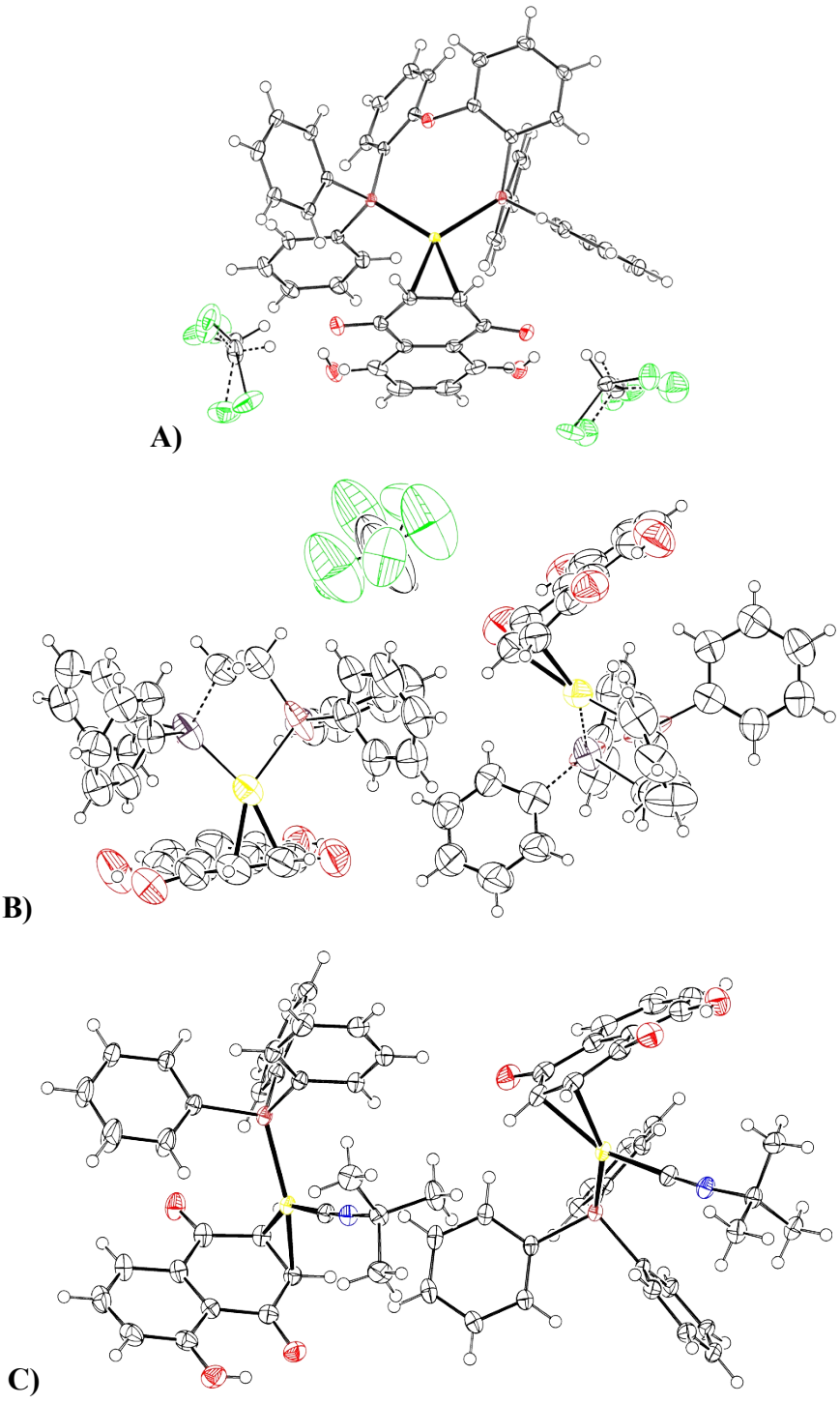

D)

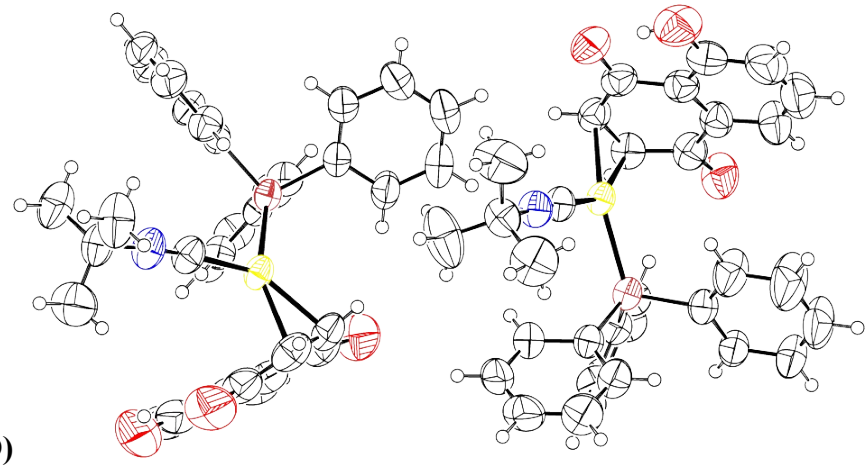

CYTOTOXICITY STATISTICAL ANALYSIS

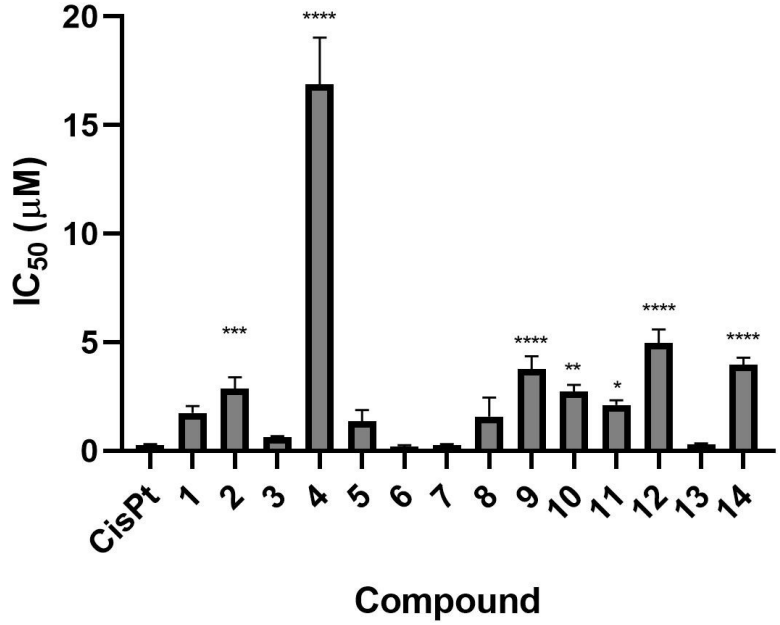

Figure **S65**. ANOVA test between IC_{50} of complexes *vs* Cisplatin (control) in A2780 cell line.

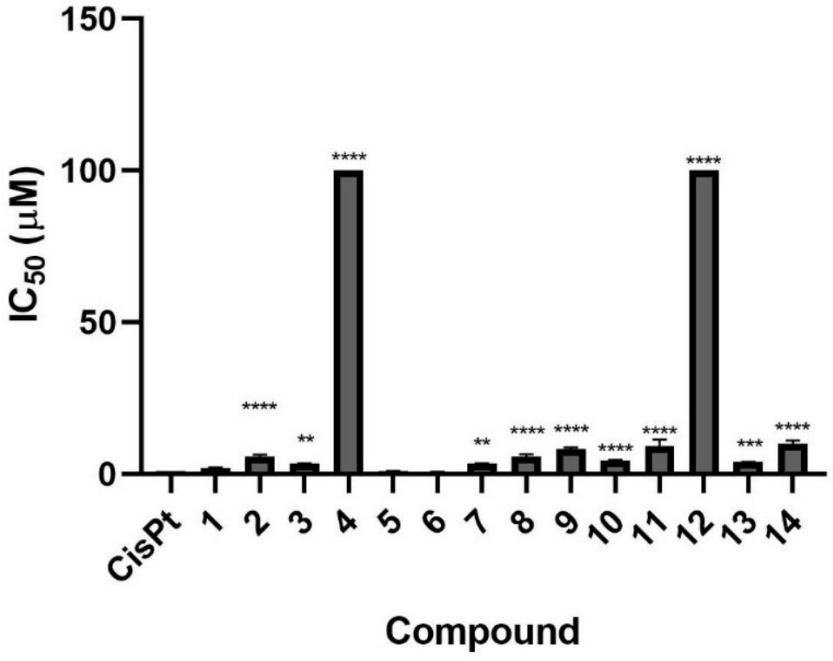

Figure **S66**. ANOVA test between IC_{50} of complexes *vs* Cisplatin (control) in OVCAR5 cell line.

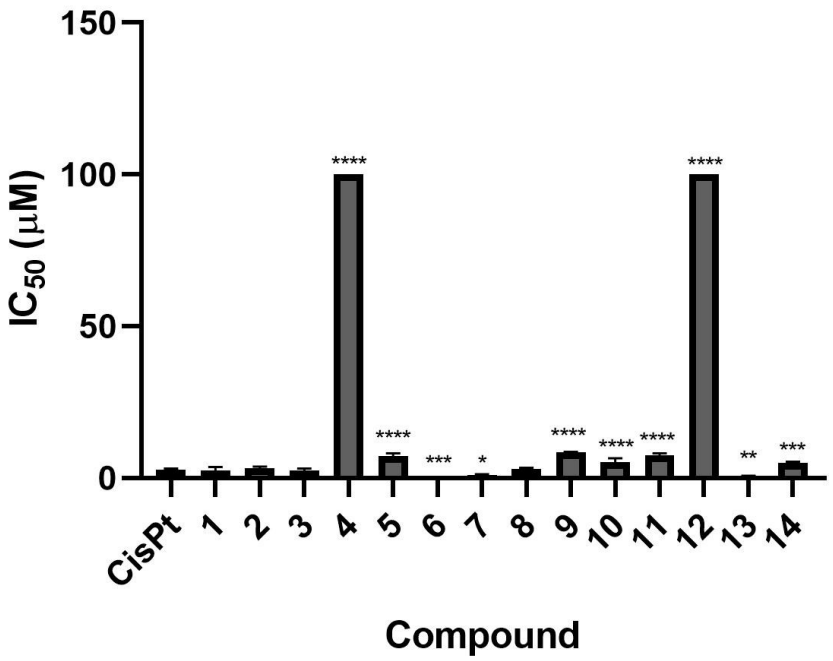

Figure **S67**. ANOVA test between IC_{50} of complexes *vs* Cisplatin (control) in KURAMOCHI cell line.

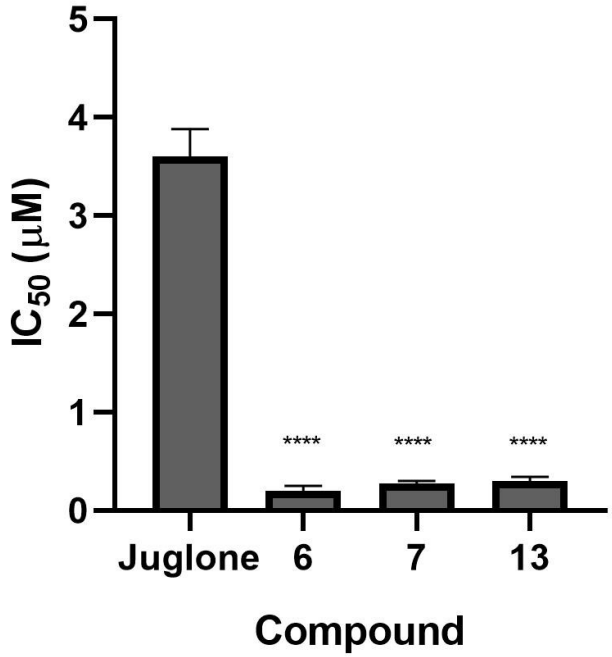

Figure **S68**. ANOVA test between IC_{50} complexes 6, 7, 13 *vs* Juglone (control) in A2780 cell line.

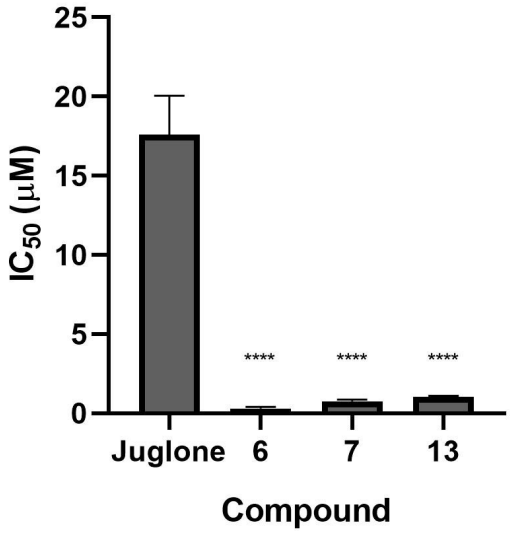

Figure **S69**. ANOVA test between IC_{50} complexes 6, 7, 13 *vs* Juglone (control) in A2780cis cell line.

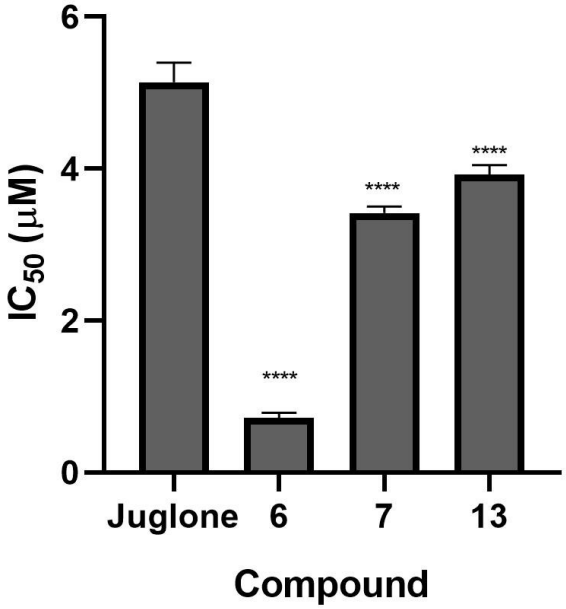

Figure **S70**. ANOVA test between IC_{50} complexes 6, 7, 13 *vs* Juglone (control) in OVCAR-5 cell line.

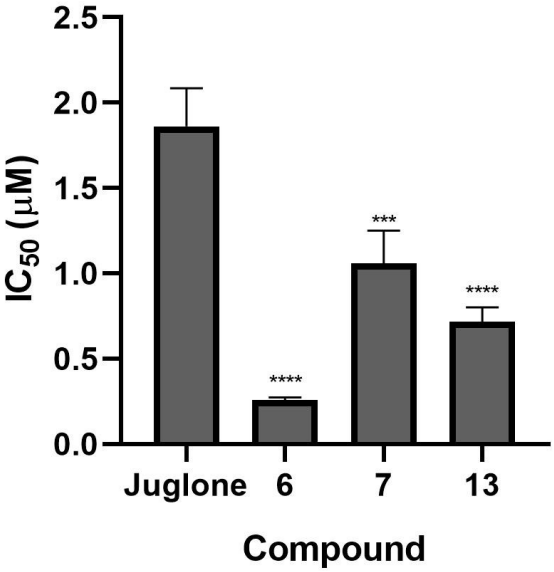

Figure **S71**. ANOVA test between IC_{50} complexes 6, 7, 13 *vs* Juglone (control) in KURAMOCHI cell line.

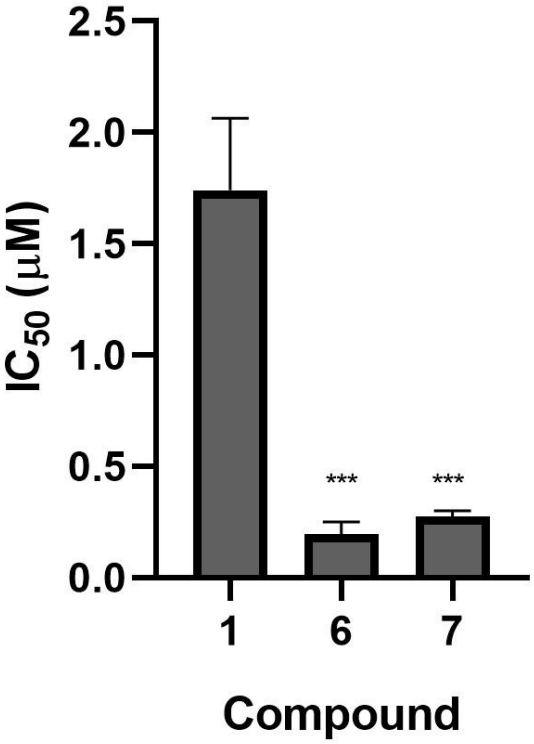

Figure **S72**. ANOVA test between IC_{50} complexes 6, 7 *vs* 1 in A2780 cell line.

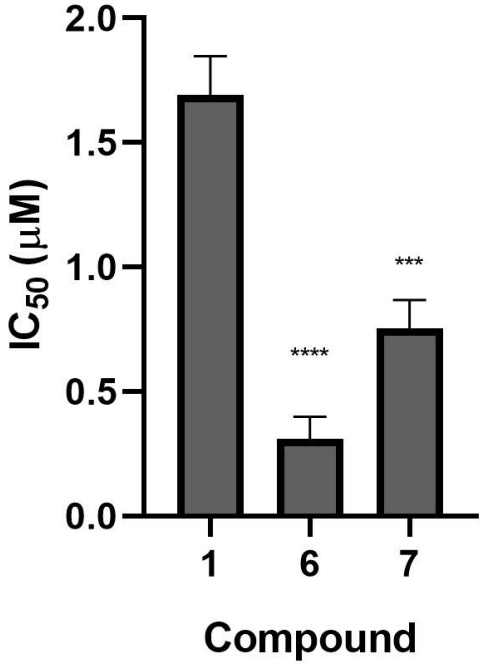

Figure **S73**. ANOVA test between IC_{50} complexes 6, 7 *vs* 1 in A2780cis cell line.

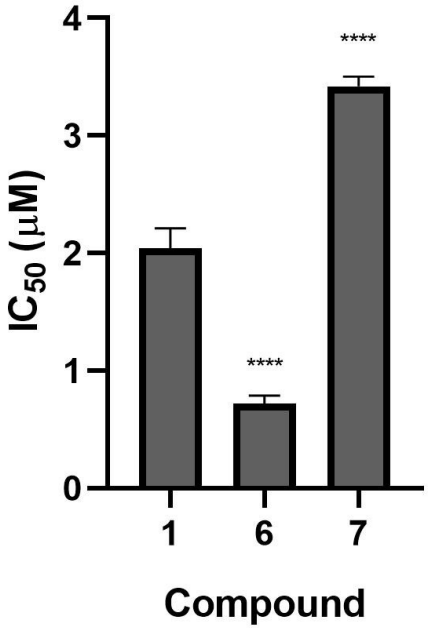

Figure **S74**. ANOVA test between IC_{50} complexes 6, 7 *vs* 1 in OVCAR-5 cell line.

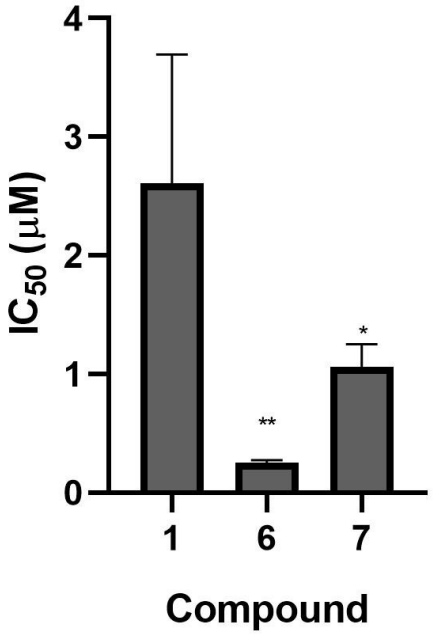

Figure **S75**. ANOVA test between IC_{50} complexes 6, 7 *vs* 1 in KURAMOCHI cell line.

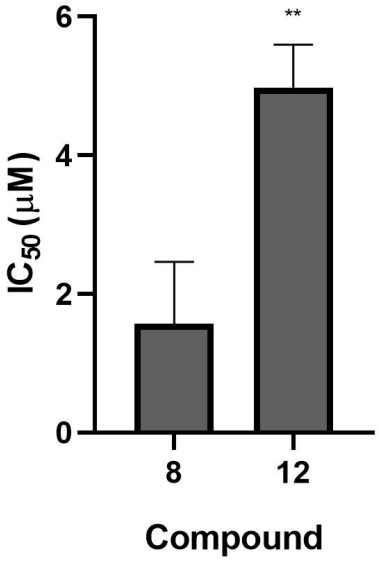

Figure **S76**. t test between IC_{50} of complex 12 *vs* 8 in A2780 cell line.

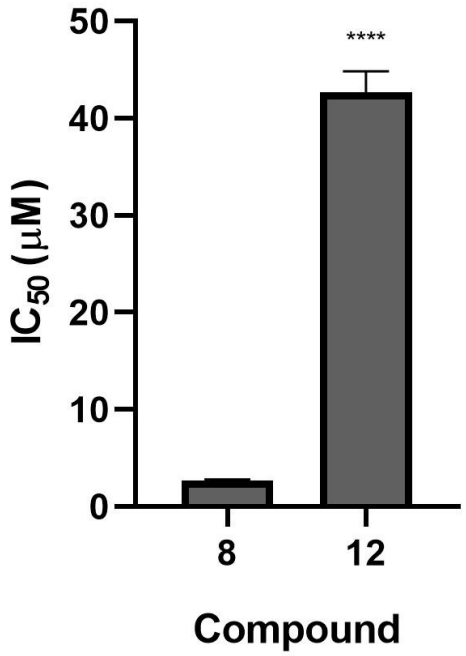

Figure **S77**. t test between IC_{50} of complex 12 *vs* 8 in A2780cis cell line.

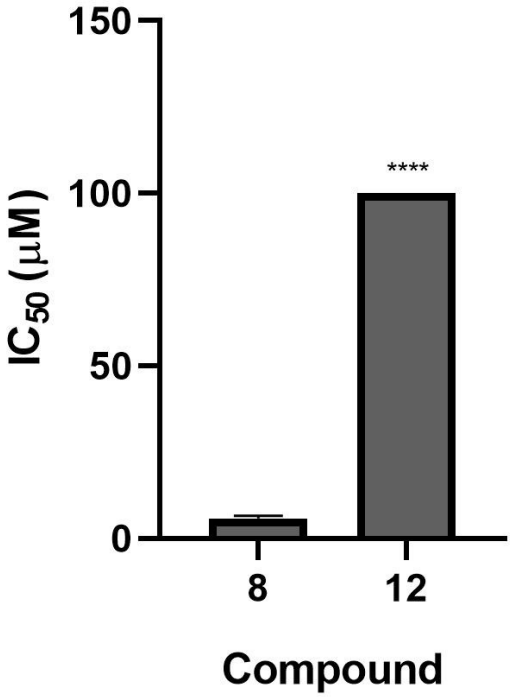

Figure **S78**. t test between IC_{50} of complex 12 *vs* 8 in KURAMOCHI cell line.

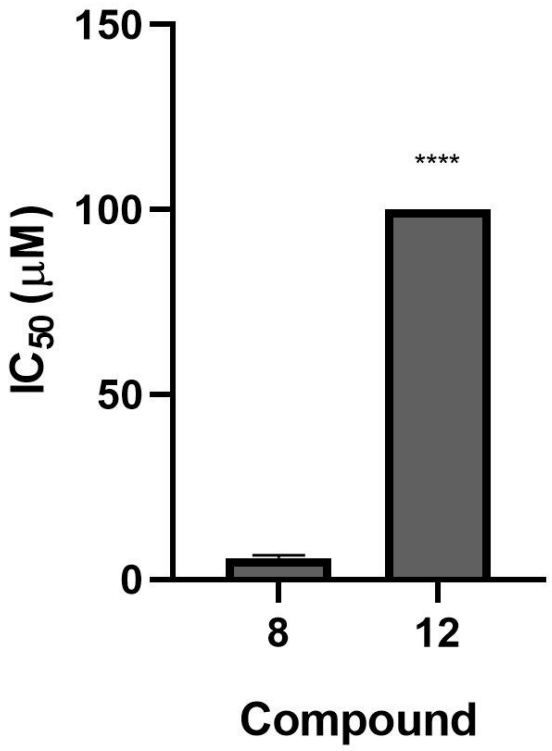

Figure **S79**. t test between IC_{50} of complex 12 *vs* 8 in OVCAR-5 cell line.